Institut für Geographische Wissenschaften der Freien Universität Berlin

Monitoring land use dynamics with optical and radar remote sensing data in western Ukraine

Inaugural-Dissertation zur
Erlangung des akademischen Grades
Doktor der Naturwissenschaften (Dr. rer. nat.)
des Fachbereichs Geowissenschaften
der Freien Universität Berlin

vorgelegt von
Jan Stefanski

Berlin, 2014

Erstgutachter: Prof. Dr. Björn Waske
Zweitgutachter: Prof. Dr. Achim Schulte

Tag der Disputation: 30.01.2015

Eidesstattliche Erklärung

Hiermit erkläre ich, dass ich die vorliegende Arbeit selbständig verfasst und keine anderen als die angegebenen Hilfsmittel benutzt habe. Die aus fremden Quellen direkt oder indirekt übernommenen Inhalte sind als solche kenntlich gemacht. Die Arbeit hat in dieser oder ähnlicher Form bisher noch keiner Prüfungsbehörde vorgelegen.

Jan Stefanski

Berlin, den 07.10.2014

Abstract

Remote sensing is a key technology for systematic and broad-scale observations of the Earth's surface and provides the basis for a large body of research and applications. However, region wide land use intensity mapping as well as monitoring of changes of land management based on remote sensing data has not yet been studied thoroughly. The main goal of this thesis was to develop and apply a framework for monitoring land management regimes that differ in land use intensity in order to advance the mapping and understanding of broad-scale land use changes based on remote sensing, and to assess the spatio-temporal patterns of land management regimes. The land management regimes defined in this thesis are large-scale cropland with a high management intensity, small-scale cropland with a potentially low management intensity, and farmland abandonment that implies no active land management.

Eastern Europe is a prime example for drastic broad-scale land use changes due to the momentous political and socio-economic changes after the collapse of the Soviet Union in 1991. In order to monitor land management regimes in western Ukraine, a combination of different strategies was used. First, a semi-automatic parameter selection was developed to optimize and economize image segmentation, which is a prerequisite for object-based analysis. To select the optimal parameters of the Superpixel Contour segmentation algorithm, a predefined range of parameters is selected by the user and the best image segmentation is subsequently assessed by the fast internal accuracy assessment of the Random Forest classifier, and, optionally, by using additional validation data. Second, by integrating optical and radar data into the object-based image analysis, the synergistic and complementary effects of both data types were used to improve the mapping and monitoring approach. For example, the radar data with its high temporal resolution provided elementary information to distinguish pasture from abandonment, as both classes have a similar grassland cover but different phenological stages. Moreover, the relatively weather independent radar data was a reliable alternative to fill gaps of optical time series that can occur, for example, due to cloud cover. Third, by using a change trajectory analysis approach, land use and land use intensity changes were monitored for western Ukraine between 1986 and 2010. The results clearly showed substantial abandonment of the large collectivized farmland in the 1990s and 2000s. With Ukraine's integration in world markets and the emerge of agri-business at the end of the 2000s, many abandoned fields were recultivated. Since the beginning of the 1990s, small-scale cropland as subsistence agriculture emerged for the greatest part directly from the conversion from large-scale cropland. Nevertheless, large-scale cropland was the dominant class in the study area at any time during the study period. To further explore the spatial patterns of land management regimes, the final classification results were overlayed by a number of spatial indicators related to the marginality of farming, such as soil type, distance to markets, and elevation. Although a large part of the abandoned farmland was located on soils not very well suited for agriculture, the analysis showed that there is still a considerable potential for recultivation and for intensifying small-scale farmland.

Zusammenfassung

Fernerkundung ist eine Schlüsseltechnologie für die systematische und großflächige Beobachtung der Erdoberfläche und bildet die Grundlage für viele Forschungsarbeiten und Anwendungen. Die großflächige, fernerkundungsbasierte Kartierung von Landnutzungsintensitäten sowie das Monitoring von Landmanagement ist bisher jedoch kaum untersucht worden. Der Schwerpunkt dieser Dissertation war die Entwicklung und Anwendung eines Systems zum Monitoring von verschiedenen Landmanagementklassen sowie ihrer jeweiligen Landnutzungsintensität, um die Kartierung und das Verständnis von großflächigen Landnutzungsveränderungen mittels Fernerkundung zu verbessern und die raum-zeitlichen Muster von Landmanagement zu bestimmen. Die Landmanagementklassen wurden wie folgt definiert: Großskaliges Ackerland mit einer intensiven Landnutzung, kleinskaliges Ackerland bzw. Subsistenzlandwirtschaft mit einer potentiell geringen Landnutzungsintensität und aufgegebene landwirtschaftliche Flächen ohne aktive Landnutzung.

Osteuropa ist ein Musterbeispiel für drastische und großflächige Landnutzungsänderungen, die durch die tiefgreifenden Umwälzungen nach dem Zerfall der Sowjetunion im Jahr 1991 entstanden sind. Um die unterschiedlichen Landmanagementklassen im Untersuchungsgebiet in der Westukraine über die Zeit zu untersuchen, wurden verschiedene Analysestrategien kombiniert. Erstens wurde eine semi-automatische Parameterbestimmung entwickelt um die Bildsegmentierung hinsichtlich ihrer Qualität und ihres Generierungsaufwandes zu optimieren. Um die optimalen Parameter des Superpixel Contour Segmentierungsalgorithmus zu erhalten, definiert der Anwender zunächst einen gewissen Parameterbereich und anschließend wird die beste Parameterkombination aus dem vordefinierten Bereich anhand der internen Genauigkeitsuntersuchung des Random Forest Klassifikators, oder optional mittels eines Referenzdatensatzes, bestimmt. Zweitens konnten durch die Integration von optischen und radargestützten Satellitendaten innerhalb der objektbasierten Bildanalyse Synergie- und Komplementäreffekte durch beide Datentypen genutzt werden, um die Kartierung und das Monitoring zu verbessern. Zum Beispiel waren die Radardaten mit ihrer hohen zeitlichen Auflösung eine Voraussetzung für die präzise Unterscheidbarkeit von Weideland und aufgegebenen landwirtschaftlichen Flächen, da beide Klassen zwar prinzipiell eine Graslandbedeckung aufweisen, jedoch unterschiedliche phänologische Phasen haben. Des Weiteren erlaubten die Radardaten Lücken in der Zeitreihe der optischen Daten effektiv zu füllen, die beispielsweise auf Grund von Wolkenbedeckung auftreten können. Drittens, durch die Nutzung von Veränderungstrajektorien konnten die Veränderungen in Landnutzung und Landnutzungsintensität in der Westukraine für den Zeitraum zwischen 1986 und 2010 effektiv bestimmt werden. Die Ergebnisse zeigten deutlich die massive Aufgabe von großen, kollektivierten landwirtschaftlichen Flächen in den 1990er und 2000er Jahren. Mit der Integration in die Weltmärkte und dem Aufkommen von Agribusiness Ende der 2000er wurden viele vormals aufgegebene Flächen rekultiviert. Seit Anfang der 1990er Jahre wurde zudem das Aufkommen von Subsistenzlandwirtschaft beobachtet, welches zum größten Teil

direkt aus den großskaligen Ackerflächen umgewandelt wurde. Dennoch nahm das großskalige Ackerland innerhalb des Untersuchungszeitraums immer die größte Fläche in Anspruch. Um die räumlichen Muster der Landmanagementklassen im Detail genauer zu untersuchen, wurden verschiedene Indikatoren zur Bestimmung der landwirtschaftlichen Eignung von Flächen, wie beispielsweise Bodenqualität, Distanzen zu Märkten oder Höhenlage mit den Klassifikationsergebnissen verglichen. Obwohl ein Großteil der aufgegebenen landwirtschaftlichen Flächen nur geringe Bodenqualität aufwies, zeigten die Analysen, dass es dennoch ein deutliches Potential zur Rekultivierung von aufgegebenen landwirtschaftlichen Flächen sowie zur Bewirtschaftungsintensivierung von kleinskaligem Ackerland gibt.

Contents

List of Figures

List of Tables

List of Abbreviations

ALOS	Advanced Land Observing Satellite
DFG	Deutsche Forschungsgemeinschaft (German research funding organisation)
DLR	Deutsches Zentrum für Luft- und Raumfahrt (German Aerospace Center)
ERS	European Remote Sensing Satellite
ESA	European Space Agency
IVM	Import Vector Machines (classifier)
LSC	Large-scale cropland
LUCAS	Land Use and Cover Area frame Survey
MAP	Maximum-a posteriori
MLC	Maximum likelihood classifier
MRS	Multiresolution segmentation
NIR	Near-infrared
OOB	Out-of-bag
PA	Producer's accuracy
PALSAR	Phased Array type L-band Synthetic Aperture Radar
Pb	Pixel-based
RESA	RapidEye Science Archive
RF	Random Forest (classifier)
SAR	Synthetic aperture radar
SLC	Single look complex
SPc	Superpixel Contour (segmentation)
SPOT	Satellite Pour l'Observation de la Terre
SRTM	Shuttle Radar Topography Mission
SSC	Small-scale cropland
SVM	Support Vector Machines (classifier)
TM	Thematic Mapper
UA	User's accuracy
USGS	United States Geological Survey

Chapter I:

Introduction

1 Land use, its environmental impact, and perspectives

"Land use" is the manifold use of the Earth's surface and its natural resources by human activities, while "land cover" denotes the biophysical character of the Earth's surface. Both terms are closely linked when it comes to land cover changes, as these are principally based on human activities and land use changes. In the case of, for example, agricultural expansion, such land use/cover changes are accompanied by the replacement of natural ecosystems and are based on individual or societal need or want (Turner et al., 1990; Ojima et al., 1994; Walker et al., 1999; Lambin & Geist, 2006).

The pressure that increasing global population puts on land use has started being central to discussions and thinking already at the end of the 18th century (cf. Malthus, 1798; Godwin, 1820). However, factors and relations are complex and not only the sheer number of people, but a composition of social organization, technology, lifestyle, and consumption patterns are likely responsible for population pressure on land use (Ehrlich & Holdren, 1971; Jolly & Torrey, 1993; Lambin & Geist, 2006). In the past, agricultural expansion led to more and more land use/cover changes, for example, cropland areas increased more than five times during the past three centuries (Goldewijk, 2001) and nowadays about 13 million hectares are converted from natural vegetation to agricultural land every year (Tilman et al., 2001; FAO, 2006). Recent studies estimate that about 80% of new agricultural land is converted from tropical forests, which are a rich reservoir for biodiversity and ecosystem services (Barlow et al., 2007; Gibbs et al., 2010). Overall, about 40% of the Earth's surface is domesticated by human use for pasture and cropland (Vitousek, 1997; Foley et al., 2005).

Next to agricultural expansion, agricultural intensification was largely responsible to meet the food demand of the world population, which more than doubled during the past five decades (Tilman, 1998; Foley et al., 2011). Agricultural intensification, also called the "Green Revolution", which started in the 1960s, remarkably increased agricultural yields by using high-yielding crops, chemical fertilizers and pesticides, improved irrigation techniques, and mechanization (Tilman, 1998; Matson et al., 1997; Evenson & Gollin, 2003).

The success of increasing agricultural production is immense and the provisioning ecosystem services (i.e., food, fiber, shelter, freshwater) were highly increased in their efficiency (MEA, 2005), but there are two sides of every coin. Both agricultural expansion and intensification have fundamental impact on the environment and other ecosystem services. The expansion of agriculture into natural ecosystems, for example due to deforestation, degrades regulating ecosystem services such as for air quality, water quality, diseases, erosion, and natural hazards (MEA, 2005). Further consequences of expanding agriculture are the loss of biodiversity, which is even aggravated by the fragmentation of landscapes, and the change of the global carbon cycle by the release of huge amounts of carbon and reducing the capacity of carbon sequestration (Guo & Gifford, 2002; Tscharntke et al., 2005; Foley et al., 2011). Agricultural intensification, on the other hand, entails negative consequences on different scales in the world. Local consequences include increased soil erosion, lower soil fertility,

and reduced biodiversity due to the high-productive monoculture cultivation (Matson et al., 1997; Altieri, 1999b). Regional consequences can be the pollution of ground water and eutrophication of rivers and lakes, due to anthropogenic nutrient inputs from fertilizers (Matson et al., 1997; Bennet et al., 2001). Global consequences of agricultural intensification affect the atmospheric constituents and the climate by the emission of greenhouse gases (Smith et al., 1997; Matson et al., 1997). In total, agriculture is responsible for up to 35% of the global greenhouse gas emissions, mainly resulting from deforestation, methane emissions from livestock and rice cultivation, and nitrous oxide emissions from fertilized soils (Foley et al., 2011).

With the contemporary land use, humanity is degrading the global environment and potentially undermines the long-term capacities of ecosystems to provide services (Tilman et al., 2001; Foley et al., 2005). Unfortunately, the situation even seems to get aggravated in the future. The increasing world population, dietary changes towards an increasing meat consumption, and the role of bioenergy suggest a global demand for agricultural products by 2050 roughly twice as high as today (Godfray et al., 2010; Foley et al., 2011). To meet the surging demand for agricultural products in an environmentally-friendly and sustainable way will be a grand challenge in the 21st century, involving both science and politics.

Ensuring both secure food supply and environmental sustainability requires the combination of different strategies: (1) The amount of food that is lost in the food chain has to be reduced. Nowadays, about one-third of the food produced for human consumption is lost, this equals around 1.3 billion tons per year (FAO, 2011). This means, on the one hand, that huge amounts of food are wasted while they are missing in some parts of the world. On the other hand, huge amounts of resources used for the food production and all associated environmental impacts are wasted. The amount of food waste in low-income and developing countries is relatively low, however, improvements in the early stages of the food supply chains can overcome their food losses, for example, due to financial support, especially for investments in infrastructure and technical equipment, such as harvesting techniques, storage and cooling conditions as well as packaging (FAO, 2011). Food losses in medium and high-income countries are mainly related to consumer and food industry behavior. Changes in this context could prevent large quantities of food from being thrown away, for example due to changes in the insufficient purchase planning, the "best-before-dates" principle, or quality standards such as imperfect shape or appearance (FAO, 2011). (2) Changes on the demand side can help to increase the rate of available human food. Currently, croplands devoted to animal feed and pasture together amount to around 75% of the world's agricultural land (Foley et al., 2011). As a result, Foley et al. (2011) estimated the potential to increase food supplies by shifting 16 major crops to human food to over a billion tonnes, which would be an increase of 28% (around 49% more calories). West et al. (2014) even estimated that about 70% more calories would become available if the crop production for animal feed and nonfood uses shifts to direct consumption. Although a worldwide complete shift away from meat-based diets is unrealistic, these studies generally show the considerable potential of

shifts in food consumption. (3) Increasing the agricultural production in sustainable ways completes the strategies to secure food supply while the negative environmental impacts are minimized.

There are mainly three ways to increase agricultural production. First, agricultural areas can be expanded into natural ecosystems. This would have large negative consequences for the environment, as mentioned above. Furthermore, the benefits for food production, for instance based on deforested tropical areas, are not very clear and seem to be limited (Foley et al., 2011). Second, existing agricultural land can be intensified in a sustainable way, which means that the yield of underperforming fields is increased while at the same time the environmental impact of cultivation is decreased (Cassman, 1999; Clough et al., 2011; Tilman et al., 2011). For example, improving the management of nutrient and water can reduce resource inputs for cultivation and as a result also reduce the environmental impact of land use (Mueller et al., 2012). Organic farming systems produce food with minimal harm to ecosystems due to its abstinence of artificial fertilizers and pesticides, its positive impact on biodiversity, and usually with a more diverse crop rotation (Shepherd et al., 2003; Bengtsson et al., 2005; Hole et al., 2005). The yielding potential of organic farming is controversial. Some studies found evidence that organic farming can produce as much as conventional agriculture (Altieri, 1999a; Pretty & Hine, 2001). However, it is likely that the yield of organic farming is contextual, so that measures like good management practices, particular crop types, and growing conditions can produce similar yields (Seufert et al., 2012). In the end, to establish organic agriculture as an essential part of sustainable agriculture to secure food supply, the factors influencing the yields of organic agriculture have to be better understood (Seufert et al., 2012). Third, abandoned farmland can be recultivated to increase agricultural production, whereby the environmental impact depends on the stage of succession and is generally less dramatic than agricultural expansion into primary forests (Barthlott et al., 2001; Barlow et al., 2007; Gardner et al., 2008). One of the greatest potentials for recultivation lies in Eastern Europe with its widespread farmland abandonment since the collapse of the Soviet Union (Kuemmerle et al., 2011; Alcantara et al., 2012; Stefanski et al., 2014a). For instance, in Russia alone, around 40 million hectares of arable land became abandoned since the 1990s (Prishchepov et al., 2012). However, parts of the former cultivated land are marginally suited for agriculture, for example due to low soil quality for agriculture or mountainous areas such as the Carpathian Mountains (Stefanski et al., 2014a; Griffiths et al., 2013). This relativizes the rate of farmland abandonment as the potential for recultivation. Furthermore, profitable recultivation depends on the costs, which are directly linked to the type and stage of succession (Larsson & Nilsson, 2005; USDA-FAS, 2008). Natural succession is mainly determined by the soil properties, climate conditions, and the time elapsed since the abandonment (Schierhorn et al., 2013). For example, the recultivation costs increase with advanced shrub land and woody vegetation in comparison to perennial weeds and grasses. In the end, recultivation is a trade-off between the agricultural potential of the land, recultivation costs, economic and institutional constraints, and, at best,

the carbon costs involved in recultivating abandoned farmland (Schierhorn et al., 2013).

All in all, the combination of different strategies to secure food supply while minimizing the negative environmental impact of agriculture is crucial (Foley et al., 2011; West et al., 2014). Remote sensing can play an important role to map and estimate the current land use and to derive potentials for intensification and recultivation. This thesis makes a contribution to a more nuanced mapping of land use to estimate and ultimately better understand land management patterns and land use intensity (i.e., high and low land use intensity as well as abandoned land).

2 Remote sensing and methodologies for monitoring land use dynamics

Remote sensing has a long history that goes back to photographies in the 1850s out of balloons, while the advent of modern earth observation started with the first commercial satellite – Landsat-1 – in 1972 (Lillesand et al., 2008). Great advances during the past decades have led to an expansion of remote sensing in diverse commercial and scientific applications as well as to an increasing support for decision-makers in economy and politics. The advances in remote sensing were enabled by both the technical development resulting in a considerable variety of sensors and the rapid progress in digital image processing with its advancing methodologies. The unique ability to acquire systematic repetitive observations of large parts of the Earth's surface with different spectral and temporal resolutions makes remote sensing to the most important tool for monitoring and mapping land use dynamics (Campbell, 2002).

Nowadays, a multitude of remote sensing satellites acquire images of the Earth's surface at different spatial resolutions, spectral regions, and temporal characteristics. While satellites with a high spatial resolution capture relatively small area coverages of the ground (e.g., RapidEye 6.5 m spatial resolution, 5 spectral bands, and about 80 km swath width), satellites such as MODIS have a swath width of 2330 km with a spatial resolution between 250 m and 1000 m, depending on the number of spectral bands, which allows to capture the entire surface of the Earth in up to two days (Sandau, 2010; Xiong et al., 2003). Therefore, choosing the optimal sensor for monitoring applications is mainly a trade-off between the spatial/spectral resolution and the ground as well as repeat coverage. In general, multispectral sensors, which record natural radiation (e.g., sunlight), offer a wide range of applications with regard to the spectral band. For example, while the blue spectrum is sensitive to water, the red and infrared spectra are sensitive to vegetation (Lillesand et al., 2008). The Landsat satellite mission acquires multispectral images of the Earth's surface since more than 40 years and the Landsat archive – in the meantime free of charge – became a fundamental basis for remote sensing based applications regarding mapping and change detection (Wulder et al., 2012). The properties of the Landsat images since Landsat-4 represent a good compromise between the area coverage (185×185 km) and the spatial resolution (30×30 m), which enable accurate

yet region-wide analyses (Mika, 1997; Williams et al., 2006). Beside of such passive satellite systems, satellites with microwave sensors, such as synthetic aperture radar (SAR), are active imaging systems that allow data acquisitions independently from the day/night cycle and the characteristic of the radar signal allows to measure through cloud cover and some rain (Moore, 1983). The radar backscatter is a function of the signal (i.e., frequency, polarization, incidence angle) and the surface parameters (Moore, 1983). For example, different radar frequencies have different penetration depths and thus provide different information about the observed surface. Generally, SAR is sensitive to soil moisture, surface roughness, vegetation cover, and soil texture (Henderson & Lewis, 1998). The ERS-1/-2 SAR mission provided continuous observations of the Earth between 1991 and 2011 and enabled a multitude of land and sea applications (Gens & van Genderen, 1996; Attema et al., 1998; Del Frate et al., 2000; Quegan et al., 2000). The ERS sensor operated at a frequency of 5.3 GHz (C-band) and a typical standard three-look image has an area coverage of 100×100 km and a spatial resolution of 25×25 m (Lehner et al., 1998; Attema et al., 2000).

Each remote sensing sensor has its own advantages and drawbacks. Therefore, the combination of different types of data is a promising avenue to benefit from the multisensory synergistic and complementing effects, and, ultimately, to make better use of remote sensing data for numerous applications. On the one hand, increasing the available spectral resolution or bandwidth due to different sensors likely improves the accuracy of more complex analyses. On the other hand, the use of multisensor data can increase the temporal resolution, which often increases the accuracy of the analysis as well as the robustness, for instance in cases where certain acquisition dates are required but not available due to cloud cover. The joint use of multitemporal SAR and multispectral data, for example with ERS SAR and Landsat data, significantly increased the accuracy of land use/cover mapping (e.g., Shupe & Marsh, 2004; Waske & van der Linden, 2008; Stefanski et al., 2014a). Especially the combination of SAR and multispectral data is beneficial, as the former is able to provide necessary image observations at specific dates because of the radar properties, and the latter provides a good spectral resolution useful for many applications.

Beside of the technical development of sensors and computers, digital image processing and analytical methods have also exhibited great progress in the past decades. Nowadays, they are used in a multitude of important areas such as medical imaging, in the field of security, intelligent sensing systems, material science, robotics and manufacturing, apart from remote sensing (Pitas, 2000). With the advent of machine learning techniques in remote sensing image analysis, many new applications became feasible. Classification methods can generally be divided into supervised and unsupervised approaches. Unsupervised classification algorithms analyze images in order to group the data into spectral categories and to assign a class to every image pixel without foreknowledge of the user or training samples. Unsupervised approaches are often performed with clustering methods like the k-means clustering and can, for example, be helpful for determining the spectral class composition prior to subsequent analysis (MacQueen, 1967; Richards & Jia, 2006). The basis of supervised methods are

typically multitemporal images, a data set for training of the classification model, and a data set for validation to estimate the achieved accuracy. Nowadays, supervised algorithms such as Support Vector Machines (SVM) or Random Forests (RF) are widely used for classification or regression analyses (e.g., Pal, 2005; Prasad et al., 2006; Waske & Benediktsson, 2007). Furthermore, such non-parametric classifier have no constrains regarding assumptions of the data distribution. Non-parametric classifier like RF can easily handle large multisensor data sets with similar or better accuracies and less training samples compared to parametric classifiers such as the maximum likelihood classifier (Waske & Braun, 2009; Na et al., 2010; Rodriguez-Galiano et al., 2012). In comparison to traditional pixel-based analysis, the use of spatial information in addition to spectral information becomes more popular (Gamanya et al., 2009; Blaschke, 2010). Image segmentation enables the partitioning of an image into homogenous regions and thus, finding objects represented of up to several pixels with regard to the object-size and spatial resolution of the image. The prior object-identification and utilization of spatial information (e.g., the segments' mean or variance value) can significantly enhance the mapping accuracy in comparison to a pixel-based approach, especially in object-relevant analysis such as agriculture and urban areas (Myint et al., 2011; Whiteside et al., 2011; Stefanski et al., 2013, 2014a). Object-based image analysis becomes more effective when the spatial resolution of the image increases. On the one hand, the identification of objects in high spatial resolution images is easier as objects are covered by more pixels. On the other hand, object-based information can help to overcome challenges when analyzing high spatial resolution images, such as spectral variations within single objects caused by crown textures, rooftops, or shadows (Yu et al., 2006; Wang et al., 2010). However, performing adequate image segmentation is often time consuming when users have to select the optimal segmentation parameters manually with a "trial-and-error" approach and, besides that, segmentation parameters cannot be transferred in most cases (Möller et al., 2007; Myint et al., 2011; Stefanski et al., 2013). The multiresolution segmentation implemented in the image analysis software eCognition is the most widely used image segmentation method for remote sensing applications (Baatz & Schäpe, 2000; Blaschke, 2010) and is therefore often used as a benchmark for new segmentation algorithms.

Satellite remote sensing acquisitions are predestined for change detection and monitoring land use dynamics because of the repeated coverage at short intervals with a relatively consistent image quality (Singh, 1989). The basic principle of many change detection approaches is a set of multitemporal imagery that is analyzed in order to detect spectral differences that represent the changes of land cover. However, not each spectral difference can necessarily be traced back to changes of the object since other factors, including atmospheric conditions, sun or observation angle, or soil moisture can also cause spectral changes (Jenson, 1983; Du et al., 2002). The use of, for example, appropriate data with similar image recording constellation, calibration methods (e.g., radiometric normalization), or supervised change detection approaches, may reduce or eliminate effects or consequences of ambiguity in spectral differences (Singh, 1989). Established change detection is mainly based on either

bi-temporal or trajectory-based approaches (McRoberts, 2013). While bi-temporal change detection is well suited to detect type and extend of land conversions (i.e., sudden changes), it is not able to detect gradual or subtle changes such as land cover modifications between the two dates. A more detailed analysis of temporal patterns is achieved with a change trajectory approach that analyzes the characteristics of every pixel in a time series of remote sensing data (Mertens & Lambin, 2000; Kennedy et al., 2007; Stefanski et al., 2014b). A common drawback of such change detection approaches, when using optical data, is that cloud cover can hinder useful image acquisitions, which causes gaps in time series that can prevent accurate change detection. To overcome such issues and to make change detection analysis more robust, it is beneficial to use a variable change detection approach including SAR data. Due to the SAR signal characteristics, SAR data can complement multispectral data and fill gaps in optical time series (Stefanski et al., 2014b).

3 Ukraine in the context of political and socio-economic changes

In the 20th century, Ukraine was an important producer of agricultural products and has therefore often been associated as the "granary of the Soviet Union" (Striewe & von Cramon-Taubadel, 1999; Aslund, 2009). At the end of the 1980s, Ukraine produced about 60% of the corn, 50% of the sugar beet, and 40% of the winter wheat and sunflower seed of the Soviet Union, even though Ukraine's arable land accounted for only around 15% of the Soviet Union's total arable land (World Bank, 1996). This is not very surprising given that the temperate continental climate and the fertile black soils make Ukraine a very favorable country for agricultural production. Ukraine can culturally and economically be divided into two parts due to a long history with both Russian/Soviet rule in the east and Polish and Austro-Hungarian rule in the west (Shulman, 1999). In general, eastern Ukraine is a center for mining and industry where the majority of the population speaks Russian in contrast to western Ukraine with its large agricultural sector and a majority of Ukrainian-speaking population (Shulman, 1999; Aslund, 2009).

The agricultural sector of the Soviet Union was characterized by large industrial and collectivized farms with high inputs of fertilizer and pesticides (Strayer, 1998). Although Soviet Ukraine's crop productivity was one of the highest within the Soviet Union, its production potential was even higher than being realized under the central planning (Striewe & von Cramon-Taubadel, 1999). Soviet agriculture was a high-cost agriculture with similar input use compared to most developed countries, however, the agricultural productivity was comparatively low (Johnson et al., 1983; Lerman et al., 2003). And the political-economic system with artificially low food prices and subsidies did not contribute to improving agricultural efficiency and competitiveness (Csaki & Lerman, 1997). Since the end of the 1970s, the increasing demand for food could not be met by the low growth of agricultural production (Johnson et al., 1983) and thus, the Soviet Union became a large grain importer until its collapse (Liefert et al., 2010).

With the collapse of the Soviet Union and its political-economic system in 1991, the Ukraine experienced drastic institutional and socio-economic changes. The direct economic impact for the Ukraine was a sharp decrease of the gross domestic product over 50% and the grain production decreased by about 20% to 25% in the 1990s (Blanchard & Kremer, 1997; Striewe & von Cramon-Taubadel, 1999; Liefert et al., 2010). With the transition from command economy to free markets, old production links broke down, for instance the state input distribution system, and old markets and trade agreements diminished (Blanchard & Kremer, 1997). Furthermore, the lack of capital investments resulted in a degradation of infrastructure (e.g., machineries and irrigation systems), a reduced technical efficiency in crop production, and ultimately limited the economic viability of farms (Johnson et al., 1994; Hostert et al., 2011). All in all, the drastic changes after the end of socialism resulted in lower profitability of farming and rural migrations, and, consequently, led to widespread farmland abandonment and the emerge of subsistence agriculture (Müller & Munroe, 2008; Hostert et al., 2011; Stefanski et al., 2014b). And although it is commonly understood that the collapse of the Soviet Union resulted in drastic impacts for the political and socio-economic systems, rates and spatio-temporal patterns of land changes remain largely unclear.

While the yields in the Ukraine declined during the 1990s, land reforms and a more stable trade policy started a period of efficiency-driven growth of the agricultural sector, including increasing yields and profits (Aslund, 2002; OECD, 2004; Liefert et al., 2010). For example, since 2006, the sunflower, corn, and soybean yields in Ukraine could almost double, and in 2009, Ukraine became the world's largest barley exporter (USDA, 2010; Deininger et al., 2013). A main source of the rising yields and Ukraine's increasing role as an important agricultural producer is the emerge of new and more productive operators as large, vertically integrated enterprises, combining the whole chain of primary agriculture, processing, distribution, and sometimes retail sale (Liefert et al., 2010; Deininger et al., 2013). These new operators mainly use former collective farms, and capital invest into current technology such as machines and irrigation systems, import high-yielding seeds, and professionalize the management practices. Both the potential for increasing yields and the availability of idle farmland with perspectives for recultivation are two of the main reasons why recent studies predict the Ukrainian's agricultural sector an important role in the future (USDA, 2010; Liefert et al., 2010; Deininger et al., 2013).

4 Aims and research questions

The main objective of this dissertation was to develop and apply a feasible methodological approach for mapping and monitoring land use dynamics, and specifically identifying the spatio-temporal patterns of land use and its intensity. As the global demand for agricultural products is surging, strategies for increasing agricultural production with a minimized environmental impact are gaining increasing attention. A prerequisite for the realization of such strategies is the mapping of current land use patterns including their land use intensity

and management. To do so, a comprehensive framework was developed that consisted of: 1) object-based image analysis with a semi-automatic parameter selection to extract additional spatial information; 2) the integration of multispectral and SAR data into a classification scheme to advance the mapping of land management regimes due to synergistic and complementing effects; and 3) the use of change trajectory analysis to monitor rates and patterns of land use intensity changes in western Ukraine.

The mapping of land management regimes that differ in field size (e.g., large-scale cropland and small-scale cropland) is challenging and hardly possible when solely analyzing spectral per-pixel information. Using multilevel segmentation (i.e., multiple segmentations with different parameter settings such as different "scales") enables the integration of different spatial information into image analysis and thus increases the sensitivity for different object sizes. Finding adequate segmentation parameters is often time consuming when the user has to select appropriate parameter settings by a "trial-and-error" approach, which is an iterative process of generating a segmentation, visually interpreting the result, and then adjusting the parameters into a direction the user believes it will improve the result in the next iteration. To raise the segmentation parameter selection to a new level in terms of evaluation of the optimal segmentation level and user-friendliness, a classification-optimized parameter selection in which the user just pre-defines the general parameter range and the selection of the optimal segmentation is done automatically appears worthwhile. Such an advanced parameter selection is even more beneficial if a multilevel segmentation is used and each segmentation level requires a class-specific optimization.

Generally speaking, land use intensity is a complex and multidimensional term. For example, land use intensity can be measured by agricultural inputs such as the application rate of fertilizer and pesticides or by agricultural outputs such as yields. As these dimensions can only rarely be measured by remote sensing analysis, the additional use of ground-based data containing intensity metrics could overcome this problem. However, such ground-based data is often not available, especially when the analysis should cover large areas, which would require extensive and expensive in-situ measurements to collect the intensity metrics. Therefore, the use of proxy variables such as field size to represent land management regimes with different intensities seems to be an interesting remote sensing-compatible approach. Moreover, the joint use of multispectral and SAR data may support a more reliable mapping of land management regimes. On the one hand, the use of SAR data ensures the provision of that particular temporal information that is necessary due to the weather independence of SAR data. On the other hand, in the case of, for example, the discrimination of vegetation species, SAR data can contribute with information about surface roughness, soil moisture, or soil texture of the Earth's surface.

The far-reaching consequences of the collapse of the Soviet Union and the following drastic institutional and socio-economic changes offer an unique opportunity to study the transition from planned to free market economy with its broad scale changes of land use and land management. Unfortunately, our understanding of the impact of major socio-economic

disturbances on land use is limited. Therefore, it is important to monitor the spatial and temporal patterns of land use and its intensity to gain information about the rate and extend of widespread land changes triggered by specific socio-economic disturbances. Moreover, the mapping and monitoring of active land use, abandonment, and recultivation by using remote sensing data offers the opportunity to assess potentials for both agricultural intensification and recultivation, which can increase agricultural production. The large image coverages with a sufficient high spatial resolution for identifying land systems acquired from remote sensing satellites such as Landsat/ERS or the upcoming Sentinel-1/-2 mission make remote sensing a key technology for monitoring land use dynamics.

Overall, the main objectives of this dissertation are addressed by the following research questions:

1. How can object-based image analysis be optimized and simplified in order to improve both the quality and feasibility of remote sensing analysis?

2. How can the representation of land use intensity be improved in order to efficiently map land use management based on remote sensing data and what are the methodological and data requirements for mapping land management regimes?

3. What were the specific rates and patterns of land use and management changes in western Ukraine since 1986?

5 Structure of this dissertation

This dissertation is divided into three core chapters (Chapter II–IV), each relating to one of the research questions that are set out above. Chapter II introduces a semi-automatic parameter selection to optimize a Superpixel Contour segmentation with a Random Forest classification-based assessment of the segmentation quality. This method was successfully tested on two study sites, one data set consisted of RapidEye images and the other one consisted of SPOT-5 images. The developed parameter selection approach was used to find optimal segmentation parameter settings for the subsequent object-based analysis regarding the study in western Ukraine. In Chapter III, land management regimes that differed in field sizes were mapped to identify different land use intensities in western Ukraine. The hierarchical, object-based approach to map the land management regimes used Landsat-5 and ERS SAR data. In Chapter IV, the changes of land management regimes between 1986 and 2010 were monitored in order to assess the spatio-temporal patterns of land use intensity changes. This approach used change trajectory analysis that were based on an extensive Landsat-5 and ERS SAR time series. Finally, Chapter V presents a synthesis of the results of the three core chapters, provides answers to the research questions, and discusses future perspectives and application potentials.

The core chapters (Chapter II–IV) of this dissertation were written as stand-alone manuscripts and published in international peer-reviewed journals:

Chapter II: Stefanski, J., Mack, B., & Waske, B. (2013). Optimization of object-based image analysis with Random Forests for land cover mapping. *IEEE Journal of Selected Topics in Applied Earth Observations and Remote Sensing*, 6, 2492–2504.

Chapter III: Stefanski, J., Kuemmerle, T., Chaskovskyy, O., Griffiths, P., Havryluk, V., Knorn, J., Korol, N., Sieber, A., & Waske, B. (2014). Mapping land management regimes in western Ukraine using optical and SAR data. *Remote Sensing*, 6, 5279–5305.

Chapter IV: Stefanski, J., Chaskovskyy, O., & Waske, B. (2014). Mapping and monitoring of land use changes in post-Soviet western Ukraine using remote sensing data. *Applied Geography*, 55, 155–164.

The final reference section includes only the literature cited in the Introduction (Chapter I) and Synthesis (Chapter V).

Chapter II:

Optimization of object-based image analysis with Random Forests for land cover mapping

IEEE Journal of Selected Topics in Applied Earth Observations and Remote Sensing, vol. 6, pp. 2492–2504, December 2013

Jan Stefanski, Benjamin Mack, and Björn Waske

© 2013 IEEE. All rights reserved.
http://dx.doi.org/10.1109/jstars.2013.2253089

Abstract

A prerequisite for object-based image analysis is the generation of adequate segments. However, the parameters for the image segmentation algorithms are often manually defined. Therefore, the generation of an ideal segmentation level is usually costly and user-depended. In this paper a strategy for a semi-automatic optimization of object-based classification of multitemporal data is introduced by using Random Forest (RF) and a novel segmentation algorithm. The Superpixel Contour (SPc) algorithm is used to generate a set of different levels of segmentation, using various combinations of parameters in a user-defined range. Finally, the best parameter combination is selected based on the cross-validation-like out-of-bag (OOB) error that is provided by RF. Therefore, the quality of the parameters and the corresponding segmentation level can be assessed in terms of the classification accuracy, without providing additional independent test data. To evaluate the potential of the proposed concept, we focus on land cover classification of two study areas, using multitemporal RapidEye and SPOT 5 images. A classification that is based on eCognition's widely used multiresolution segmentation algorithm (MRS) is used for comparison. Experimental results underline that the two segmentation algorithms SPc and MRS perform similar in terms of accuracy and visual interpretation. The proposed strategy that uses the OOB error for the selection of the ideal segmentation level provides similar classification accuracies, when compared to the results achieved by manual-based image segmentation. Overall, the proposed strategy is operational and easy to handle and thus economizes the findings of optimal segmentation parameters for the Superpixel Contour algorithm.

1 Introduction

Earth Observation (EO) data provide diverse information for decision support and environmental monitoring systems. In this context the mapping of land cover and land use is one of the major issues and remotely sensed land cover maps support a wide-range of applications, e.g., in the field of forestry (Walker et al., 2010), natural hazards (Stumpf & Kerle, 2011), urban climatology (Chen et al., 2006), and agriculture (Lobell et al., 2003; Skriver et al., 2011).

While most land cover classifications focus on pixel-based image analyses, object-based image analyses have been emerged over the past decade (Blaschke, 2010). Although, the classification accuracy of Landsat-like data can be improved by image segmentation (Dorren et al., 2003; Myint et al., 2008), object-based image analyses are even more attractive regarding EO data with higher spatial resolution (Wang et al., 2010).

In general, segmentation means the process of partitioning an image into multiple homogenous regions. Neighboring pixels are aggregated to segments, which simplify the representation of an image. This enables the derivation of additional features like the segments' mean

value or variance. The derivation of the segments' mean value can overcome the problem of random noise (Blaschke et al., 2000; Wang et al., 2010), which is particularly a problem in high spatial resolution imagery. Thus, subsequent filter operations are often obsolete (Voorde et al., 2007). Moreover, image segmentation enables the extraction of spatial information of the image objects, which can be included in subsequent image analysis, e.g.: van der Werff & van der Meer (2008) analyzed objects with identical spectral information to distinguish them on the basis of spatial information. Segl et al. (2003) show that the fusion of spectral and shape features improves the differentiation of urban surface cover.

However, the definition of an adequate segmentation scale is critical. An inaccurate segmentation can decrease classification accuracy and different classes and data sets often require different segmentation levels (cf. Song et al., 2005; van der Linden et al., 2007; Waske & van der Linden, 2008). Waske & van der Linden (2008) discussed a joint classification of different segmentation scales from multisensor images using SAR and optical data sets. They show that different segmentation scales contribute unequally to the classification accuracy of various rural land cover classes. While one scale is well suited for a specific data set and/or to describe a class, another scale is more adequate for others.

Similar results were reported in context of classifying urban structure types, using airborne hyperspectral data. Although segment-based maps visually appear more homogeneous, positive and negative impacts on the classification accuracies can be observed. Consequently, no ideal single segmentation scale can be defined, where an increase in classification accuracy is significant for all urban classes (van der Linden et al., 2007).

Behind these facts, a general accepted segmentation strategy, which produces high quality results for different types of images and study sites, would be attractive. An adequate segmentation algorithm as well as recommendations for universally valid default values could foster object-based image analyses, also in context of large-scale and operational applications.

In most remote sensing applications, the multiresolution segmentation algorithm (MRS) (Baatz & Schäpe, 2000) in Definiens eCognition is used (Duro et al., 2012b; Myint et al., 2011; Whiteside et al., 2011). Although a statistical significant difference between pixel-based and object-based classification is not necessarily achieved (Duro et al., 2012b), in several studies object-based classifications result in significant higher accuracies when compared to the pixel-based approach (Myint et al., 2011; Whiteside et al., 2011). In addition, the results show that usually manual input (e.g., segmentation parameters like scale level) is required to generate adequate segmentation results (Myint et al., 2011; Duro et al., 2012b). However, parameter settings cannot be transferred in the very most cases, i.e., diverse remote sensing images and study sites require specific parameters (Arbiol et al., 2006). Thus, the determination of optimal parameters is labour intensive, because it is usually based on a manual "trial-and-error" principle, i.e., the user tests different parameter settings, often by visual interpretation (Lowe & Guo, 2011). This widely-used technique to determine segmentation parameters is especially time consuming for non-experienced users. Behind this fact, Duro et al. (2012b) underlined the demand for strategies, which can reduce the time needed for selecting the

optimal input parameters for image segmentation, while the quality of the segmentation should be comparable or even superior. Anders et al. (2011) developed a technique for semi-automated geomorphologic mapping, which includes a systematic selection of the scale parameter of eCognition's multiresolution segmentation. The segment quality is evaluated by determining a segmentation error based on frequency matrices of the generated objects and training data. Tarabalka et al. (2012) developed an approach to generate automated segmentations by a marker-based segmentation, whereas the markers have to be found by a pixel-wise classification before the segmentation. One prerequisite for a correct segmentation is that the initial classification must marker all objects, since each region in the segmentation map contains one marker. Furthermore, some studies introduced approaches for selecting segmentation parameters (Espindola et al., 2006; Dragut et al., 2010; Dongping Ming et al., 2012). The segmentation quality criterion of these approaches is the maximization of intrasegment homogeneity and intersegment heterogeneity. All these parameter selections have in common that they optimize segment properties before a classification. However, a systematic parameter selection, which comprises all relevant segmentation parameters, combined with an unbiased classification-based quality assessment, would be desirable.

To overcome these problems, an alternative segmentation strategy is proposed that enables the semi-automated adaption of relevant parameters for image segmentation. Therefore, the Superpixel Contour (SPc) algorithm (Mester et al., 2011) is introduced in context of remote sensing. Furthermore, the region-based SPc segmentation technique is combined with the Random Forest classifier (Breiman, 2001). Random Forest (RF) is a supervised classifier and has demonstrated excellent performance in terms of classifying diverse remote sensing data sets (Gislason et al., 2006; Waske & van der Linden, 2008; Waske & Braun, 2009; Stumpf & Kerle, 2011; Palsson et al., 2012; Duro et al., 2012a). Moreover, Duro et al. (2012a) used RF for a multiscale object-based image analysis and feature selection. They generated a large set of features based on four segmentation scales and five different object-feature types. Finally, RF was used to select only the "relevant" features concerning the overall classification. In general, RF performs well with small training sample sets and often outperforms other methods in terms of accuracy and computation time (Waske & Braun, 2009). Moreover, the method offers a cross-validation-like accuracy measure, which will be used for the parameter selection of the segmentation algorithm. Overall, this study demonstrates that the proposed concept minimizes manual input for the segmentation procedure in conclusion with an efficient classification method.

In order to evaluate the potential of the proposed concept, we focus on three main research questions:

1. Is object-based classification capable to significantly increase classification accuracy compared to a pixel-based approach?

2. Can the Superpixel Contour algorithm perform similar like the widely-used segmentation method eCognition's multiresolution segmentation?

3. Is the proposed strategy able to enhance and economize the optimization of segmentation parameters?

2 Methods

2.1 Superpixel Contour

A wide-range of segmentation algorithms, which are based on different partitioning techniques: 1) pixel-based; 2) edge-based; 3) region-based; and 4) combined, have been introduced (Blaschke, 2010). The Superpixel Contour algorithm (Mester et al., 2011) is an iterative, region-based segmentation procedure based on a stochastic model capable to separate images into homogenous regions, i.e., segments or superpixels. These regions are created by the aggregation of neighboring pixels, following certain criteria like homogeneity of pixel values or shape of the segments. A detailed description on the general concept of the SPc algorithm is given by Mester et al. (2011). A brief summary is given below.

The principle of the SPc algorithm is to optimize a non-specified initial segmentation along its boundaries. This so-called contour relaxation is based on the statistical distribution of each region. The distributions of two neighboring regions are derived for the case that a contour pixel belongs to one region or to the other. The pixel is assigned to the region that maximizes the posterior distribution. The idea behind this is a maximum-a-posteriori (MAP) segmentation running iteratively until the optimal segmentation is found.

The fast and efficient processing is enabled by the principle of the SPc algorithm to consider only the pixels at the boundary of each region. Therefore, the image is scanned several times with a systematically varying pixel visiting scheme. In every pass through the image, to minimize the bias of the results, pixels are visited from all four possible directions: 1) left-right, up-down; 2) left-right, down-up; 3) right-left, up-down; and 4) right-left, down-up.

SPc is based on the assumption that the considered image is separable into meaningful regions and the probability measure can be derived, e.g., the statistical distribution must be known. Let x be the vector of measurements (e.g., spectral values of a remotely sensed imagery). The first step of the segmentation framework is the generation of an initial segmentation $Q_0 = \{R_1, R_2, \ldots, R_n\}$ with the maximum number of superpixels n. We propose an initial grid with equal distances defined by parameter G (in pixel) as a presegmentation. Each region R_i receives a parameter vector $\Theta_i = \Theta(R_i)$, which comprises the stochastic component.

The next step is the contour relaxation based on the prior distribution $p(Q)$ and the likelihood function $p(x \mid Q)$ of x given Q. For an efficiently generation of optimized segments, the SPc considers systematically the contour pixels and only the direct neighborhood of grid pixels x_0 is taken into account. The current region label $q(x_0)$ depends on the potential of the 8 cliques that include pixel x_0. Clique potentials are defined as pairs of neighboring pixels and depend on whether the label values are identical or not. The probability for a

label change at the contour of a region is

$$p(Q) = k_1 \cdot \exp\left(-n'_B B - n'_C C\right) \tag{II-1}$$

with the constant k_1. B and C are the cost factors for inhomogeneous paraxial (horizontal/vertical) and diagonal cliques, respectively. Depending on a change of $q(x_0)$, the numbers of inhomogeneous cliques are expressed by n'_B and n'_C.

The conditional likelihood function of the image x given the partition Q is obtained by

$$p(x \mid Q) = k_2 \cdot \prod_{\{R_j\}} p(x(R_j) \mid \Theta(R_j)). \tag{II-2}$$

This equation consists of a constant k_2 and a variable term depending on $q(x_0)$. The model parameter Θ are determined by a maximum-likelihood estimation (MLE).

Every contour pixel x_0 obtains the specific label that maximizes

$$p(x, Q) = k_1 \cdot k_2 \cdot \exp\left(-n'_B B - n'_C C\right) \cdot \prod_{\{R_j\}} p(x(R_j) \mid \Theta(R_j)) \tag{II-3}$$

based on equation II-1 and II-2. Due to practical applicability, the negative logarithm (energy function) of equation II-3 is minimized.

In this study the maximum likelihood estimation is computed under a given Gaussian distribution. However, the SPc allows the use of different probability density functions (pdf), depending on the distribution of input data.

Overall, SPc has four parameters: B and C are the cost factors for inhomogeneous cliques, G is the initial grid size and *max_iter* is the maximum number of iterations. However, the presented algorithm is simple to handle because only 2 out of these 4 parameters have to be adapted to each application. We propose to set the clique costs B between 0 and 1 and $C = B/\sqrt{2}$. The cost factor B controls the shape of the segments, i.e., a large cost factor leads to more block-like segments. The user can control the segment size by varying the initial grid size G (scale factor). Preliminarily results suggest 10 as the maximum number of iterations, since no further significant changes in segment quality and subsequently classification accuracy could be observed.

2.2 Random Forest

In the presented study, the Random Forest classifier, an ensemble of classification trees, is used. A detailed description on the general concept of the RF is introduced by (Breiman, 2001). An overview in the context of remote sensing is given by (Gislason et al., 2006; Waske & Braun, 2009). A brief summary of the RF algorithm is given below.

The principle of the RF is to build a set of k randomly generated decision trees, which are independent from each other. During the tree building process, m features (i.e., bands) are randomly chosen at each split rule, with $m < D$ and D as the number of bands. Moreover,

each tree within the ensemble is constructed using a randomly generated subset from the original training data by sampling with replacement. Because the selection is done with replacement, some training samples can be selected several times for a specific training set, whereas other samples are not considered in this particular sample set. A majority vote over the results of the different trees is used to generate the final classification result. While for every tree different, randomly selected training samples are used, the remaining samples are not considered for the training of this particular tree. These remaining sample subsets are called "out-of-bag" (OOB) and can be used for an unbiased estimation of the classification error (Breiman, 2001).

Random Forest is a classification algorithm with a number of advantages. Due to its underlying principle, the RF is robust against outlier and overfitting (Breiman, 2001). Furthermore, the RF is easy to handle, because it relies on only two user-defined parameters, i.e., k and m, which are reactively insensitive in terms of the classification result. Thus, default values or recommendations for the two parameters can be provided. The default settings for the number of trees k is 500. However, parameter k can easily be adapted during the classifier training by using the OOB error rate. The number of randomly selected variables m is usually set to the square root of the number of input features (Breiman, 2001; Gislason et al., 2006). Due to limiting the number of variables at each internal node of a tree, the computational complexity of the classifier is simplified. As a result the RF is adequate for handling high-dimensional data sets, even with a small number of training samples.

2.3 Optimization of segmentation parameters

The proposed approach semi-automatically optimizes segmentation parameters by minimizing the unbiased OOB error of all trees of the Random Forest. Therefore, SPc systematically generates a set of segments with different combinations of parameters. The set of parameters G and B is generated in a user-defined range and the best combination for G and B is selected based on the OOB error. Finally, the segmentation with the best parameter set is used for generating the final land cover map. By using the internal unbiased accuracy assessment of the RF, the parameters for the segmentation can be determined without providing additional independent test data. This method is comparable to a cross-validation, for example for estimating the error rate of a prediction rule (Efron & Gong, 1983) or the selection of kernel parameters in context of a classification by Support Vector Machines.

The criterion to assess the segmentation quality is the overall classification accuracy, using the OOB error. This means that the proposed method does not necessarily produce the "best" visual segmentation result, however, it produces the optimal segmentation result regarding the classification accuracy. Furthermore, it is possible to optimize the parameter selection for only one or a few classes by weighting the class-specific OOB error rates. The experiments were performed with an in-house SPc implementation and a freely available RF code (Jaiantilal, 2009). Both algorithms are combined in a single work flow in MATLAB.

3 Study area and data

Two multitemporal data sets from different study sites were used in this study. The first study site lies in Luxembourg (*Lux*) and covers approximately 360 km^2 (Figure II-1A). The rural study area is characterized by agricultural land use, forests and urban regions, with grassland, corn and winter wheat being the main agricultural classes. The classification aims on identifying the following 8 agricultural land cover classes: *grassland*, *potatoes*, *corn*, *spring barley*, *winter barley*, *winter rape*, *winter triticale* and *winter wheat*. A multitemporal RapidEye data set containing three images, acquired on May 02, June 27 and September 25, 2011, is available. The RapidEye images have a spatial resolution of 5 meters and consist of 5 spectral bands: blue (440–510 nm), green (520–590 nm), red (630–685 nm), red-edge (690–730 nm) and near-infrared (760–850 nm). The data was ordered in level 3A format and thus has already been radiometric and geometric corrected.

The second study site is located near Bonn in Germany (*Ger*) and covers approximately 144 km^2 (Figure II-1C). The almost flat study site is dominated by agricultural use, with cereals and sugar beets as main crops. The following 8 land cover classes are investigated in the second study area: *grassland*, *orchards*, *cereals*, *corn*, *rape*, *root crops*, *forest* and *urban*. The data set consists of two SPOT 5 images, acquired on June 24 and July 17, 2006. The SPOT 5 images have a spatial resolution of 10 meters and consists of 4 spectral bands: green (500–590 nm), red (610–680 nm), near-infrared (780–890 nm) and mid-infrared (1580–1750 nm).

For both study areas, detailed land cover information is available on field plot basis for classifier training and validation of the results. The reference data was randomly separated (each 50% for training and testing) on field plot level to generate independent and spatially disjoined training and test data. Consequently, training and test samples are not included in the same field plot.

4 Experimental Results

Several land cover maps were generated, using different combinations of the multitemporal data sets and two segmentation techniques: SPc and multiresolution technique (MRS) in eCognition. In this study, the derived segments' mean values were used in addition to the pixel-based values. Therefore, a feature vector in the object based classification contains the pixel values of each band as well as the segments' mean values of each band. Consequently, the pixel-based approach of two images (e.g., June+July with each 5 dimensions) uses a 10-d feature vector, while the joint object-based classification is based on a 20-d feature vector. Although the pixel-object combination led to a relative large feature vector, Random Forests are capable to cope with large data sets and experimental results showed that, overall, the combined pixel-object classification improved the accuracy compared to object-based classification. Moreover, these results were compared to a standard pixel-based classification.

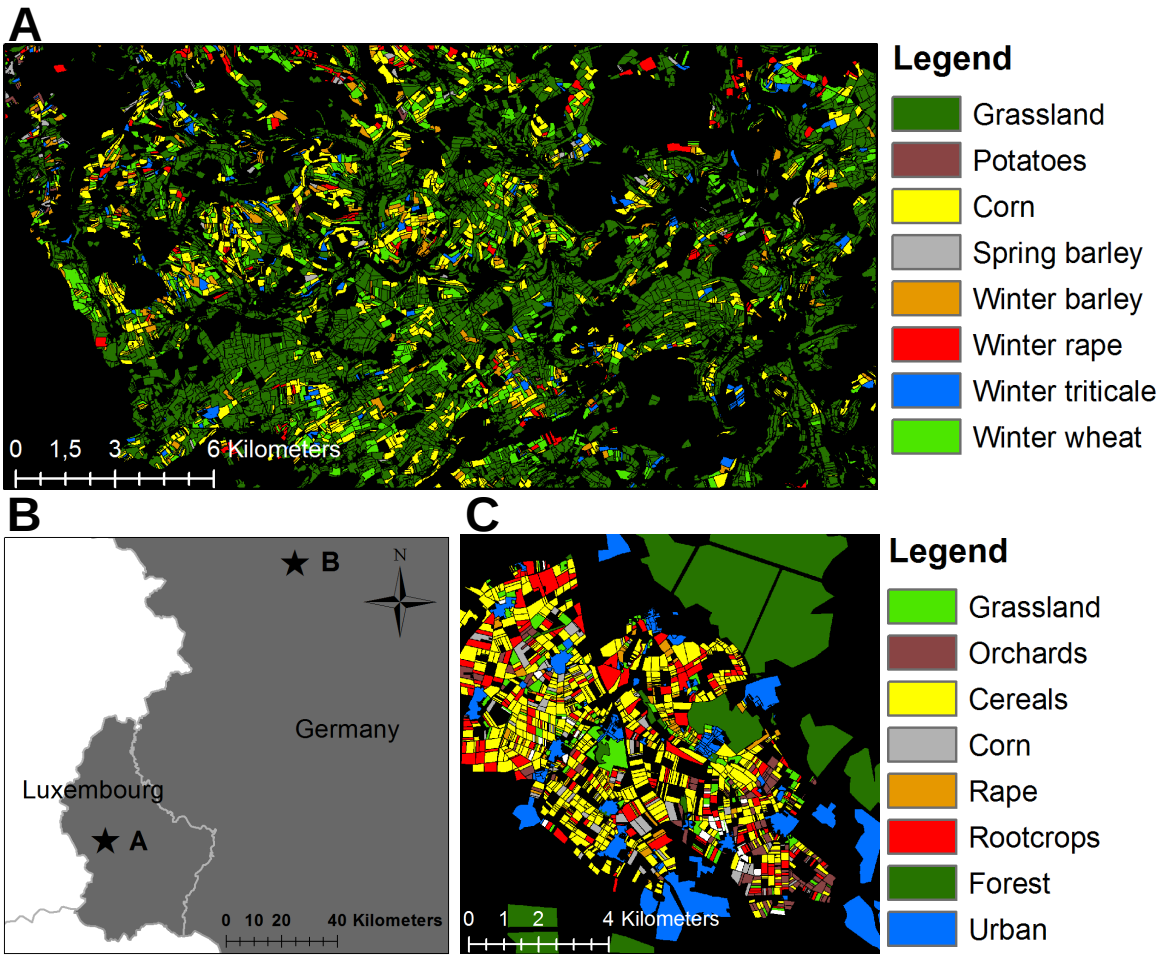

Figure II-1: A: Reference data in Luxembourg (*Lux*); B: Study areas located in Luxembourg and Germany, Europe; C: Reference data in Germany (*Ger*).

Accuracy assessments were performed using confusion matrices on pixel-basis in order to derivate the overall, producer's and user's accuracies. Furthermore, statistical-based comparison was assessed to determine the statistical difference between the different classification results (i.e., pixel-based, SPc, and MRS), using a McNemar test with a 95% confidence interval (Foody, 2004). For generating the final training sample set, an equalized random sampling was performed, selecting 500 training samples per class.

4.1 Optimization of segmentation parameters

The semi-automatic process of selecting the ideal segmentation parameters for the SPc algorithm combined with the quality assessment by Random Forest's OOB error is demonstrated in this section. In the initial phase the parameter B is set to 1, while G is tested in a range between 1 and 50. Figure II-2 shows the OOB error and the test error rate achieved on the joint classification of the multitemporal data, using different values for G. For both study areas, both error rates have the highest values at $G = 1$ and asymptotically decrease with an

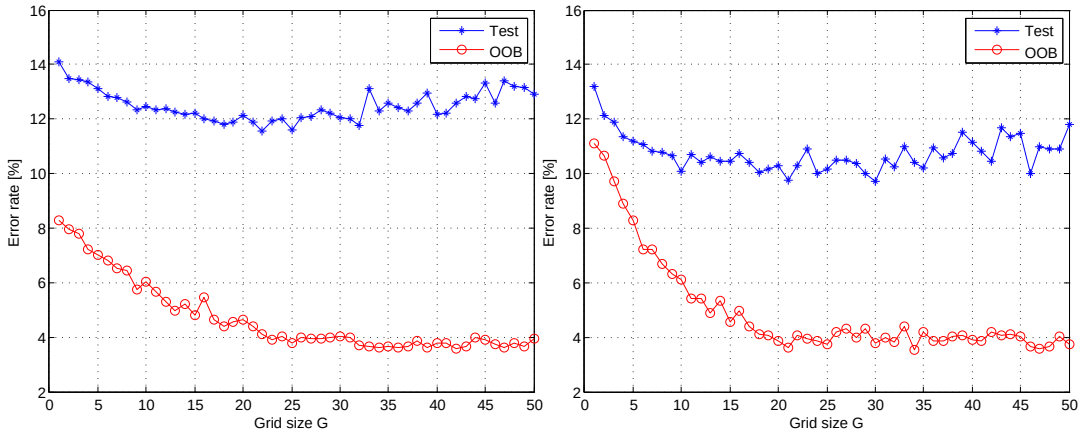

Figure II-2: Comparison of the classification error using test data (stars) and OOB data (circles) with different segmentation grid sizes G; Left: Based on the Luxembourg data set (joint classification of May + June + Sep.); Right: Based on the German data set (joint classification of June + July).

increasing value for G. The minimum error, i.e., highest overall accuracy, is achieved with $G = 25$ for the Luxembourg data set and $G = 21$ for the German data set. Using a G value above 25 or 21 for *Lux* or *Ger*, respectively, the test error rate increases again, while the OOB rate approximately remains on the same level.

Behind these facts, the parameter G is ideally set to the smallest potential value with regard to the OOB error (i.e., *Lux*: $G = 25$, *Ger*: $G = 21$). While the OOB error rate steadily decreases up to $G = 25$ for *Lux* or $G = 21$ for *Ger*, no appreciable changes/improvements can be observed for values above. Therefore, for example, values $G = 32 - 38$ for *Lux* and $G = 34$ for *Ger* are not recommended for use (Figure II-2).

The results also confirm the general findings in terms of object-based image analysis (Bruzzone & Carlin, 2006). While an under-segmentation (i.e., high G parameter) can result in misclassifications, because an image segment can include more than one object, the positive impact of image segmentation is limited by an over-segmentation (i.e., small G parameter).

Some applications focus on the classification of specific classes (van der Linden et al., 2007; Walker et al., 2010). Therefore, class specific OOB error rates are used to determine the optimal segmentation parameters. Figure II-3 illustrates the F-measure (Baeza-Yates & Ribeiro-Neto, 1999) of *winter wheat* and *corn* based on OOB and test data for *Lux* and *Ger*, respectively. The pixel-based classification accuracy of *corn*, for example, is significantly improved by object-based analysis under the assumption of using the optimal value of G, since the F-measure of the test set is decreased from about 34% ($G = 1$) to less than 23% ($G = 21$) for *Ger*. Although the ideal class-specific segmentation parameters are identical with the respective global optimum, the results confirm the use of OOB error rates to determine adequate segmentation parameters for individual classes, since the OOB error behaves similar compared to the independent test error.

The determination of parameter B is executed with different values of G. Figure II-4 depicts the OOB error for evaluating B from 0 to 1 with different grid sizes G. The results demonstrate that parameter B is not very sensitive with regard to the classification results (e.g., *Lux*: error rate of $G = 25$ between 3.7% and 4.2%), however, SPc tends to provide better results with a B close to 1 (e.g., *Ger*: error rate of $G = 21$ from 4.8% with $B = 0$ to 4.1% with $B = 1$). Therefore, the parameter B is set to 1 during this study.

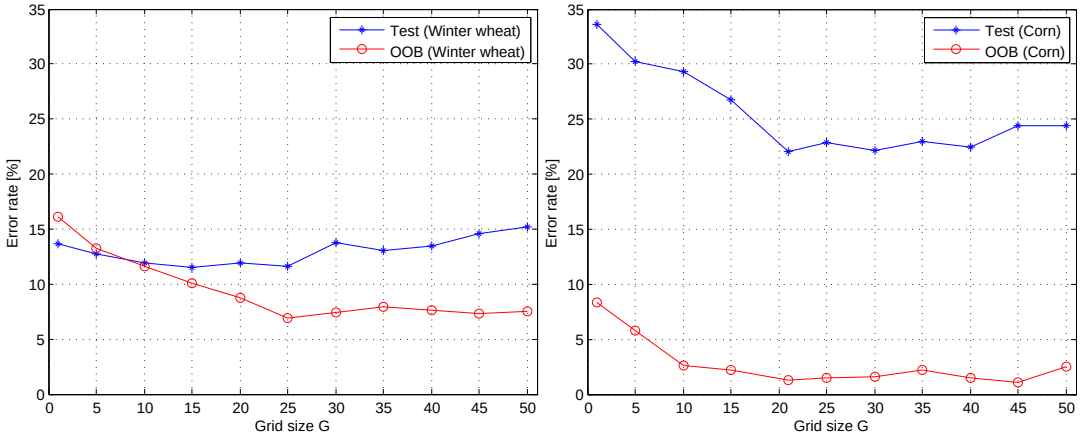

Figure II-3: Comparison of class specific classification errors (F-measure) using test data and OOB data with different segmentation grid sizes G; Left: Based on the Luxembourg data set (joint classification of May + June + Sep.); Right: Based on the German data set (joint classification of June + July).

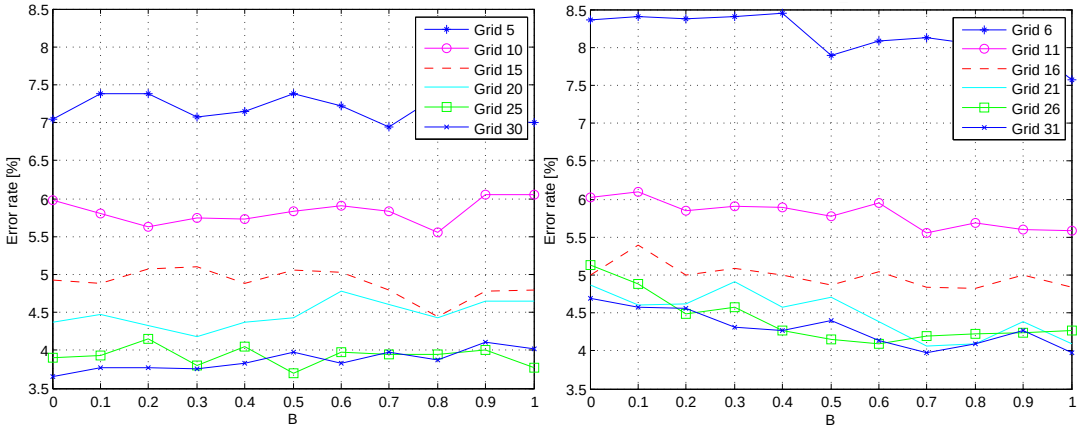

Figure II-4: Determination of Superpixel Contour parameter B with different values of G based on the OOB error rate; Left: Based on the Luxembourg data set (joint classification of May + June + Sep.); Right: Based on the German data set (joint classification of June + July).

4.2 Superpixel segmentation

Various classifications were performed, using different input images and following the method described above, i.e., the parameters for the Superpixel Contour algorithm were semi-automatically optimized.

The classification accuracies for different pixel-based and object-based classifications of the Luxembourg data set are shown in Table II-1. The results demonstrate the positive impact of image segmentation in terms of accuracy, independently of the input images and the land cover classes.

Table II-1: Accuracy assessment for *Lux*: Comparison of pixel-based and SPc classification, with different input data sets (Pb = pixel-based, PA = producer's accuracy, UA = user's accuracy)

Land cover	**Pb (Jun)**		**SPc (Jun)**		**Pb (Jun+Sep)**		**SPc (Jun+Sep)**	
	PA [%]	UA [%]	PA [%]	UA [%]	PA [%]	UA [%]	PA [%]	UA [%]
Grassland	80.4	89.0	88.2	88.0	88.8	92.6	91.4	92.5
Potatoes	48.7	13.7	41.8	37.5	53.6	20.6	50.4	53.5
Corn	53.1	81.6	62.8	80.1	86.7	91.9	89.3	91.3
Spring barley	39.9	10.9	38.1	20.4	38.2	16.2	30.2	23.7
Winter barley	84.3	62.4	85.2	64.7	83.8	68.4	85.0	68.2
Winter rape	88.2	61.0	84.4	71.6	88.6	76.1	88.1	79.2
Winter triticale	54.2	27.9	51.2	31.5	53.1	33.5	49.8	36.3
Winter wheat	63.2	82.2	72.7	84.3	64.1	88.4	73.4	88.6
Overall accuracy	67.2%		73.7%		78.2%		81.6%	
Kappa	0.60		0.67		0.73		0.77	

The use of SPc increases the overall accuracy and kappa statistics for June from 67.2% and 0.60 to 73.7% and 0.67, respectively. Particularly user's accuracies are significantly increased and thus more balanced producer's and user's accuracies are achieved. The producer's accuracies of *grassland*, *corn* and *winter wheat* are improved by approximately 9% by SPc. Furthermore, the user's accuracies of *potatoes* and *winter rape* are increased by more than 10% based on June + SPc.

The object-based classification of June + September shows overall improvements for all classes, when compared to the accuracies achieved on pixel-level. The overall accuracy and kappa statistics increase from 78.2% and 0.73 to 81.6% and 0.77, respectively. Particularly *potatoes*, which are difficult to classify on pixel-level, are more accurately classified due to image segmentation. Similar results were found for other single-month and two-month classifications.

Table II-2 shows the pixel-based and object-based classification results of the second data set. These results confirm the positive impact of image segmentation to improve classification accuracies, since nearly all producer's and user's accuracies are increased. The overall accuracy from June to SPc (June) is improved by 5.4% and the overall accuracy from July to SPc (July) is increased from 77.5% to 84.6% by about 7.1%.

The results achieved with the whole multitemporal data sets, i.e., the joint classification of

Table II-2: Accuracy assessment for *Ger*: Comparison of pixel-based and SPc classification, with different input data sets (Pb = pixel-based, PA = producer's accuracy, UA = user's accuracy)

Land cover	**Pb (Jun)**		**SPc (Jun)**		**Pb (Jul)**		**SPc (Jul)**	
	PA [%]	UA [%]	PA [%]	UA [%]	PA [%]	UA [%]	PA [%]	UA [%]
Grassland	40.9	32.1	48.2	36.8	59.1	35.4	59.1	42.6
Orchards	51.4	37.5	61.3	45.0	65.2	34.4	60.0	45.1
Cereals	76.7	93.2	83.7	93.2	66.0	90.6	77.4	90.0
Corn	49.9	27.4	49.4	43.3	64.1	36.4	66.6	54.5
Rape	81.8	39.1	79.7	67.0	64.3	21.3	47.0	27.7
Root crops	78.6	77.5	79.3	77.8	84.1	84.5	90.1	84.8
Forest	93.5	96.8	97.0	98.0	87.5	97.6	94.1	98.6
Urban	81.8	86.6	92.6	95.4	79.8	82.4	89.7	89.3
Overall accuracy	80.7%		86.1%		77.5%		84.6%	
Kappa	0.75		0.82		0.72		0.80	

all acquisitions, clearly demonstrates the benefit of multitemporal information for land cover mapping (Table II-3). The pixel-based overall classification accuracies of the Luxembourg and German data sets can be increased with the three-month and two-month data sets in comparison to the one-month data. However, the accuracies achieved on pixel-level are already very high (*Lux*: OA: 86.4%; *Ger*: OA: 87.5%). Therefore, the classification accuracy improvement due to image segmentation is lower when compared to the results achieved on monotemporal data sets.

Moreover, the McNemar tests showed statistically significant differences between the pixel- and object-based classifications ($z = 3.09 > 1.96$ for *Lux* and $z = 4.24 > 1.96$ for *Ger*).

Table II-3: Classification accuracy of the joint multitemporal data set *Lux* (June + May + Sep.) and *Ger* (June + July)

Data set	**Pixel-based**	**SPc**
Lux	86.4%	88.5%
Ger	87.5%	90.6%

4.3 Superpixel in comparison to MRS

To assess the general performance of the SPc algorithm, results were compared to an object-based classification, using eCognition's multiresolution segmentation algorithm for image segmentation. Various parameter settings were manually tested to get the optimal segmentation result for the latter approach, while the SPc parameters were optimized by the proposed approach. Table II-4 and Table II-5 show the defined image segmentation parameters and the number of the corresponding segments.

The initial grid size G of SPc is comparable to the *scale* level of MRS. They define the relative size of the segments and mainly the total number of segments. For agricultural land cover mapping homogeneously and thus more block-like objects are advantageous,

Table II-4: Segmentation parameters and number of segments for *Lux*

Parameters	**SPc**	**MRS**	**Parameters**
G	25	102	*scale*
B	1	0.8	*shape*
		0.5	*compactness*
# segments	22,895	22,828	

Table II-5: Segmentation parameters and number of segments for *Ger*

Parameters	**SPc**	**MRS**	**Parameters**
G	21	20	*scale*
B	1	0.8	*shape*
		0.5	*compactness*
# segments	3363	3341	

because they better represent typical spatial patterns of a rural study site. Consequently, high values for the parameters B and *shape* were used to generate blocky objects. The third multiresolution segmentation parameter is *compactness*, which has been kept at the default value of 0.5. Both segmentation algorithms generated almost the same number of segments for *Lux* with 22,895 and 22,828 and for *Ger* with 3363 and 3341 for SPc and MRS, respectively.

Different segmentation results for the Luxembourg data set are depicted in Figure II-5 (A-F). A visual assessment of the segmentation results demonstrates that Superpixel Contour and multiresolution segmentation produce similar results. The segments, generated with ideal parameters (Figure II-5B and E) are well adapted to the field plot boundaries and show a good separation of the different types of fields. To avoid highly fractal objects $B = 1$ for SPc and $shape = 0.8$ for MRS prove to be suitable. Lower scale levels yield in a high over-segmentation, where fields are mostly represented by several segments (Figure II-5A and D). On the other hand, high scale levels lead to an under-segmentation (Figure II-5C and F).

Similar segmentation results are achieved for the German data set shown in Figure II-5 (G-L). As for the other study site, the proposed strategy results in adequate segments that are well adapted to the natural objects in the very most cases (Figure II-5H). However, some segment boundaries are not perfectly matched with regard to the June scene. Although, many different parameter values were tested for the MRS, no better segmentation result was achieved by the multiresolution segmentation (Figure II-5K). Both segmentation algorithms have some missing boundaries regarding the June scene (Figure II-5H and K), however, in contrast to the SPc segmentation, MRS has difficulties to detect the correct boundary between two fields whereby the spectral differences are very apparent in most cases.

The detailed accuracy assessment of the three classification approaches for *Lux* is shown in Table II-6. Both segmentation methods improve the producer's and user's accuracies in the most cases. *Potatoes* have the highest increase of the user's accuracy from 48.4%

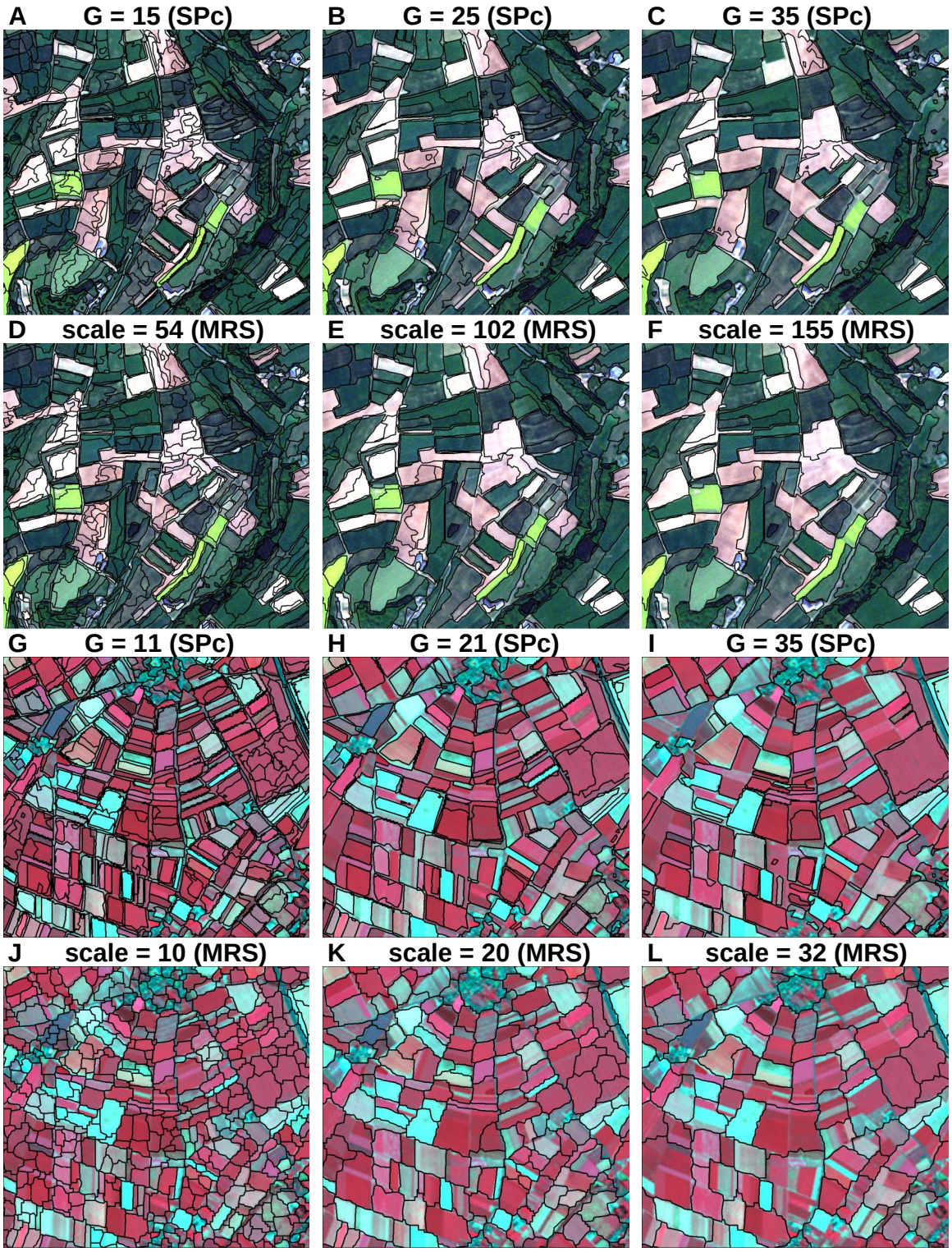

Figure II-5: Segmentation comparison of Superpixel Contour and eCognition's Multiresolution Segmentation of *Lux* (RGB: May) and *Ger* (nIR-R-G: June). SPc (*Lux*): A,B,C with grid size $G = 15, 25, 35$. MRS (*Lux*): D,E,F with $scale = 54, 102, 155$; SPc (*Ger*): G,H,I with grid size $G = 11, 21, 31$. MRS (*Ger*): J,K,L with $scale = 10, 20, 32$.

(pixel-based) to 78.8% and 79.7% (SPc and MRS, respectively), whereas the producer's accuracy is decreasing by about 10%. *Spring barley* has a similar behavior compared to *potatoes*. The producer's accuracy of *winter wheat* is increased by approximately 5% – 6%, when comparing pixel-based and object-based classification results.

Table II-6: Accuracy assessment of three classification approaches based on the Luxembourg data set: joint classification of May, June and September (PA = producer's accuracy, UA = user's accuracy)

Land cover	**Pixel-based**		**SPc**		**MRS**	
	PA [%]	UA [%]	PA [%]	UA [%]	PA [%]	UA [%]
Grassland	94.3	95.3	96.1	94.1	96.3	94.5
Potatoes	67.9	48.4	54.8	78.8	57.9	79.7
Corn	92.1	94.3	94.1	93.6	94.0	93.7
Spring barley	70.7	44.2	61.9	63.7	59.5	57.8
Winter barley	85.1	71.5	86.1	72.7	85.7	72.3
Winter rape	97.0	95.1	97.0	95.1	97.0	95.5
Winter triticale	64.1	46.1	60.5	54.6	63.2	53.9
Winter wheat	77.5	93.6	83.2	92.9	82.4	93.6
Overall accuracy	86.4%		88.5%		88.5%	
Kappa	0.83		0.85		0.85	

Table II-7 shows the detailed accuracy assessment of the three classification approaches for *Ger*. Most producer's and user's accuracies are improved by the SPc and MRS segmentation approaches. The highest increase of the producer's accuracy can be observed for *urban* land cover from 87.1% to 93.8% and 92.9% for SPc and MRS, respectively. The pixel-based producer's accuracy of *corn* can be improved from 71.1% to 76.2% for SPc, whereas the producer's accuracy decreases to 70.1% for MRS. The user's accuracy of *corn* can be increased by about 15% from 63.5% to 78.4% and 79.0% for SPc and MRS, respectively. In general, the findings from the other study area are underlined, as the image segmentation improves most classification accuracies.

Furthermore, the McNemar tests showed no statistically significant differences between the classification results provided by SPc and MRS ($z = 0.19 < 1.96$ for *Lux* and $z = 1.20 < 1.96$ for *Ger*).

Classification maps of the three classification approaches of *Lux* are depicted in Figure II-6. In general, the pixel-based classification (Figure II-6B) shows a good classification of most agricultural field plots. Nevertheless, some noise and misclassifications are inherent and a few borders between individual agricultural field plots appear slightly blurred. *Grassland* and *corn* is classified clearly by all three approaches, which is supported by the accuracy assessment in Table II-6. *Potatoes* and *winter wheat* have the largest uncertainties in the pixel-based classification, which is improved by SPc (Figure II-6C) and MRS (Figure II-6D). For example, the large *winter triticale* field in the lower left corner has an error of commission, as some parts of the field are classified as *winter wheat*.

Figure II-7 shows the land cover maps of the three classification approaches of the second data set. Overall, the pixel-based approach generates a visually correct map. However,

Table II-7: Accuracy assessment of three classification approaches based on the Germany data set: joint classification of June and July (PA = producer's accuracy, UA = user's accuracy)

Land cover	**Pixel-based**		**SPc**		**MRS**	
	PA [%]	UA [%]	PA [%]	UA [%]	PA [%]	UA [%]
Grassland	63.1	48.6	64.7	49.3	64.9	46.6
Orchards	75.6	47.3	74.5	58.1	73.2	58.9
Cereals	85.1	94.7	88.2	94.4	86.0	93.5
Corn	71.1	63.5	76.2	78.4	70.1	79.0
Rape	81.3	69.5	79.6	75.6	78.7	64.3
Root crops	88.4	84.7	89.4	87.0	89.3	84.5
Forest	94.6	98.1	97.3	98.8	97.9	99.0
Urban	87.1	90.8	93.8	96.1	92.9	96.9
Overall accuracy	87.5%		90.6%		89.8%	
Kappa	0.84		0.88		0.87	

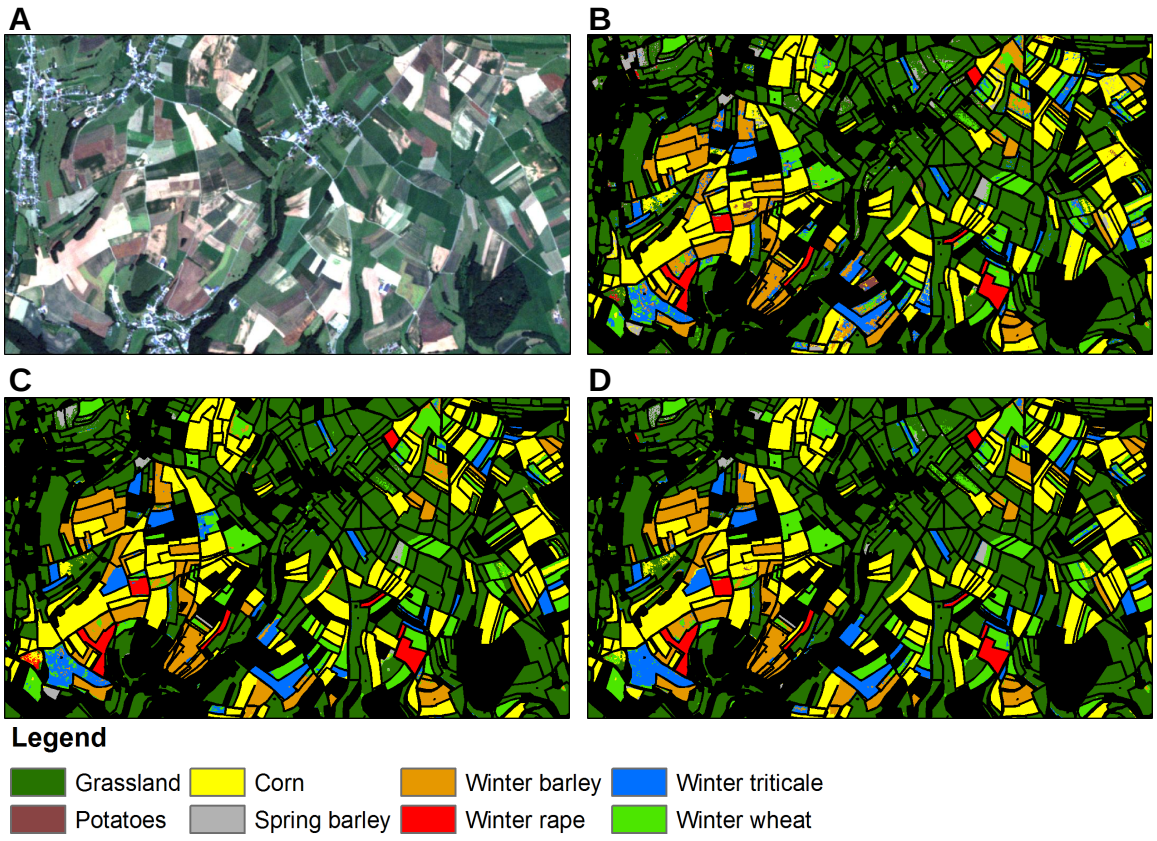

Figure II-6: *Lux* study site: A: RapidEye (RGB: June); B: Pixel-based classification; C: SPc classification; D: MRS classification; (black: area of no reference).

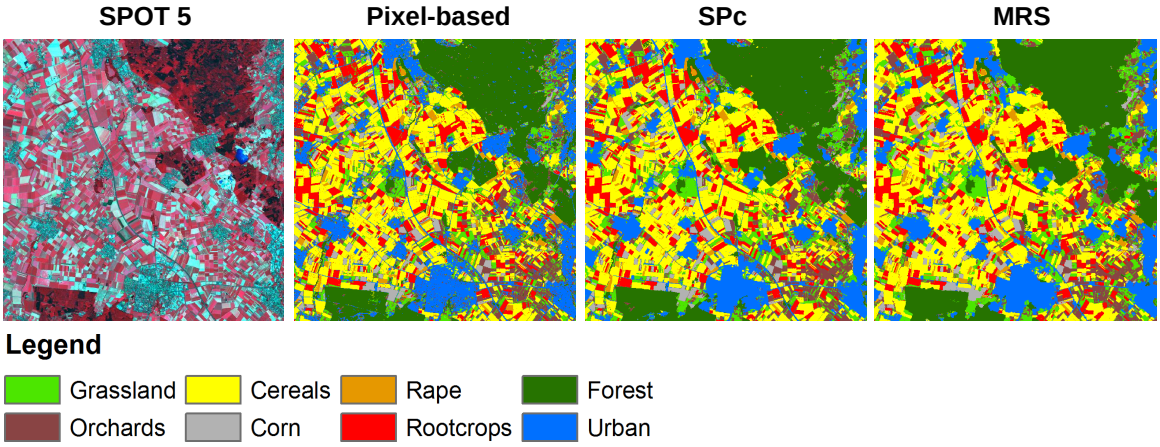

Figure II-7: *Ger* study site: SPOT 5 scene (June 24, 2006; nIR-R-G); Pixel-based, SPc and MRS based classification maps.

in comparison to the SPc and MRS based land cover map, the pixel-based result is more noisy and some misclassifications can be observed. Only a few differences occur, when comparing the two maps achieved by SPc and MRS. Thus, the visual comparison confirms the independent accuracy assessment.

5 Discussion

5.1 Impact of image segmentation

The use of image segmentation proves useful to improve the accuracy of land cover mapping. Irrespective of the segmentation algorithm, the object-based classifications outperform the classifications on pixel-level in terms of overall, producer's and user's accuracies. Moreover, the class accuracies (producer's and user's accuracies) are usually more balanced. However, the generation of adequate image segments is critical. An inadequate value for the SPc parameter G decreases the positive impact of image segmentation on the classification accuracy. Thus, the results are in accordance with previous studies (Song et al., 2005; Waske & van der Linden, 2008). Even though only one segmentation level is generated, the resulting segments are adequate for the different land cover classes in the very most cases. Nevertheless, the methods can be easily adapted for a multi-level classification approach (Waske & van der Linden, 2008; Bruzzone & Carlin, 2006), e.g., by generating class-specific segmentation levels.

As in other studies (Song et al., 2005; Shackelford & Davis, 2003; Aguirre-Gutiérrez et al., 2012), the segments' mean values were derived and added as additional feature for the subsequent classification. However, other object information, such as texture, shape and neighborhood relations can be extracted. Behind these facts, the use of RF is particularly useful because the method is well suited for high dimensional feature spaces. Moreover, the method is non-parametric and can even handle categorical variables.

It is worth to underline that in particular the single-date classifications are significantly improved by image segmentation. In some cases, similar accuracies are achieved when compared to the accuracies achieved by multitemporal data sets. Although the accuracy of a multitemporal classification is increased by object-based analysis, the positive effect is lower, when compared to the single-date classifications. Nevertheless, adequate temporal information is still required for an accurate classification result and cannot be fully replaced by image segmentation alone. This might be one reason for the relatively low classification accuracy of spring barley in *Lux*, using the June and September image.

Both segmentation algorithms, SPc and MRS, perform similar in terms of visual examination (Figure II-5) and classification accuracy (Table II-6 and II-7). Beside the increase of the producer's accuracies of most classes, segmentation supports the correctness of the generated land cover maps, i.e., the user's accuracies are improved in comparison to the pixel-based approach. Particularly the user's accuracies for classes like *potatoes*, *spring barley* and *winter triticale*, which are difficult to map on pixel-level, are increased. Moreover, the producer's and user's accuracies are more balanced. However, some producer's and user's accuracies are still relatively low. Reasons for this could be the environmental setting of the study site and the spectral characteristics of land cover classes. Orchards, for example, usually consists of individual trees on grassland. Hence the class *orchards* can appear as mixture between *forest* and *grassland*. The study sites are characterized by typical high-frequent land cover changes between individual plots. Moreover, some agricultural field plots are relatively small. Thus, the classification accuracy can be decreased (Smith et al., 2002, 2003).

5.2 Optimization of segmentation parameters

As stated in the introduction and it is reported in several studies, object-based image analysis requires manual input to determine adequate parameters for image segmentation (Myint et al., 2011; Duro et al., 2012b). The optimal parameters are usually determined by visual interpretation and/or "trial-and-error" and therefore, the parameter selection is often time-consuming as well as user-dependent. However, independently from the segmentation algorithm the positive impact of segmentation on the classification accuracy is decreased by suboptimal parameter settings.

The proposed semi-automatic parameter selection for the SPc algorithm is based on minimizing the classification error, indicated by the OOB error estimation. The OOB error estimation is a cross-validated accuracy estimation, since for the kth tree the respective out-of-bag samples were not used for classifier training. Thus, the quality of image segmentation can be assessed in terms of the map accuracy, without providing additional test data. Results of both study areas prove that the OOB error is appropriate for the parameter selection. While most applications aim on the generation of an optimal overall accuracy, the accuracy of individual single land cover classes can be optimized by class-specific OOB error rates.

Furthermore, the utilization of the RF to optimize and evaluate the segmentation parameters proves useful regarding the computational time. Whether a small or large training set

is used, the time for generating the classification model with the RF is relatively fast.

Although a more detailed grid-search is possible, intervals of $G = 5$ seems adequate for the parameter optimization method (Figure II-3). The classification results are relatively insensitive to the SPc parameter B in terms of the accuracy. Thus, it is recommended to test parameter B for the best three grid sizes G.

6 Conclusions

Object-based image analysis is frequently used to optimize the accuracy of various land cover maps. However, accurate image segmentation is a prerequisite to generate an adequate classification result.

In the presented study, an object-based classification strategy was presented that enables the semi-automatic determination of optimal segmentation parameters in terms of the classification accuracy. The approach is based on the Random Forest and the Superpixel Contour algorithm, which is newly introduced in context of remote sensing. Segmentation parameters are systematically tested in a user-defined range and the quality of the image segmentation is evaluated by the OOB error provided by the RF. Consequently, no additional test set is required for the parameter selection. Furthermore, the good classification results for separating agricultural classes, which are often difficult to map by monotemporal data sets, underline the benefit of multitemporal analyses.

Three research questions were stated in the beginning regarding: 1) the impact of the object-based classification compared to pixel-based classification; 2) the performance of the SPc algorithm; and 3) the parameter optimization in terms of the classification accuracy. Experimental results show that image segmentation can significantly increase the accuracy of land cover maps, which is in accordance to previous studies. Furthermore, the Superpixel Contour algorithm provides very similar results in comparison to the well established and widely-used multiresolution segmentation in eCognition. The SPc algorithm is simple to handle, because it mainly depends on two parameters and provides accurate segmentation maps. The proposed approach, the use of the OOB error rate for parameter determination proves useful and results in optimized image segmentation in terms of classification accuracy. Therefore, the manual and subjective parameter selection, which is usually required in object-based image analysis, is economized and optimized. Another benefit of the proposed parameter optimization is the scale-invariance, as the optimal parameters are determined only with respect to the classification accuracy. Besides the functional OOB error, the use of RF seems particularly interesting with their simple handling and fast training times. In addition, RF is well suited for the classification of different remote sensing data sets, even with a small number of training samples. Overall, the proposed concept, the combination of SPc and RF with a semi-automatic parameter selection, constitutes a feasible approach and a useful modification of regular object-based image analysis.

Acknowledgments

This work was supported by the German Research Foundation (DFG - WA 2728/2-1). RapidEye data was provided from the RapidEye Science Archive (RESA) by DLR under the proposal id490. Ground truth data was made available by RPG-AGRICOLE 2011 (c) Ministre de l'Agriculture, de la Viticulture et du Développement rural, Grand Duché of Luxembourg. The authors would like to thank the anonymous reviewers for their comments and suggestions which helped us to improve the manuscript.

References

Aguirre-Gutiérrez, J., Seijmonsbergen, A. C., & Duivenvoorden, J. F. (2012). Optimizing land cover classification accuracy for change detection, a combined pixel-based and object-based approach in a mountainous area in Mexico. *Applied Geography*, *34*, 29–37.

Anders, N. S., Seijmonsbergen, A. C., & Bouten, W. (2011). Segmentation optimization and stratified object-based analysis for semi-automated geomorphological mapping. *Remote Sensing of Environment*, *115*, 2976–2985.

Arbiol, R., Zhang, Y., & Pala, V. (2006). Advanced classification techniques: A review. ISPRS Commission VII Mid-term Symposium "From Pixel to Processes", Enschede, NL, 8-11 May 2006.

Baatz, M., & Schäpe, A. (2000). Multiresolution segmentation: An optimization approach for high quality multi-scale image segmentation. In J. Strobl, T. Blaschke, & G. Griesebner (Eds.), *Angewandte Geographische Informationsverarbeitung XII* (pp. 12–23). Wichmann Verlag.

Baeza-Yates, R. A., & Ribeiro-Neto, B. (1999). *Modern Information Retrieval*. Boston, MA, USA: Addison-Wesley Longman Publishing Co., Inc.

Blaschke, T. (2010). Object based image analysis for remote sensing. *ISPRS Journal of Photogrammetry and Remote Sensing*, *65*, 2–16.

Blaschke, T., Lang, S., Lorup, E., Strobl, J., & Zeil, P. (2000). Object based image analysis for remote sensing. In *Cremers, A., Greve, K. (Eds.), Environmental Information for Planning, Politics and the Public* (pp. 555–570). Metropolis Verlag volume 2.

Breiman, L. (2001). Random Forests. *Machine Learning*, *45*, 5–32.

Bruzzone, L., & Carlin, L. (2006). A multilevel context-based system for classification of very high spatial resolution images. *Geoscience and Remote Sensing, IEEE Transactions on*, *44*, 2587–2600.

Chen, X.-L., Zhao, H.-M., Li, P.-X., & Yin, Z.-Y. (2006). Remote sensing image-based analysis of the relationship between urban heat island and land use/cover changes. *Remote Sensing of Environment*, *104*, 133–146.

Dongping Ming, Tianyu Ci, Hongyue Cai, Longxiang Li, Cheng Qiao, & Jinyang Du (2012). Semivariogram-based spatial bandwidth selection for remote sensing image segmentation with mean-shift algorithm. *IEEE Geoscience and Remote Sensing Letters*, *9*, 813–817.

Dorren, L. K., Maier, B., & Seijmonsbergen, A. C. (2003). Improved Landsat-based forest mapping in steep mountainous terrain using object-based classification. *Forest Ecology and Management*, *183*, 31–46.

Dragut, L., Tiede, D., & Levick, S. R. (2010). Esp: A tool to estimate scale parameter for multiresolution image segmentation of remotely sensed data. *International Journal of Geographical Information Science*, *24*, 859–871.

Duro, D. C., Franklin, S. E., & Dubé, M. G. (2012a). Multi-scale object-based image analysis and feature selection of multi-sensor Earth observation imagery using Random Forests. *International Journal of Remote Sensing*, *33*, 4502–4526.

Duro, D. C., Franklin, S. E., & Dubé, M. G. (2012b). A comparison of pixel-based and object-based image analysis with selected machine learning algorithms for the classification of agricultural landscapes using SPOT-5 HRG imagery. *Remote Sensing of Environment*, *118*, 259–272.

Efron, B., & Gong, G. (1983). A leisurely look at the bootstrap, the jackknife, and cross-validation. *The American Statistician*, *37*, 36–48.

Espindola, G. M., Camara, G., Reis, I. A., Bins, L. S., & Monteiro, A. M. (2006). Parameter selection for region–growing image segmentation algorithms using spatial autocorrelation. *International Journal of Remote Sensing*, *27*, 3035–3040.

Foody, G. (2004). Thematic map comparison: Evaluating the statistical significance of differences in classification accuracy. *Photogrammetric Engineering and Remote Sensing*, *70*, 627–633.

Gislason, P. O., Benediktsson, J. A., & Sveinsson, J. R. (2006). Random Forests for land cover classification. *Pattern Recognition Letters*, *27*, 294–300.

Jaiantilal, A. (2009). Classification and regression by randomForest-matlab. Available at http://code.google.com/p/randomforest-matlab.

van der Linden, S., Janz, A., Waske, B., Eiden, M., & Hostert, P. (2007). Classifying segmented hyperspectral data from a heterogeneous urban environment using support vector machines. *Journal of Applied Remote Sensing*, *1*, 1–17.

Lobell, D. B., Asner, G. P., Ortiz-Monasterio, J. I., & Benning, T. L. (2003). Remote sensing of regional crop production in the Yaqui Valley , Mexico: estimates and uncertainties. *Agriculture, Ecosystems & Environment*, *94*, 205–220.

Lowe, S., & Guo, X. (2011). Detecting an optimal scale parameter in object-oriented classification. *Selected Topics in Applied Earth Observations and Remote Sensing, IEEE Journal of*, *4*, 890–895.

Mester, R., Conrad, C., & Guevara, A. (2011). Multichannel segmentation using contour relaxation: Fast super-pixels and temporal propagation. In *Proceedings of the 17th Scandinavian conference on Image analysis* SCIA'11 (pp. 250–261). Berlin, Heidelberg: Springer-Verlag.

Myint, S. W., Gober, P., Brazel, A., Grossman-Clarke, S., & Weng, Q. (2011). Per-pixel vs. object-based classification of urban land cover extraction using high spatial resolution imagery. *Remote Sensing of Environment*, *115*, 1145–1161.

Myint, S. W., Yuan, M., Cerveny, R. S., & Giri, C. P. (2008). Comparison of remote sensing image processing techniques to identify tornado damage areas from Landsat TM data. *Sensors*, *8*, 1128–1156.

Palsson, F., Sveinsson, J. R., Benediktsson, J. A., & Aanaes, H. (2012). Classification of pansharpened urban satellite images. *Selected Topics in Applied Earth Observations and Remote Sensing, IEEE Journal of*, *5*, 281–297.

Segl, K., Roessner, S., Heiden, U., & Kaufmann, H. (2003). Fusion of spectral and shape features for identification of urban surface cover types using reflective and thermal hyperspectral data. *ISPRS Journal of Photogrammetry and Remote Sensing*, *58*, 99–112.

Shackelford, A., & Davis, C. (2003). A combined fuzzy pixel-based and object-based approach for classification of high-resolution multispectral data over urban areas. *Geoscience and Remote Sensing, IEEE Transactions on*, *41*, 2354 – 2363.

Skriver, H., Mattia, F., Satalino, G., Balenzano, A., Pauwels, V., Verhoest, N., & Davidson, M. (2011). Crop classification using short-revisit multitemporal SAR data. *Selected Topics in Applied Earth Observations and Remote Sensing, IEEE Journal of*, *4*, 423–431.

Smith, J. H., Stehman, S. V., Wickham, J. D., & Yang, L. (2003). Effects of landscape characteristics on land-cover class accuracy. *Remote Sensing of Environment*, *84*, 342–349.

Smith, J. H., Wickham, J. D., Stehman, S. V., & Yang, L. (2002). Impacts of patch size and land-cover heterogeneity on thematic image classification accuracy. *Photogrammetric Engineering & Remote Sensing*, *68*, 65–70.

Song, M., Civco, D. L., & Hurd, J. D. (2005). A competitive pixel-object approach for land cover classification. *International Journal of Remote Sensing*, *26*, 4981–4997.

Stumpf, A., & Kerle, N. (2011). Object-oriented mapping of landslides using Random Forests. *Remote Sensing of Environment*, *115*, 2564–2577.

Tarabalka, Y., Tilton, J., Benediktsson, J., & Chanussot, J. (2012). A marker-based approach for the automated selection of a single segmentation from a hierarchical set of image segmentations. *Selected Topics in Applied Earth Observations and Remote Sensing, IEEE Journal of*, *5*, 262–272.

Voorde, T. V. D., Genst, W. D., & Canters, F. (2007). Improving pixel-based VHR land-cover classifications of urban areas with post-classification techniques. *Photogrammetric Engineering & Remote Sensing*, *73*, 1017–1027.

Walker, W., Stickler, C., Kellndorfer, J., Kirsch, K., & Nepstad, D. (2010). Large-area classification and mapping of forest and land cover in the Brazilian Amazon: A comparative analysis of ALOS/PALSAR and Landsat data sources. *Selected Topics in Applied Earth Observations and Remote Sensing, IEEE Journal of*, *3*, 594–604.

Wang, Z., Jensen, J. R., & Im, J. (2010). An automatic region-based image segmentation algorithm for remote sensing applications. *Environmental Modelling & Software*, *25*, 1149–1165.

Waske, B., & Braun, M. (2009). Classifier ensembles for land cover mapping using multitemporal SAR imagery. *ISPRS Journal of Photogrammetry and Remote Sensing*, *64*, 450–457.

Waske, B., & van der Linden, S. (2008). Classifying multilevel imagery from SAR and optical sensors by decision fusion. *Geoscience and Remote Sensing, IEEE Transactions on*, *46*, 1457–1466.

van der Werff, H., & van der Meer, F. (2008). Shape-based classification of spectrally identical objects. *ISPRS Journal of Photogrammetry and Remote Sensing*, *63*, 251–258.

Whiteside, T. G., Boggs, G. S., & Maier, S. W. (2011). Comparing object-based and pixel-based classifications for mapping savannas. *International Journal of Applied Earth Observation and Geoinformation*, *13*, 884–893.

Chapter III:

Mapping land management regimes in western Ukraine using optical and SAR data

Remote Sensing, vol. 6, pp. 5279–5305, June 2014

Jan Stefanski, Tobias Kuemmerle, Oleh Chaskovskyy, Patrick Griffiths, Vassiliy Havryluk, Jan Knorn, Nikolas Korol, Anika Sieber, and Björn Waske

© 2014 by the authors; licensee MDPI, Basel, Switzerland.
http://dx.doi.org/10.3390/rs6065279

Abstract

The global demand for agricultural products is surging due to population growth, more meat-based diets, and the increasing role of bioenergy. Three strategies can increase agricultural production: (1) expanding agriculture into natural ecosystems; (2) intensifying existing farmland; or (3) recultivating abandoned farmland. Because agricultural expansion entails substantial environmental trade-offs, intensification and recultivation are currently gaining increasing attention. Assessing where these strategies may be pursued, however, requires improved spatial information on land use intensity, including where farmland is active and fallow. We developed a framework to integrate optical and radar data in order to advance the mapping of three farmland management regimes: (1) large-scale, mechanized agriculture; (2) small-scale, subsistence agriculture; and (3) fallow or abandoned farmland. We applied this framework to our study area in western Ukraine, a region characterized by marked spatial heterogeneity in management intensity due to the legacies from Soviet land management, the breakdown of the Soviet Union in 1991, and the recent integration of this region into world markets. We mapped land management regimes using a hierarchical, object-based framework. Image segmentation for delineating objects was performed by using the Superpixel Contour algorithm. We then applied Random Forest classification to map land management regimes and validated our map using randomly sampled in-situ data, obtained during an extensive field campaign. Our results showed that farmland management regimes were mapped reliably, resulting in a final map with an overall accuracy of 83.4%. Comparing our land management regimes map with a soil map revealed that most fallow land occurred on soils marginally suited for agriculture, but some areas within our study region contained considerable potential for recultivation. Overall, our study highlights the potential for an improved, more nuanced mapping of agricultural land use by combining imagery of different sensors.

1 Introduction

Human-caused land use and land cover change is one of the major drivers of global environmental change (Foley et al., 2005; Turner et al., 2007). Historically, agricultural expansion was the principal mode of land use change leading to, for example, an increasement of cropland areas by about 550% over the last three centuries (Goldewijk, 2001). Nowadays, up to 38% of the land surface is used for agriculture and every year about 13 million hectares covered by natural vegetation are transformed into agricultural land (Foley et al., 2005; FAO, 2006). Next to agricultural expansion, agricultural intensification has recently become an important mode of reaching higher agricultural outputs (Siebert et al., 2010; Ellis et al., 2013; Erb et al., 2013). Especially since the advent of industrial fertilizer and the green revolution, intensification has been responsible for the majority of yield increases in recent decades (Matson et al., 1997; Rounsevell et al., 2012; Erb et al., 2013; Ellis et al., 2013).

Both agricultural expansion and intensification entail substantial environmental trade-offs. Approximately 35% of the anthropogenic CO_2 emissions since 1850 are directly traced back to land use changes (Foley et al., 2005). On the one hand, expansion of agriculture into native ecosystems is the major driver of biodiversity loss, releases huge amounts of carbon and plays a major role in changing the global carbon cycle (Brooks et al., 2002). On the other hand, agricultural intensification can increase soil erosion, lower soil fertility, threaten biodiversity, pollute ground water and lead to the eutrophication of rivers and lakes, and contribute to climate change via the emission of CO_2 and other green-house gases (Matson et al., 1997). Mapping the extent and the intensity of agriculture is therefore important for assessing environmental and socio-economic trade-offs of agriculture.

As demand for agricultural products (e.g., food, feed, bioenergy) continues to increase and land resources are increasingly becoming scarce (Lambin & Meyfroidt, 2011; Godfray et al., 2010), identifying strategies for increasing agricultural production in sustainable ways has become a research priority (Foley et al., 2011; Mueller et al., 2012). There are three strategies that could lead to increasing agricultural production: (1) cultivation of new farmland; (2) intensifying existing farmland; or (3) recultivation of unused or abandoned farmland. However, assessing where sustainable intensification or recultivation could be fostered, requires improved maps that go beyond broad land cover classes such as cropland and are sensitive to land use intensity and that include information on active and fallow/abandoned agriculture. Unfortunately, such information does not exist for most parts of the globe (Kuemmerle et al., 2013; Fritz et al., 2013).

Satellite remote sensing has doubtless become the most important technology to monitor agricultural land use and changes therein (Rudorff, Bernardo Friedrich Theodor et al., 2010; Skriver et al., 2011; Atzberger, 2013; Sieber et al., 2013; Li et al., 2014). Yet, existing approaches to do so have mainly focused on cropland extent and the proximate drivers, leading to changes in cropland area (e.g., deforestation due to agricultural expansion, agricultural abandonment) (Alcantara et al., 2012; Souza, Jr, Carlos et al., 2013). What is generally lacking are methods able to capture the heterogeneity and the varying management intensity within the broad agricultural class.

One reason for the lack of approaches sensitive to land use intensity is that intensity in itself is a complex and multidimensional term. Agricultural land use intensity can be measured via inputs to agriculture (e.g., fertilizer, pesticide application rate), the outputs from agriculture (e.g., yields), or in terms of system properties that change due to management (e.g., human appropriation of net primary production) (Turner & Doolittle, 1978; Kleijn et al., 2009; Kuemmerle et al., 2013). Unfortunately, remote sensing can only rarely measure any of these dimensions directly and therefore a combination of remote sensing and ground-based data is often needed to determine land use intensity metrics. This is problematic because comprehensive and detailed in-situ data on land management is unavailable for most parts of the world, either because of the lack of monitoring schemes or the confidentiality issues (Zaks & Kucharik, 2011; Verburg et al., 2011; Kuemmerle et al., 2013). Approaches that allow

to better characterize management intensity directly from satellite imagery are therefore potentially highly beneficial for a better understanding of the impacts of agriculture on the environment.

A promising avenue for a more nuanced representation of agriculture is to identify and map management regimes with different intensities (Kuemmerle et al., 2013; Verburg et al., 2011). Such management regimes (or land systems) may be easier to map than all the individual dimensions of management intensity itself, yet provide a proxy variable for tracking changes in management intensity and their impacts (e.g., shifts from subsistence to capital intensive farming). A few studies have used such approaches recently at the global scale. For example, combining land cover data with human population density allowed deriving anthromes of varying land use intensity (Ellis & Ramankutty, 2008). Or, using clustering techniques on a comprehensive set of environmental and socio-economic variables allowed to map land system archetypes (Václavík et al., 2013).

Likewise, combining global data sets on cropland extent, yield gaps, livestock distribution, and market accessibility allowed to map different "land use systems", which represented different levels of management intensity (Asselen & Verburg, 2012; Václavík et al., 2013). Examples relying on remote sensing data to characterize land management regimes are even scarcer. At the regional scale, Landsat images were used to map swidden agricultural systems of varying management intensities for Laos (Hett et al., 2012). Furthermore, the spatial distribution of farming types in Ethiopia was analyzed based on Landsat, but additionally to remote sensing data, local spatial contextual information was needed (Wästfelt et al., 2012). While these studies highlight the value of mapping management intensity regimes, there is a general lack of studies developing methods to map management regimes using remote sensing data.

One important indicator to characterize agricultural land use intensity is field size, which is a proxy variable for the degree of mechanization. While small fields indicate low levels of mechanization, often accompanied by low levels of fertilizer and pesticide use, large fields tend to require a high degree of mechanization and are typical for industrialized agriculture (Killeen et al., 2008; Rodriguez & Wiegand, 2009). Mapping land management regimes that differ in field sizes (e.g., large-scale cropland and small-scale cropland) is challenging due to spectral similarities of fields and mixed signatures within groups of small fields. Studies mapping field sizes based on remote sensing data are scarce. While some remote sensing-based studies used predefined vector data or texture measures to analyze field sizes (Ferguson et al., 1986; Aplin & Atkinson, 2001; Lloyd et al., 2004; Ozdogan & Woodcock, 2006; Kuemmerle et al., 2009) or an object-based approach using Landsat data to extract fields (Yan & Roy, 2014), there is no classification-based approach to directly derive management regimes differing in field sizes up to now.

Object-based approaches use additional information compared to pixel-by-pixel approaches, for example, spatial context and object-based features such as spectral mean or variance. Object-based classification of land use and land cover often results in higher accuracies, when

compared to pixel-based classifications (Cleve et al., 2008; Moskal et al., 2011; Whiteside et al., 2011; Stefanski et al., 2013). Some studies also used hierarchical classification approaches, mainly to integrate different data types into a comprehensive mapping framework (Dai & Khorram, 1998; Jones et al., 2009; Sulla-Menashe et al., 2011; Li et al., 2013). However, to our knowledge, no study has used segmentation algorithms to make better use of field size information inherent in satellite images in order to improve the mapping of agricultural management intensity.

Landsat has arguably become the most important sensor to characterize land cover and land use at regional to landscape scale (Cohen & Goward, 2004; Loveland et al., 2008; Griffiths et al., 2013; Kindu et al., 2013), especially since the recent opening of the United States Geological Survey (USGS) Landsat archives (Woodcock et al., 2008). However, Landsat data availability can be limited in regions of persistent cloud cover or due to the relatively low revisiting rates of the Landsat sensors (16 days). For example, the limits regarding image acquisition dates and temporal coverage are critical for the mapping accuracy of agricultural abandonment (Prishchepov et al., 2012; Kovalskyy & Roy, 2013).

Contrary to optical data, synthetic aperture radar (SAR) data are almost independent from weather conditions. Thus, multitemporal data sets covering any stage from one growing season in regions like Central Europe can reliably be produced by using SAR sensors. Several studies used SAR data for land use and land cover mapping (Waske & Braun, 2009; Bargiel & Herrmann, 2011; Cable et al., 2014). In addition, SAR data provides different, but complementary information on land cover, when compared to optical data. For example, discriminating vegetation species can be difficult due to their similar spectral signature. In this case, radar can contribute with signal differences in surface roughness, shape, and moisture content of the observed ground (Pohl & Van Genderen, 1998).

Jointly using optical and SAR data to map land use and land cover change is therefore an attractive option, but has so far rarely been employed. This is unfortunate because such multisensor approaches can result in more reliable maps than using only one data source alone. For example, the fusion of multispectral and SAR data from an agricultural area outperforms the mono-sensorial approach in terms of the classification accuracy (Waske & Benediktsson, 2007). Overall, several studies noted higher accuracies in the differentiation of classes by the combined use of optical and SAR data in context of land use and land cover mapping (Kuplich et al., 2000; Shupe & Marsh, 2004; Waske & van der Linden, 2008; Gong et al., 2011), for example by minimizing spectral ambiguities and improving the characterization of phenological variability (Griffiths et al., 2010). However, none of these studies have assessed how the combined use of optical and SAR data can advance the mapping of management intensity of cropland.

Here, we explore the synergetic effect of multispectral Landsat and SAR data to map land management regimes, as proxies of land use intensity, in our study area in western Ukraine. Land use intensity here refers to the management intensity in terms of capital-related inputs such as industrial fertilizer, pesticides, or heavy machinery. Eastern Europe and

especially western Ukraine are particular interesting for mapping land management regimes (Kuemmerle et al., 2006; Müller et al., 2009; Alcantara et al., 2012). Land management in the region has changed drastically in recent decades, triggered by the breakdown of the Soviet Union in 1991, when industrialized and the large agricultural fields, established during Soviet times, were abandoned (Baumann et al., 2011; Ioffe et al., 2012). Furthermore, large fields were converted to small fields as subsistence agriculture became important after 1991 (UNEP, 2005; Kuemmerle et al., 2006; Baumann et al., 2011; Kuemmerle et al., 2011). Recently, global trends in food prices have led to a growing interest in the region, which triggered the recultivation of much farmland and a renaissance of industrial agriculture, including a consolidation of small fields into large ones (Sabates-Wheeler, 2002). The rates and patterns of these trends remain unclear, however, especially with regard to changes in management intensity, which in this region is intimately linked to changes in agricultural field size. Mapping land management regimes can therefore offer important insights about land use change and ultimately the effect of economic and institutional drivers on land change in western Ukraine.

The overall goal of our study was to develop an approach for mapping agricultural land management regimes of different intensities for our study area in western Ukraine, and to use this methodology to assess the patterns and rates of agricultural land use in this region. To do so, we used field size (large-scale cropland and small-scale cropland) as a proxy for management intensity and evaluated the potential of object-based image analysis to merge multispectral and SAR images within a hierarchical classification framework in order to discriminate different land cover/use categories, including different land management regimes. Specifically, our objectives were to:

1. Analyze whether object-based mapping improves the separation of land management regimes
2. Assess whether the combination of multispectral and SAR data enhances the classification of land management regimes.
3. Map land management regimes and analyze them across gradients of soil marginality, elevation, and distance to markets.

2 Material

2.1 Study area

Our study area is located in Volynska and Lvivska Oblasts in western Ukraine and covers about 7500 km^2 (Figure III-1). The study area contains seven raions (*i.e.*, administrative unit at the district-level). In addition, the three cities Volodymyr-Volynsky, Novovolynsk, and Chervonograd are self-governing municipalities. Elevation in the study area varies from about 150 m to 300 m. The climate is temperate continental with average temperatures from

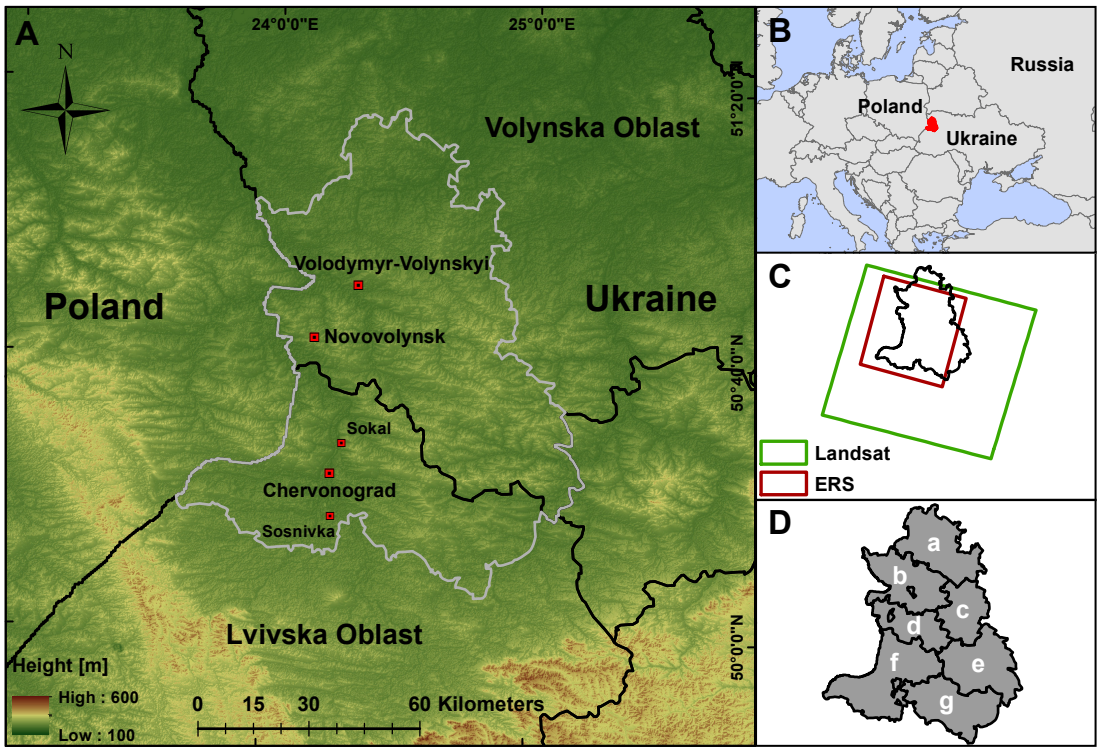

Figure III-1: Map of the study area in western Ukraine. (**A**) Study area boundaries (grey); (**B**) Location of the study area in Europe; (**C**) Landsat footprint (green) and ERS footprint (red); (**D**) Administrative boundaries of (a) Turiyskyi Raion; (b) Volodymyr-Volynskyi Raion; (c) Lokachynskyi Raion; (d) Ivanychivskyi Raion; (e) Horokhivskyi Raion; (f) Sokalskyi Raion; and (g) Radekhivskyi Raion.

−2.9 °C in January to 19.0 °C in July (NOAA, 2011). The region is dominated by agricultural land use and forests. Soil types vary within the study area with mainly Podzols and Gleysols in the wooded northern and southern part and Phaeozems as well as Chernozems in the central part. Approximately half of the population in the region is living in rural areas (State Statistics Committee of Ukraine, 2001).

The study area in western Ukraine is particular interesting to investigate land management regimes because it comprises a large variability of socio-economic and environmental conditions, resulting in a large heterogeneity of management practices. The Soviet land management was characterized by collectivized and large-scale farmland (Kuemmerle et al., 2011). With the collapse of the Soviet Union in 1991, the region experienced drastic changes in institutions and socio-economic conditions. For example, the collapse of the Soviet Union and associated economic changes (e.g., price liberalization, rising competition, and breakaway of former markets) resulted in the substantial abandonment of agricultural fields on the one hand, and an emergence of a substantial subsistence agriculture sector on the other hand (Sabates-Wheeler, 2002; Kuemmerle et al., 2006; Baumann et al., 2011). Furthermore, changes in the land ownership lead to farmland fragmentation (Sabates-Wheeler, 2002). More recently, recultivation of abandoned land and conversion of subsistence farming to

Table III-1: Land categories, defined classes, class descriptions.

Categories	Classes	Description
Agriculture	Large-scale cropland	Potentially intensive use; large fields (100 ha) indicating a high degree of mechanization and other capital-related inputs (e.g., pesticides, fertilizer)
Agriculture	Small-scale cropland	Kitchen gardens, subsistence agriculture; small field size indicates high labor intensity, but low intensity in terms of capital related inputs
Agriculture	Pasture	Grassland used for grazing of cattle, sheep, or goats
Agriculture	Fallow	Areas without sign of management, including perennial vegetation (willow, alder, or birch shrubs), all indicating potentially abandoned agricultural land
Forestry	Forest	Mixed forest or forests dominated by coniferous or deciduous forests species
Urban	Urban	Dense settlements or cities

large-scale farming has become common.

We decided to map the following land use and land cover classes (Table III-1). The four agricultural management regimes we mapped comprised *large-scale cropland* (LSC), *small-scale cropland* (SSC), *fallow* and *pasture* (Figure III-2). While *LSC* is a potential indicator for intensive agricultural use, *fallow* areas are abandoned or currently unused fields. *SSC* refers to subsistence agriculture and kitchen gardens, and thus indicates low management intensity. *Forest* and *urban* completed the land use/cover categories in the study area.

2.2 Data set and preprocessing

To map the different land use/cover classes including our land management intensity regimes, we acquired multispectral Landsat TM data (30 m resolution) and ERS-2 SAR data (about 25 m spatial resolution). We used a total of two Landsat scenes (7 June 2010 and 14 November 2010, path/row 185/25) and nine ERS-2 scenes (each month in 2010 except for January, May, and August). The Landsat images were already preprocessed to level L1T, which ensures a sufficient geometric and radiometric accuracy for our analysis (USGS, 2013). The ERS-2 data were ordered in a single look complex (SLC) image format. Preprocessing of SAR data was carried out with NEST-4C. Standard SAR preprocessing was applied, containing radiometric and geometric corrections as well as multitemporal speckle-filtering. The ERS-2 images were resampled to a 30 meter pixel size to match the resolution of the Landsat TM data for all subsequent analysis.

We used additional data to analyze the land management regimes map. To receive information about soil qualities, an Ukrainian soil map with a scale of 1:1,000,000 was digitized in-house. Elevation data was derived from the digital elevation model of the Shuttle Radar Topography Mission (SRTM) (Figure III-1A). Furthermore, a map with buffer zones

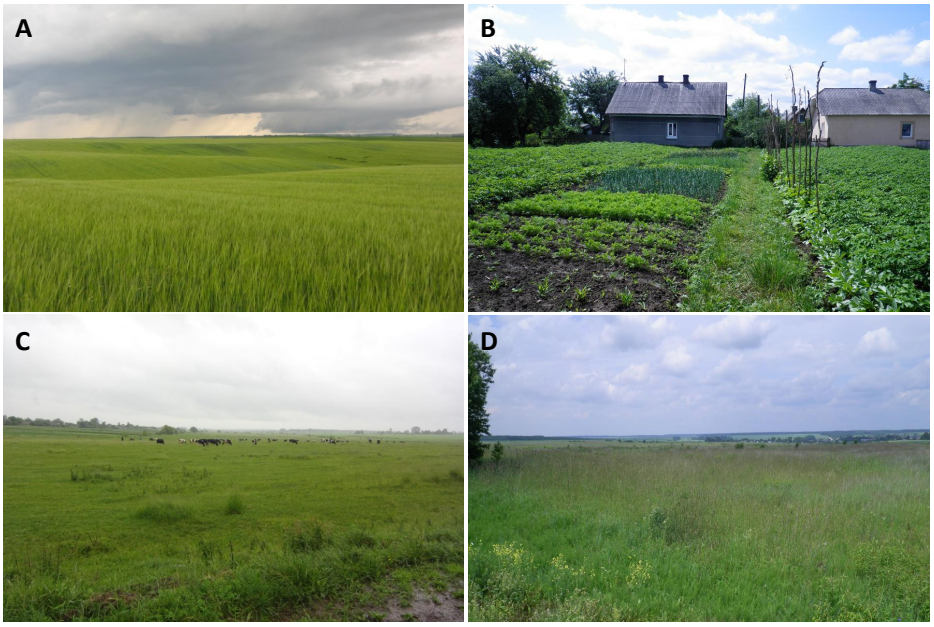

Figure III-2: Photos of the agricultural category taken during our field campaign. (**A**) Large-scale cropland (**B**) Small-scale cropland (**C**) Pasture (**D**) Fallow/potential abandoned, high grass with some bushes.

around the cities was prepared with GIS analysis. We used a city layer created on the basis of a topographic map from OpenStreetMaps (OSM) and visual interpretation. Only cities with more than 10,000 inhabitants were taken into account (Figure III-1A).

We acquired in-situ data during an extensive field campaign in 2012 and controlled the data for validity in the study period (2010) by visually inspecting high-resolution imagery. We used a random clustered sampling technique to allocate 357 points to be used for the validation data set. To do so, we generated 40 clusters, where each cluster contained five points in a (+) shape with a distance of 100 m between points along the horizontal and vertical axis. Three teams, each containing two to three surveyors, accessed each point in the field, noted the land use/cover at the point and photo documented the area in each direction from the point. The survey protocol was derived from the Land Use and Cover Area frame Survey (LUCAS) guidelines (EUROSTAT, 2009). We created a field protocol with land use and land cover categories based on the LUCAS guidelines, which contained hierarchical land cover categories (e.g., agriculture → arable land → cereals/root crops → wheat/potatoes) and as well as land use categories (e.g., agriculture/fallow and abandoned land/kitchen gardens). In a last step, we expanded the set of five points assessed in the field to a nine point (3 × 3) grid, using the field photos and on-screen interpretation of high-resolution RapidEye data to determine the land use/cover category of the additional four points per cluster. Three sample points were removed, due to inaccessibility in the field and uncertainty in on-screen interpretation. Thus, the reference set contains 357 points.

The training data acquisition was also based on the field campaign and was additionally

supported by visual interpretation of RapidEye data. The training data was generated independently from the test data set. To do so, we ensured that the (1) training and test data are spatially disjoint and (2) no training and test data are located within the same field plot.

3 Methods

To map land management regimes in our study region, we compare (1) a pixel-based (Landsat); (2) an object-based (Landsat); and (3) a hierarchical object-based classification approach (Landsat+ERS) in terms of the mapping accuracy. The following sections introduce the underlying methods for these three approaches.

3.1 Random Forest classifier

We chose a Random Forest (RF) classifier for all three approaches. RF performs efficiently with large data sets, is robust to outliers and overfitting, and its parameter selection is user-friendly (Breiman, 2001). The RF has demonstrated excellent performance in terms of classifying diverse remote sensing data sets (Gislason et al., 2006; Waske & Braun, 2009; Stumpf & Kerle, 2011; Rodriguez-Galiano et al., 2012; Stefanski et al., 2013) and especially joint optical and radar data sets (Waske & van der Linden, 2008; Zhu et al., 2012).

Random Forests are based on a combination of a set of k different decision tree classifiers. Decision trees have a tree-like hierarchy, consisting of a root node, which includes all samples, internal or split nodes that contain a decision rule, and final leave nodes, representing the different classes. A majority vote is used to combine the outputs by the k decisions trees to generate the final classification result. Each tree in the RF is trained by a randomly selected subset of the training data. The remaining training samples, which are called "out-of-bag" (OOB), enable a cross-validation-like accuracy measure through the OOB error estimate. The RF split rules are based on a subset m of all n features, whereby m is a user-defined value, with $m < n$. As RF parameters, we used standard values such as 500 trees for k and the square root of the total input features for m. However, the classification accuracy is relatively insensitive to the RF parameters (Breiman, 2001; Gislason et al., 2006).

In this study, the classification model was generated with 1000 training samples per class, which were selected by an equalized random sampling out of the training set.

3.2 Superpixel Contour segmentation

To perform an image segmentation, we used the Superpixel Contour (SPc) segmentation algorithm in combination with a semi-automatic parameter selection (Stefanski et al., 2013). The SPc, introduced by Mester et al. (2011), is an iterative, region-based segmentation algorithm. The principle of the SPc is to optimize a non-specified initial segmentation to separate the image into homogenous regions (*i.e.*, segments or superpixels, ideally represent-

ing real-world objects). Therefore, the initial segmentation is optimized along its boundaries based on the statistical distribution of each region. The boundary pixels are assigned to the region that maximizes the posterior distribution. The general principle behind this is an iteratively running maximum-a-posteriori (MAP) segmentation. The SPc algorithm is computationally efficient as only the boundary pixels of each region are taken into account for the optimization process.

The SPc segmentation algorithm has four parameters. However, SPc is generally user-friendly as only two (parameter G and B) out of four parameters have to be adapted to the respective application (Stefanski et al., 2013). The user can control the scale of the segments with G and the shape of the segments with B. Stefanski et al. (2013) introduced a concept to semi-automatically select the optimal segmentation parameters with respect to the classification accuracy, which was used in this study. The basic idea of the concept is to define a set of parameters for G and B that are segmented by SPc and evaluated by the OOB error rate of the RF. Then, the best parameter combination based on the classification accuracy can be used for subsequent object-based classifications. This approach is comparable with a grid-search which is, for example, frequently used to select the parameters of Support Vector Machines (Hsu et al., 2003).

The identification of an ideal segmentation level for all classes is often challenging. Moreover, different segmentation levels can provide different types of information (Bruzzone & Carlin, 2006; Waske & van der Linden, 2008). Waske & van der Linden (2008) proposed a multilevel segmentation strategy for the classification of SAR and multispectral data. They demonstrated that both aspects, the combination of information from different sensor sources as well as the use of multiple segmentation levels, proved useful in terms of accuracy. Thus, using the parameter optimization approach mentioned above, we analyzed various segmentation levels (*i.e.*, segmentation scales based on different values for G) for the land management regimes in our study area. The class-specific OOB error rate, provided by the RF, enables the detection of the "optimal" representation for each class in terms of the segmentation level and the classification accuracy. For example, the classification accuracy of *large-scale cropland* increased with higher segmentation levels while the effect was vice versa with the accuracy of urban areas. Initial tests showed that the subclasses of *active agriculture* (*i.e.*, *LSC*, *SSC*, and *pasture*) were difficult to classify solely on pixel-level due to spectral similarities. We used object-based analysis to overcome this issue, however, the class-specific analysis showed that there is no single object-size that results in a high classification accuracy. This can be explained by the inhomogeneous object-sizes within *SSC* and *pasture*.

Therefore, we used three segmentation levels (G = 15, 20, 25) in addition to the original pixel information. As object-based features, we derived the mean value for Landsat and the mean value and standard deviation for ERS-2 SAR. Thus, the dimension of the feature space is 111, containing the pixel information from the two Landsat images (*i.e.*, 2 images $\times$ 6 bands) and 9 SAR images (*i.e.*, 9 images $\times$ 1 band), the segments' mean derived from

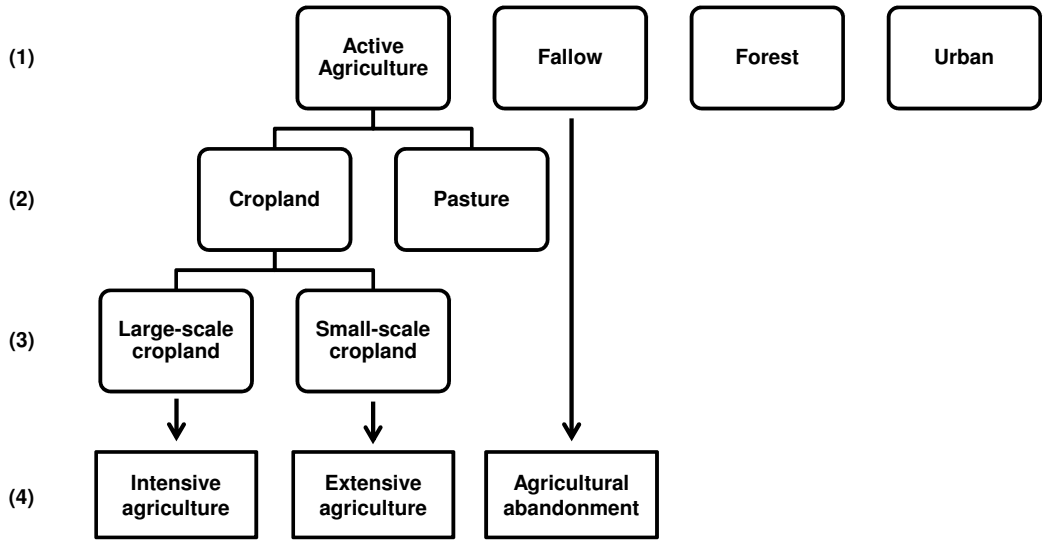

Figure III-3: Diagram showing the hierarchical classification framework and derived indicators for management intensity. (1) Classification of active agriculture, fallow, forest and urban; (2) Classification of cropland and pasture within active agriculture; (3) Classification of large-scale and small-scale cropland; (4) Indicators of land management, derived from the hierarchical classification.

Landsat ($2 \times 6 \times 3$ segmentation levels) and ERS-2 SAR (*i.e.*, $9 \times 1 \times 3$ segmentation levels), and the standard deviation from ERS-2 SAR (*i.e.*, $9 \times 1 \times 3$ segmentation levels).

3.3 Hierarchical classification framework

We used a hierarchical classification framework to integrate optical and SAR data as well as object-based features from different scales into one classification scheme (Figure III-3). For each of the three classification levels (1–3), a separate classification model was generated. (1) First, *active agriculture*, *fallow*, *forest* and *urban* were classified. For this step, a single-level object-based approach based on Landsat and ERS-2 features was used; (2) Second, *active agriculture* was separated further in either *cropland* or *pasture*. To do so, a multilevel, object-based classification based on Landsat and ERS-2 data was used; (3) The last classification differentiated *cropland* into *large-scale* and *small-scale cropland*, using the same input features as in Step 2. After performing the classification, indicators for land management intensity were derived from the generated map (cf. Figure III-3(4)).

3.4 Accuracy assessment

We assessed our results by using a randomly clustered field-based validation set. Validation points were fully independent from the training data. We calculated confusion matrices, producer's, user's, and overall accuracies, and corrected mapped areas for classification errors in the error estimates (Foody, 2002; Olofsson et al., 2013). To quantitatively evaluate the classification, error-adjusted area estimates with 95% confidence intervals were calculated by

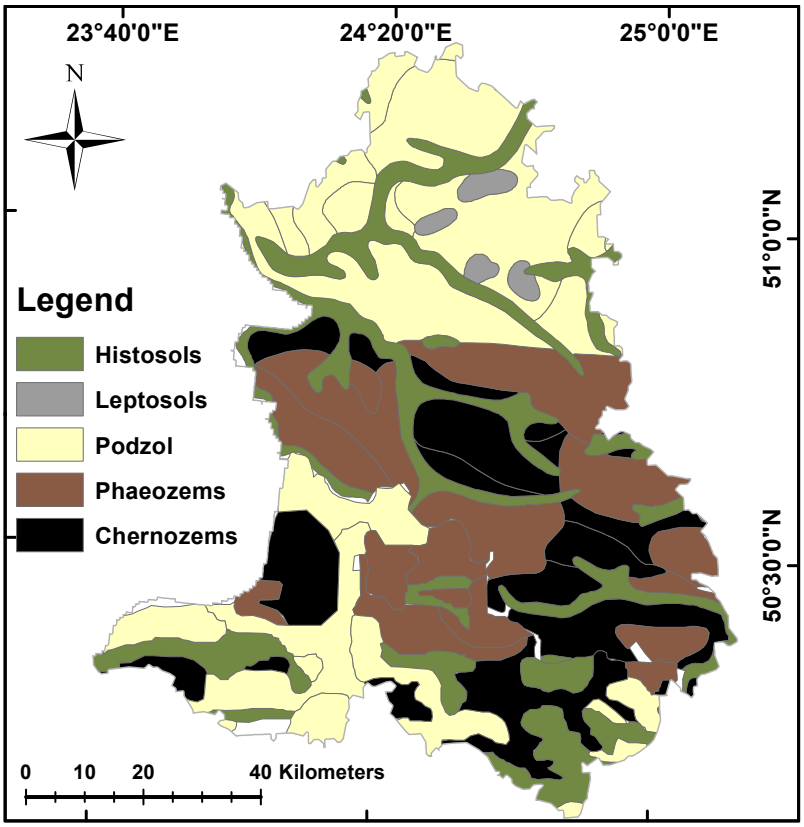

Figure III-4: Map showing the distribution of soil in our study area.

using a poststratified estimator (Olofsson et al., 2013). To assess whether our classifications were statistically significantly different from each other, we performed a McNemar test (Foody, 2004).

3.5 Exploring spatial patterns in land management regimes

To further explore the spatial pattern of land management intensity regimes in our study area, we overlay our final classification result with a number of spatial indicators related to the marginality of farming. First, we analyzed if there were spatial correlation between the classes *large-scale cropland*, *small-scale cropland*, *pasture*, *fallow*, and *forest* on the one hand and the quality of the soil for farming on the other hand. To do so, we used a soil map to calculate the ratio of each class to the underlying soil type (Figure III-4). The occurring soil types were: histosols (marshy area; not attractive for agriculture), leptosols (stony, chalky; not suitable for agriculture), podzol (sandy, nutrient-poor, acidic soils; not attractive for agriculture), phaeozems (dark humus, fertile soil; very attractive for agriculture), and chernozems (black soil, rich in organic matter; very attractive for agriculture) (IUSS Working Group WRB, 2006).

Second, to reveal the spatial relationships between our land management classes and market access (or in other words the remoteness of an agricultural plot), we analyzed the

proportion of each management regime in several buffer zones around the cities. To do so, the proportion of the different agricultural classes were summarized in buffer zones with the Euclidean distances of 0.5, 1, 2, 4, 6, 8, and 10 km from the city boundaries.

Third, we analyzed the distribution of each class in relation to elevation by overlaying the management regimes and other land cover classes with the digital elevation model based on the SRTM.

4 Results

We used three classification approaches – (1) pixel-based (Landsat); (2) object-based (Landsat); and (3) hierarchical object-based (Landsat + ERS) – to map land management intensity regimes. Generally, our classifications showed the substantial potential of improved characterizations of land management regimes when using multispectral and SAR data jointly in a hierarchical framework (Table III-2). The overall accuracy of the pixel-based classification (67.4%) was increased markedly in the object-based classification (78.3%). The hierarchical classification, integrating Landsat and ERS data as well as object-based features, outperformed both other approaches in terms of the classification accuracy (83.4%).

The confusion matrix of the pixel-based classification indicated the difficulty to classify *large-scale cropland* (*LSC*) and *small-scale cropland* (*SSC*) solely on pixel-level due to spectral ambiguities (*i.e.*, field size cannot reliably be differentiated spectrally) (Table III-3). Furthermore, there was a noticeable confusion within *active agriculture* (*LSC*, *SSC*, *pasture*) as well as between *active agriculture* and *fallow agriculture*. This caused relatively low producer's and user's accuracies for the agricultural classes in the pixel-based classification (Table III-2).

The object-based classification reduced the confusion between *LSC* and *SSC* as well as the *fallow* class substantially (Table III-4). Specifically, the misclassification of *SSC* within *LSC* was reduced from 25.8% to 10.1% and the misclassification of *fallow* within *LSC* from 25.8% to 5.6%. As a result, the producer's accuracy of *LSC* increased by about 34% from 51.6% to

Table III-2: Accuracy assessment: comparison of pixel-based, object-based and hierarchical classification (PA = producer's accuracy, UA = user's accuracy, OA = overall accuracy) with error-adjusted estimates.

LS classes	**Pixel-based**		**Object-based**		**Hierarchical**	
	PA [%]	UA [%]	PA [%]	UA [%]	PA [%]	UA [%]
LSC	51.6	70.8	85.4	89.0	85.1	89.7
SSC	73.2	43.3	92.5	56.3	91.8	71.4
Pasture	56.5	55.0	74.3	56.6	62.5	65.9
Fallow	67.3	69.4	58.0	81.9	74.0	79.2
Forest	96.8	95.1	92.3	96.1	94.1	96.2
Urban	54.5	76.9	29.5	77.8	63.2	80.0
OA	67.4%		78.3%		83.4%	

Table III-3: Confusion matrix for the pixel-based classification of LS.

Classified	**Reference**						
	LSC	SSC	Pas.	Fal.	For.	Urb.	Tot.
LSC	34	4	5	3	1	1	48
SSC	23	29	5	6		4	67
Pasture	7	2	22	9			40
Fallow	23	4	5	75	1		108
Forest	1		1	2	77		81
Urban	1	2				10	13
Total	89	41	38	95	79	15	357

Table III-4: Confusion matrix for the object-based classification of LS.

Classified	**Reference**						
	LSC	SSC	Pas.	Fal.	For.	Urb.	Tot.
LSC	73			4	3	2	82
SSC	9	36	2	11		6	64
Pasture	2	2	30	19			53
Fallow	5	2	5	59	1		72
Forest			1	2	74		77
Urban		1			1	7	9
Total	89	41	38	95	79	15	357

85.4% and the user's accuracy of *LSC* rose by about 20% to 89.0%. Similar improvements between the pixel-based and object-based classification were observed for the producer's accuracies of *SSC* and *pasture*. However, there was still considerable remaining confusion between *fallow* and *SSC* as well as *pasture*. Thus, the producer's accuracy of *fallow* as well as the user's accuracy of *SSC* and *pasture* were still relatively low at about 56.0% (Table III-2).

With the use of additional SAR data within the hierarchical classification framework, the detection of *fallow* areas was improved substantially, which consequently reduced the confusion between *SSC* and *pasture* (Table III-5). This led to an increase in the producer's accuracy of *fallow* (74.0%) as well as the user's accuracies of *SSC* (71.4%) and *pasture* (65.9%) (Table III-2).

Tests of statistical significance based on the McNemar statistics indicated that the object-based classification resulted in a significantly more accurate map ($p < 0.001$) compared to the pixel-based classification (Table III-6). The hierarchical classification performed well with regard to the classification accuracy, resulting in an overall accuracy that was significantly higher in comparison to the pixel-based ($p < 0.001$) and object-based ($p < 0.05$) approach. (Table III-6).

The map of land management regimes and land cover of our study area showed a heteroge-

Table III-5: Confusion matrix for the hierarchical classification of LS.

Classified	**Reference**						
	LSC	SSC	Pas.	Fal.	For.	Urb.	Tot.
LSC	70	1	2	2	2	1	78
SSC	7	35	2	4		1	49
Pasture		3	27	11			41
Fallow	12		6	76	1	1	96
Forest			1	2	75		78
Urban		2			1	12	15
Total	89	41	38	95	79	15	357

Table III-6: Results of McNemar's tests for the statistical significance of differences between the pixel-based, object-based, and hierarchical classification approaches.

Methods		$\|z\|$	p
Pixel-based	Object-based	3.41	< 0.001
Pixel-based	Hierarchical	5.18	< 0.001
Object-based	Hierarchical	2.07	< 0.05

neous landscape with mainly *forest* and *fallow* in the northern part of Volodymyr-Volynskyi Raion and the southern part of Sokalskyi (Figure III-5). Ivanychivskyi and Horokhivskyi in the center of the study area were mainly covered by *active farmland*. *Pasture* was mostly concentrated in the northern, southern, and western central part of the study area. The *SSC*, mainly subsistence agriculture, can contain individual houses or small villages, since *urban* represented cities with wide impervious surfaces and large urban structures. Consequently, the majority of the urban population lived in the big cities solely located in the western part of the study area while rural populations were concentrated in the central and eastern parts of the study area.

According to the error-adjusted area estimates (Figure III-6), our study area was mostly covered by *large-scale cropland* (29%, ≈190,000 ha). *Small-scale cropland* covered 15% (≈94,000 ha) and *pasture* 12% (≈77,000 ha). Therefore, the agricultural categories with active land use occupied approximately 53% of the study area, whereas about 22% (≈141,000 ha) of the study area was *fallow* land. *Forests* accounted for about 20% of the study area and the cities covered about 2% of the study region.

Comparing the distribution of land management regimes and land cover types along indicators of the marginality of agriculture revealed interesting patterns. Soil quality is a key element for agricultural productivity. As expected, our analysis revealed that the majority of *large-scale cropland* and *small-scale cropland* was cultivated in areas with comparatively good soils (Figure III-7). About 54% of the *LSC* was cultivated on Phaeozems (28%) and Chernozems (25%). Even 60% of *SSC* occurred on Phaeozems and Chernozems. *Forest*,

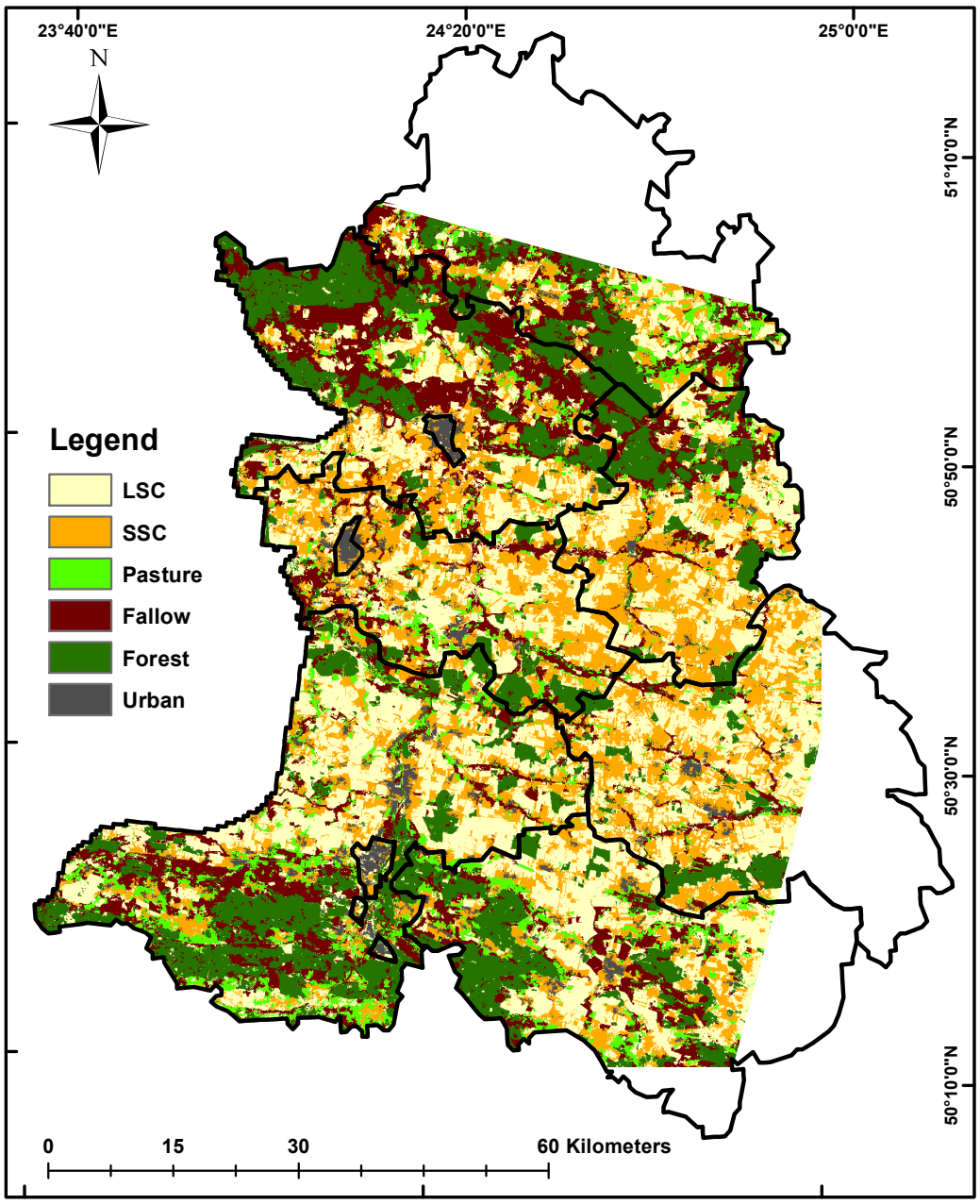

Figure III-5: Agricultural land management regimes and additional land cover classes, mapped using the hierarchical classification based on Landsat and ERS data (LSC = large-scale cropland, SSC = small-scale cropland).

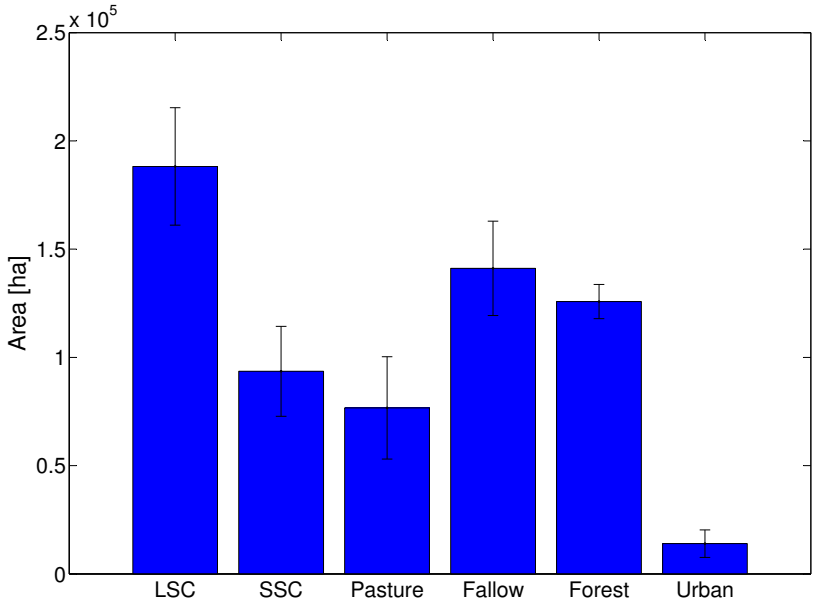

Figure III-6: Error-adjusted area estimates of the hierarchical classification with 95% confidence intervals (LSC = large-scale cropland, SSC = small-scale cropland).

pasture and *fallow* areas were mainly located on Podzols (>40%), the sum of these classes on Phaeozems or Chernozems was below 20%.

The distribution of each class also varied substantially with distance to cities (Figure III-8). The areas very close to the cities (0.5 km) in the study area contained over 25% of *SSC* and only about 13% of *LSC*, 4% *pasture*, and 6% *fallow*. With an increasing distance to cities (and thus local markets), *SSC* decreased while the share of *LSC* and *pasture* increased steadily. The dominance of land management regimes near cities changed from *small-scale cropland* to *large-scale cropland* between 2 and 4 km away from cities. *Fallow* areas increased rapidly up to a distance of 4 km around cities.

Analyzing the distribution of our land management and land cover classes along elevation gradients showed interesting differences between the land management regimes (Figure III-9). The active farmland classes (*LSC* and *SSC*) had their peaks at about 220 meter elevation, whereby *LSC* was more equally distributed compared to *SSC*. *Pasture*, *fallow*, and *forest* occurred mainly at elevations between 180 and 200 m, whereby *pasture* and *fallow* were similarly distributed.

5 Discussion

A growing world population, diet changes, and an increasing role of bioenergy all contribute to a surging demand for agricultural products, and unless major shifts in consumptive behavior occur, this requires potentially a doubling of agricultural production by 2050 (FAO, 2009; Godfray et al., 2010; Foley et al., 2011; Tilman et al., 2011; Ray et al., 2013). Production increases can be achieved following three options: (1) expanding agriculture

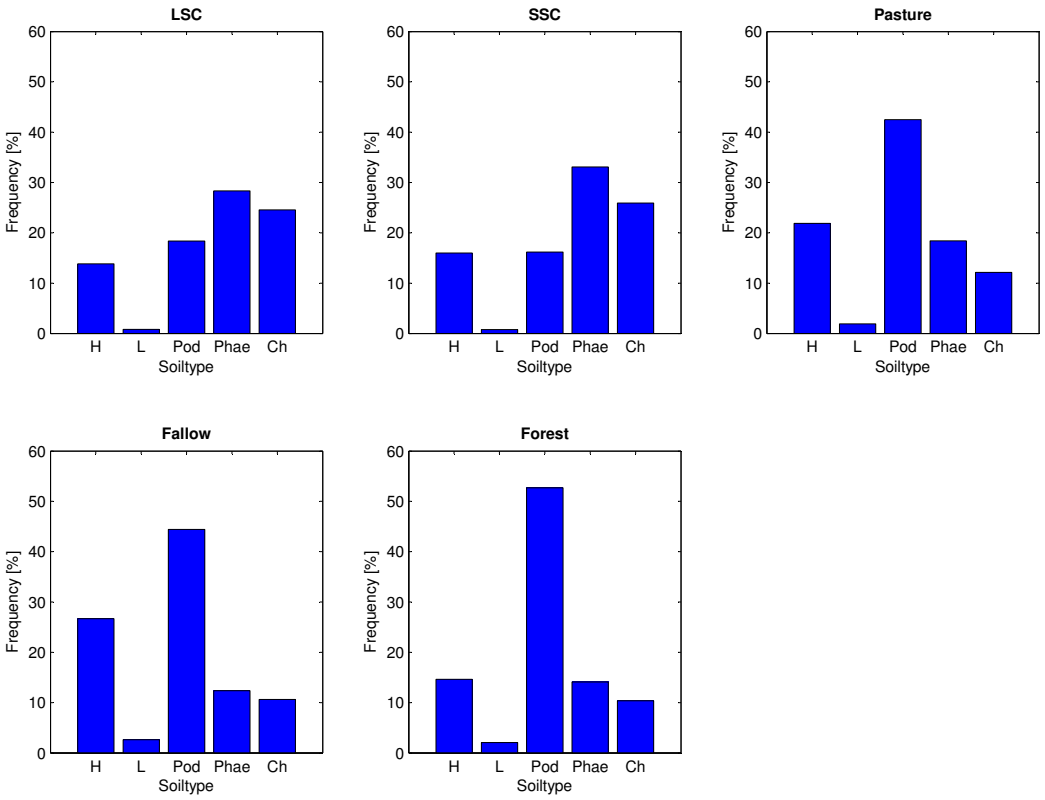

Figure III-7: Distribution of the area of each class across underlying soil types (H: Histosols, L: Leptosols, Pod: Podzol, Phae: Phaeozems, Ch: Chernozems).

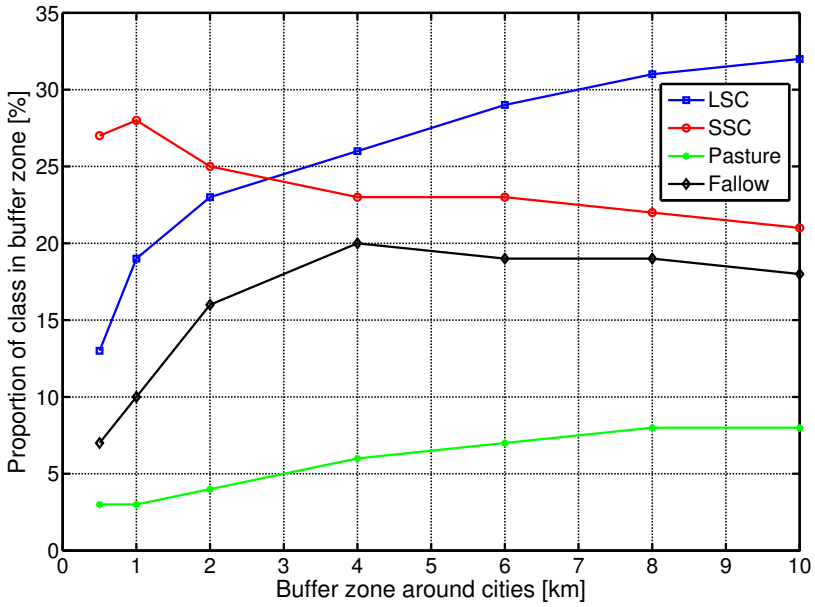

Figure III-8: Distribution of the agricultural classes in dependency of the distance to cities.

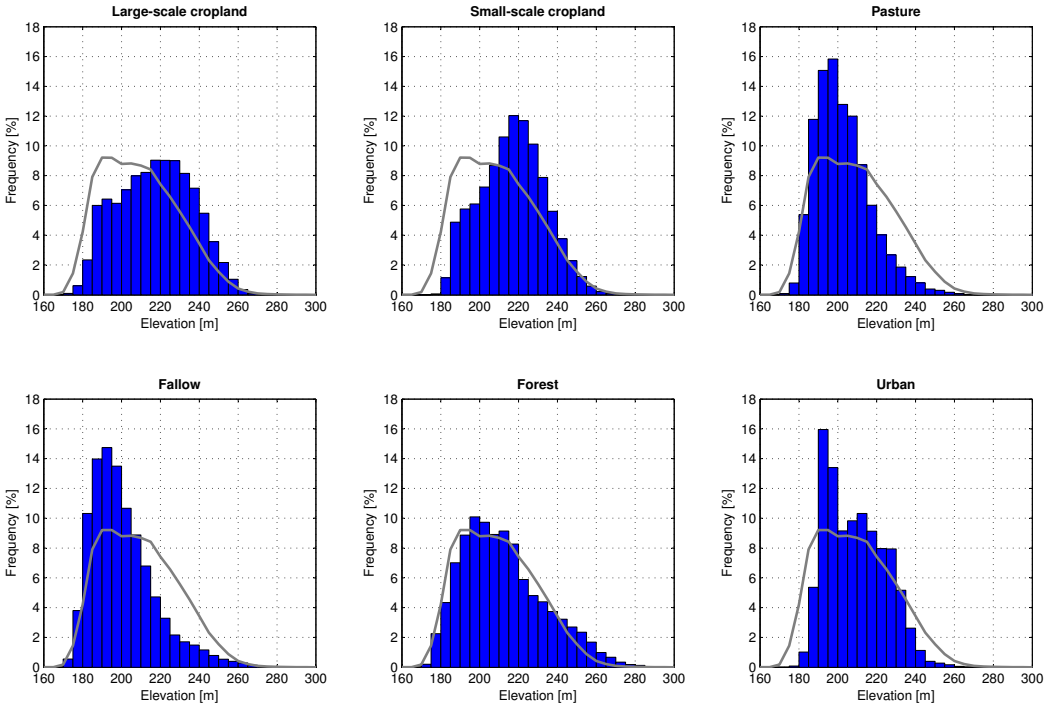

Figure III-9: Histogram showing the distribution of each class in dependency of the elevation; Grey lines show the overall distribution of the elevation in the study area.

into natural ecosystems; (2) intensifying existing farmland; or (3) recultivating abandoned farmland. To decide which strategy is attractive to increase production while mitigating the environmental trade-offs of agriculture, first and foremost it is important to better map and understand spatial heterogeneity in agricultural management intensity, ranging from industrialized to abandoned lands. Mapping agricultural management regimes such as *large-scale cropland*, and *small-scale cropland* (indicating high and low management intensity, respectively), and *fallow* land with remote sensing data provides interesting avenues to improve our understanding of the patterns of agricultural land use intensity, particularly where ground-data on the different aspects of management are scarce.

Our first objective was to analyze the value of an object-based approach in comparison with a pixel-based classification to map land management regimes. Our analyses clearly showed that the pixel-based approach was not capable of differentiating *large-scale cropland* and *small-scale cropland* with high accuracies (Table III-2), likely because of similar spectral characteristics of these classes. In our case, additional object-based features from a multilevel segmentation with different segment scales helped to overcome this problem. The spatial relationships and the different features within the segments provided information about (1) relatively homogenous large fields with one crop type and (2) small fields with inhomogeneous spectral characteristics due to multiple crops within a cluster of kitchen gardens, which is not included in pixel-by-pixel information. Therefore, multilevel object-based features were the key elements to distinguish large and small fields, and thus *large-scale cropland* and

small-scale cropland in our study area.

Our second objective was to assess the value of SAR data (ERS-2 images in our case) within a hierarchical classification framework to enhance the mapping of land management regimes compared to using optical data (Landsat images in our case) alone. As we already noted, *pasture* and *fallow* fields can have similar spectral signatures as well as spatial similarities contrary to *large-scale cropland* and *small-scale cropland*. Therefore, the object-based approach, which was based on the optical data alone, did not noticeably improve the classification accuracy of *pasture* and *fallow* land in comparison to the pixel-based classification. However, the integration of SAR data within the hierarchical classification approach did appreciably improve the classification accuracies of both classes. This was likely due to two reasons. On the one hand, SAR data included complementary information to optical data. On the other hand, additional temporal information of SAR data (*i.e.*, nine available scenes over the year), which enabled an enhanced extraction of information about different phenological stages of pasture and fallow, likely contributed to the higher classification accuracies, when using optical and SAR data jointly.

In general our results emphasize that the integration of both sources, *i.e.*, multisensor data as well as object-based features from different scales, proved useful in terms of the mapping accuracy. This is in accordance with the results achieved by other studies (Shupe & Marsh, 2004; Waske & van der Linden, 2008; Gong et al., 2011), for example, where crop type mapping was enhanced by classifying multiple segmentation levels from SAR and multispectral data (Waske & van der Linden, 2008).

The algorithms that were used in our study proved to be well suited for mapping land management regimes. The Superpixel Contour algorithm was able to separate the Landsat images into meaningful regions, as the visual inspection and the significant improvement of the classification accuracies by the generated objects confirmed. This is also in accordance with the results achieved by Stefanski et al. (2013), where the Superpixel Contour algorithm was analyzed in more detail. The Random Forest classifier also performed very well, as it was already shown in previous studies (Waske & van der Linden, 2008; Stumpf & Kerle, 2011; Rodriguez-Galiano et al., 2012), and seems adequate for handling multisensor data as well as different multilevel features.

Our third objective was to explore the spatial distribution of land management regimes. Generally, the patterns observed in our study region were well in accordance with patterns that we would predict based on classical land rent theory (Ricardo, 1821; Von Thünen, 1966)—*i.e.*, less intensive or no land use on the most marginal plots (higher elevations, less suitable soils, far away from markets). Interestingly, small-scale cropland was most widespread in the vicinity of cities (Figure III-8), whereas large-scale agriculture (*i.e.*, potentially more capital intensive) was found away from cities. Two factors explain this pattern. First, during the Soviet time, large industrialized farms were established and these were often far away from settlements and cities. Second, with the breakdown of the Soviet Union, subsistence agriculture became more important and thus farmland in the vicinity of cities was used for

small-scale farming and gardening, explaining the concentration of *small-scale cropland* close to the cities.

The pattern of the class distribution with regard to elevation can be explained by the local topography. *Large-scale cropland* and *small-scale cropland* is basically concentrated in the center of the study area, where the elevation is higher compared to the north and south, where *pasture*, *fallow*, and *forest* occurred mainly. The occurrence of farmland abandonment in Eastern Europe on lower elevations was surprising, and on first glance not in line with land rent theory. However, other studies (Baumann et al., 2011) have found similar patterns and the factors mentioned above (*i.e.*, collapse of large corporate farms after the breakdown of the Soviet Union, concentration of farming around settlements) explain these patterns as well. Furthermore, some of the lower areas in our study region are frequently flooded (especially as drainage dikes were abandoned), making these areas not well-suited for agriculture.

Earlier studies have found substantial potential for recultivation in the region (Baumann et al., 2011). Our results suggest—about 22% of the whole study area was fallow in 2010—some potential for recultivation of abandoned farmland. However, advanced processes of forest succession (*i.e.*, high amount of woodland) causes increasing recultivation costs (Larsson & Nilsson, 2005). In this context, the additional use of approaches that quantify succession seems sensible (Bergen & Dronova, 2007). About 15% of the study area was *small-scale cropland* with low intensive farming, which suggests some potential for agricultural intensification. We caution though, that the socio-economic and environmental impacts of intensification, and recultivating currently idle cropland, have to be taken into account carefully.

Our study demonstrated that agricultural management regimes can be reliably determined from remote sensing imagery alone when field size can be used as a proxy, which is an important finding given that ground data on management practices is not available for large parts of the world (Kuemmerle et al., 2013; Fritz et al., 2013). Nevertheless, several avenues for further improving our approach are possible. First, auxiliary data may be capable of improving the precision of area estimates. For example, spatial relationships can contribute to classify land management regimes more accurately or population density data may be useful to improve the precision of land cover change estimation (Stehman, 2009). In this context, non-parametric methods that can deal with continues and categorical data like Random Forests appear to be appropriate to integrate and classify diverse datasets, including multisensor data, terrain models, or categorical variables, for example, derived from soil maps (Gislason et al., 2006).

Second, ground data on management or yields could further help to generate a better map of intensity, whereby geostatistical approaches are suitable to integrate such data. Analyzing management regimes over several years may also further improve the precision of mapping management regimes. For example, using previous analyses as prior knowledge or prior probabilities may improve mapping accuracies (McIver & Friedl, 2002).

Third, auxiliary data can be used to avoid misinterpretations of land management regimes

maps. For example, Figure III-6 implied that 22% of the study area was *fallow* and therefore this region should offer great potential for recultivation. However, analyzing the proportion of *fallow* land regarding its underlying soil type revealed that 45% of the *fallow* areas were on Podzol (Figure III-7). As Podzols are generally less attractive soils for cropping due to the low nutrient status, low level of available moisture, and low pH values (IUSS Working Group WRB, 2006), realistic potentials for recultivation in this region have to be further analyzed.

6 Conclusions

Our study aimed at mapping land management regimes as proxies for agricultural land use intensity from satellite imagery. To do so, we compared pixel-based, object-based, and hierarchical classification approaches using Superpixel Contour for segmentation and Random Forests for classification. The proposed classification strategy constitutes a very feasible approach, because the underlying methods (Superpixel Contour/Random Forest) depend only on a few parameters. The object-based approach produced significantly better classification accuracies compared to the pixel-based approach. The hierarchical, multisensor classification based on Landsat and SAR data outperformed both other approaches and yielded a reliable land management intensity regime map.

As demand for agricultural products continues to increase and land resources are increasingly becoming scarce, identifying strategies for increasing agricultural production in sustainable ways has become a research priority and this necessitates better maps on land management. We emphasize the value of our hierarchical multi-sensor approach for mapping land management regimes, as we derive adequate indicators for land use intensity by remote sensing for our study area. This can be a first step to further evaluate trade-offs and benefits from different management regimes as well as methods to systematically asses potentials for increasing agricultural production. The use of auxiliary data as soil maps enable more detailed analysis of the spatial patterns and supports to evaluate the potential of agriculture and recultivation of abandoned farmland in western Ukraine.

Overall, our methodology contributes to new methods for mapping land use intensity, using multisensor remote sensing data. Regarding recent and upcoming missions with increased revisit times and better spatial resolutions as, for example, RapidEye and TerraSAR-X as well as Sentinel-1/-2, the use of multisensor data become even more attractive. In addition, it seems interesting to make full sense of the unique image record that the Landsat image archives provide.

Acknowledgments

This work was supported by the German Research Foundation (DFG-WA 2728/2-1; WA 2728/2-2) and the State Fund of Fundamental Research of Ukraine (N 0113U002752). ERS

data was provided by ESA (C1P.10962). RapidEye data was provided from the RapidEye Science Archive (RESA) by DLR under the proposal id490.

References

Alcantara, C., Kuemmerle, T., Prishchepov, A. V., & Radeloff, V. C. (2012). Mapping abandoned agriculture with multi-temporal MODIS satellite data. *Remote Sensing of Environment*, *124*, 334–347.

Aplin, P., & Atkinson, P. M. (2001). Sub-pixel land cover mapping for per-field classification. *International Journal of Remote Sensing*, *22*, 2853–2858.

Asselen, S., & Verburg, P. H. (2012). A Land System representation for global assessments and land-use modeling. *Global Change Biology*, *18*, 3125–3148.

Atzberger, C. (2013). Advances in remote sensing of agriculture: Context description, existing operational monitoring systems and major information needs. *Remote Sensing*, *5*, 949–981.

Bargiel, D., & Herrmann, S. (2011). Multi-temporal land-cover classification of agricultural areas in two european regions with high resolution spotlight TerraSAR-X data. *Remote Sensing*, *3*, 859–877.

Baumann, M., Kuemmerle, T., Elbakidze, M., Ozdogan, M., Radeloff, V. C., Keuler, N. S., Prishchepov, A. V., Kruhlov, I., & Hostert, P. (2011). Patterns and drivers of post-socialist farmland abandonment in western Ukraine. *Land Use Policy*, *28*, 552–562.

Bergen, K. M., & Dronova, I. (2007). Observing succession on aspen-dominated landscapes using a remote sensing-ecosystem approach. *Landscape Ecology*, *22*, 1395–1410.

Breiman, L. (2001). Random Forests. *Machine Learning*, *45*, 5–32.

Brooks, T. M., Mittermeier, R. A., Mittermeier, C. G., Da Fonseca, G. A. B., Rylands, A. B., Konstant, W. R., Flick, P., Pilgrim, J., Oldfield, S., Magin, G., & Hilton-Taylor, C. (2002). Habitat loss and extinction in the hotspots of biodiversity. *Conservation Biology*, *16*, 909–923.

Bruzzone, L., & Carlin, L. (2006). A multilevel context-based system for classification of very high spatial resolution images. *Geoscience and Remote Sensing, IEEE Transactions on*, *44*, 2587–2600.

Cable, J., Kovacs, J., Shang, J., & Jiao, X. (2014). Multi-temporal polarimetric RADARSAT-2 for land cover monitoring in Northeastern Ontario, Canada. *Remote Sensing*, *6*, 2372–2392.

Cleve, C., Kelly, M., Kearns, F. R., & Moritz, M. (2008). Classification of the wildland–urban interface: A comparison of pixel-and object-based classifications using high-resolution aerial photography. *Computers, Environment and Urban Systems*, *32*, 317–326.

Cohen, W., & Goward, S. (2004). Landsat's role in ecological applications of remote sensing. *Bioscience*, *54*, 535–545.

Dai, X., & Khorram, S. (1998). A hierarchical methodology framework for multisource data fusion in vegetation classification. *International Journal of Remote Sensing*, *19*, 3697–3701.

Ellis, E., Kaplan, J., Fuller, D., Vavrus, S., Goldewijk, K., & Verburg, P. (2013). Used planet: A global history. *Proceedings of the National Academy of Sciences of the United States of America*, *110*, 7978–7985.

Ellis, E. C., & Ramankutty, N. (2008). Putting people in the map: Anthropogenic biomes of the world. *Frontiers in Ecology and the Environment*, *6*, 439–447.

Erb, K.-H., Haberl, H., Jepsen, M. R., Kuemmerle, T., Lindner, M., Müller, D., Verburg, P. H., & Reenberg, A. (2013). A conceptual framework for analysing and measuring land-use intensity. *Current Opinion in Environmental Sustainability*, *5*, 464–470.

EUROSTAT (2009). Lucas 2009 (Land Use / Cover Area Frame Survey) - Instructions for Surveyors. `http://epp.eurostat.ec.europa.eu/portal/page/portal/lucas/documents/LUCAS2009_C1-Instructions_Revised20130925.pdf` (accessed on 5 June 2014).

FAO (2006). *Global Forest Resources Assessment 2005. Progress towards sustainable forest management* volume 147. Rome: FAO.

FAO (2009). Global agriculture towards 2050. Rome, FAO.

Ferguson, M., Badhwar, G., Chhikara, R., & Pitts, D. (1986). Field size distributions for selected agricultural crops in the United States and Canada. *Remote Sensing of Environment*, *19*, 25–45.

Foley, J., Defries, R., Asner, G., Barford, C., Bonan, G., Carpenter, S., Chapin, F., Coe, M., Daily, G., Gibbs, H., Helkowski, J., Holloway, T., Howard, E., Kucharik, C., Monfreda, C., Patz, J., Prentice, I., Ramankutty, N., & Snyder, P. (2005). Global consequences of land use. *Science*, *309*, 570–574.

Foley, J. A., Ramankutty, N., Brauman, K. A., Cassidy, E. S., Gerber, J. S., Johnston, M., Mueller, N. D., O'Connell, C., Ray, D. K., West, P. C., Balzer, C., Bennett, E. M., Carpenter, S. R., Hill, J., Monfreda, C., Polasky, S., Rockström, J., Sheehan, J., Siebert, S., Tilman, D., & Zaks, D. P. M. (2011). Solutions for a cultivated planet. *Nature*, *478*, 337–342.

Foody, G. M. (2002). Status of land cover classification accuracy assessment. *Remote Sensing of Environment*, *80*, 185–201.

Foody, G. M. (2004). Thematic map comparison: Evaluating the statistical significance of differences in classification accuracy. *Photogrammetric Engineering & Remote Sensing*, *70*, 627–633.

Fritz, S., See, L., You, L., Justice, C., Becker-Reshef, I., Bydekerke, L., Cumani, R., Defourny, P., Erb, K., Foley, J., Gilliams, S., Gong, P., Hansen, M., Hertel, T., Herold, M., Herrero, M., Kayitakire, F., Latham, J., Leo, O., McCallum, I., Obersteiner, M., Ramankutty, N., Rocha, J., Tang, H., Thornton, P., Vancutsem, C., van der Velde, M., Wood, S., & Woodcock, C. (2013). The need for improved maps of global cropland. *Eos, Transactions American Geophysical Union*, *94*, 31–32.

Gislason, P. O., Benediktsson, J. A., & Sveinsson, J. R. (2006). Random Forests for land cover classification. *Pattern Recognition Letters*, *27*, 294–300.

Godfray, H. C. J., Beddington, J. R., Crute, I. R., Haddad, L., Lawrence, D., Muir, J. F., Pretty, J., Robinson, S., Thomas, S. M., & Toulmin, C. (2010). Food security: The challenge of feeding 9 billion people. *Science*, *327*, 812–818.

Goldewijk, K. K. (2001). Estimating global land use change over the past 300 years: The HYDE database. *Global Biogeochemical Cycles*, *15*, 417–433.

Gong, B., Im, J., & Mountrakis, G. (2011). An artificial immune network approach to multi-sensor land use/land cover classification. *Remote Sensing of Environment*, *115*, 600–614.

Griffiths, P., Hostert, P., Gruebner, O., & van der Linden, S. (2010). Mapping megacity growth with multi-sensor data. *Remote Sensing of Environment*, *114*, 426–439.

Griffiths, P., Müller, D., Kuemmerle, T., & Hostert, P. (2013). Agricultural land change in the Carpathian ecoregion after the breakdown of socialism and expansion of the European Union. *Environmental Research Letters*, *8*, 1–12.

Hett, C., Castella, J.-C., Heinimann, A., Messerli, P., & Pfund, J.-L. (2012). A landscape mosaics approach for characterizing swidden systems from a REDD+ perspective. *Applied Geography*, *32*, 608–618.

Hsu, C.-W., Chang, C.-C., & Lin, C.-J. (2003). *A Practical Guide to Support Vector Classification*. Technical Report Department of Computer Science, National Taiwan University, Taipei, Taiwan.

Ioffe, G., Nefedova, T., & De Beurs, K. (2012). Land abandonment in Russia. *Eurasian Geography and Economics*, *53*, 527–549.

IUSS Working Group WRB (2006). *World reference base for soil resources 2006*. World Soil Resources Reports No. 103. FAO, Rome.

Jones, D. A., Hansen, A. J., Bly, K., Doherty, K., Verschuyl, J. P., Paugh, J. I., Carle, R., & Story, S. J. (2009). Monitoring land use and cover around parks: A conceptual approach. *Remote Sensing of Environment*, *113*, 1346–1356.

Killeen, T. J., Anna Guerra, Miki Calzada, Lisette Correa, Veronica Calderon, Liliana Soria, Belem Quezada, & Marc K. Steininger (2008). Total historical land-use change in Eastern Bolivia: Who, where, when, and how much? *Ecology and Society*, *13*, 1–27.

Kindu, M., Schneider, T., Teketay, D., & Knoke, T. (2013). Land use/land cover change analysis using object-based classification approach in Munessa-Shashemene Landscape of the Ethiopian Highlands. *Remote Sensing*, *5*, 2411–2435.

Kleijn, D., Kohler, F., Baldi, A., Batary, P., Concepcion, E., Clough, Y., Diaz, M., Gabriel, D., Holzschuh, A., Knop, E., Kovacs, A., Marshall, E., Tscharntke, T., & Verhulst, J. (2009). On the relationship between farmland biodiversity and land-use intensity in Europe. *Proceedings of the Royal Society B: Biological Sciences*, *276*, 903–909.

Kovalskyy, V., & Roy, D. (2013). The global availability of Landsat 5 TM and Landsat 7 ETM+ land surface observations and implications for global 30m Landsat data product generation. *Remote Sensing of Environment*, *130*, 280–293.

Kuemmerle, T., Erb, K., Meyfroidt, P., Müller, D., Verburg, P. H., Estel, S., Haberl, H., Hostert, P., Jepsen, M. R., Kastner, T., Levers, C., Lindner, M., Plutzar, C., Verkerk, P. J., van der Zanden, E. H., & Reenberg, A. (2013). Challenges and opportunities in mapping land use intensity globally. *Current Opinion in Environmental Sustainability*, *5*, 484–493.

Kuemmerle, T., Hostert, P., St-Louis, V., & Radeloff, V. C. (2009). Using image texture to map farmland field size: A case study in Eastern Europe. *Journal of Land Use Science*, *4*, 85–107.

Kuemmerle, T., Olofsson, P., Chaskovskyy, O., Baumann, M., Ostapowicz, K., Woodcock, C. E., Houghton, R. A., Hostert, P., Keeton, W. S., & Radeloff, V. C. (2011). Post-Soviet farmland abandonment, forest recovery, and carbon sequestration in western Ukraine. *Global Change Biology*, *17*, 1335–1349.

Kuemmerle, T., Radeloff, V. C., Perzanowski, K., & Hostert, P. (2006). Cross-border comparison of land cover and landscape pattern in Eastern Europe using a hybrid classification technique. *Remote Sensing of Environment*, *103*, 449–464.

Kuplich, T., Freitas, C. d. C., & Soares, J. (2000). The study of ERS-1 SAR and Landsat TM synergism for land use classification. *International Journal of Remote Sensing*, *21*, 2101–2111.

Lambin, E. F., & Meyfroidt, P. (2011). Inaugural article: Global land use change, economic globalization, and the looming land scarcity. *Proceedings of the National Academy of Sciences*, *108*, 3465–3472.

Larsson, S., & Nilsson, C. (2005). A remote sensing methodology to assess the costs of preparing abandoned farmland for energy crop cultivation in northern Sweden. *Biomass and Bioenergy*, *28*, 1–6.

Li, P., Feng, Z., Jiang, L., Liao, C., & Zhang, J. (2014). A review of swidden agriculture in Southeast Asia. *Remote Sensing*, *6*, 1654–1683.

Li, Y., Gong, J., Wang, D., An, L., & Li, R. (2013). Sloping farmland identification using hierarchical classification in the Xi-He region of China. *International Journal of Remote Sensing*, *34*, 545–562.

Lloyd, C. D., Berberoglu, S., Curran, P. J., & Atkinson, P. M. (2004). A comparison of texture measures for the per-field classification of Mediterranean land cover. *International Journal of Remote Sensing*, *25*, 3943–3965.

Loveland, T. R., Cochrane, M. A., & Henebry, G. M. (2008). Landsat still contributing to environmental research. *Trends in Ecology & Evolution*, *23*, 182–183.

Matson, P. A., Parton, W. J., Power, A. G., & Swift, M. J. (1997). Agricultural intensification and ecosystem properties. *Science*, *277*, 504–509.

McIver, D., & Friedl, M. (2002). Using prior probabilities in decision-tree classification of remotely sensed data. *Remote Sensing of Environment*, *81*, 253–261.

Mester, R., Conrad, C., & Guevara, A. (2011). Multichannel segmentation using contour relaxation: Fast super-pixels and temporal propagation. In *Proceedings of the 17th Scandinavian conference on Image analysis* SCIA'11 (pp. 250–261). Berlin, Heidelberg: Springer-Verlag.

Moskal, L. M., Styers, D. M., & Halabisky, M. (2011). Monitoring urban tree cover using object-based image analysis and public domain remotely sensed data. *Remote Sensing*, *3*, 2243–2262.

Mueller, N. D., Gerber, J. S., Johnston, M., Ray, D. K., Ramankutty, N., & Foley, J. A. (2012). Closing yield gaps through nutrient and water management. *Nature*, *490*, 254–257.

Müller, D., Kuemmerle, T., Rusu, M., & Griffiths, P. (2009). Lost in transition: Determinants of post-socialist cropland abandonment in Romania. *Journal of Land Use Science*, *4*, 109–129.

NOAA (2011). NCDC (National Climate Data Center). Available through National Oceanic and Atmospheric Administration (NOAA): `http://www.ncdc.noaa.gov/` (accessed on 5 June 2014).

Olofsson, P., Foody, G. M., Stehman, S. V., & Woodcock, C. E. (2013). Making better use of accuracy data in land change studies: Estimating accuracy and area and quantifying uncertainty using stratified estimation. *Remote Sensing of Environment*, *129*, 122–131.

Ozdogan, M., & Woodcock, C. E. (2006). Resolution dependent errors in remote sensing of cultivated areas. *Remote Sensing of Environment*, *103*, 203–217.

Pohl, C., & Van Genderen, J. L. (1998). Review article multisensor image fusion in remote sensing: Concepts, methods and applications. *International Journal of Remote Sensing*, *19*, 823–854.

Prishchepov, A. V., Radeloff, V. C., Dubinin, M., & Alcantara, C. (2012). The effect of Landsat ETM/ETM+ image acquisition dates on the detection of agricultural land abandonment in Eastern Europe. *Remote Sensing of Environment*, *126*, 195–209.

Ray, D. K., Mueller, N. D., West, P. C., Foley, J. A., & Hart, J. P. (2013). Yield trends are insufficient to double global crop production by 2050. *PLoS ONE*, *8*, 1–8.

Ricardo, D. (1821). *On the Principles of Political Economy and Taxation*. John Murray.

Rodriguez, C., & Wiegand, K. (2009). Evaluating the trade-off between machinery efficiency and loss of biodiversity-friendly habitats in arable landscapes: The role of field size. *Agriculture, Ecosystems & Environment*, *129*, 361–366.

Rodriguez-Galiano, V., Chica-Olmo, M., Abarca-Hernandez, F., Atkinson, P., & Jeganathan, C. (2012a). Random Forest classification of Mediterranean land cover using multi-seasonal imagery and multi-seasonal texture. *Remote Sensing of Environment*, *121*, 93–107.

Rodriguez-Galiano, V., Ghimire, B., Rogan, J., Chica-Olmo, M., & Rigol-Sanchez, J. (2012b). An assessment of the effectiveness of a Random Forest classifier for land-cover classification. *ISPRS Journal of Photogrammetry and Remote Sensing*, *67*, 93–104.

Rounsevell, M. D., Pedroli, B., Erb, K.-H., Gramberger, M., Busck, A. G., Haberl, H., Kristensen, S., Kuemmerle, T., Lavorel, S., Lindner, M., Lotze-Campen, H., Metzger, M. J., Murray-Rust, D., Popp, A., Pérez-Soba, M., Reenberg, A., Vadineanu, A., Verburg, P. H., & Wolfslehner, B. (2012). Challenges for land system science. *Land Use Policy*, *29*, 899–910.

Rudorff, Bernardo Friedrich Theodor, de Aguiar, Daniel Alves, da Silva, Wagner Fernando, Sugawara, L. M., Adami, M., & Moreira, M. A. (2010). Studies on the rapid expansion of sugarcane for ethanol production in São Paulo State (Brazil) using Landsat data. *Remote Sensing*, *2*, 1057–1076.

Sabates-Wheeler, R. (2002). Consolidation initiatives after land reform: Responses to multiple dimensions of land fragmentation in Eastern European agriculture. *Journal of International Development*, *14*, 1005–1018.

Shupe, S. M., & Marsh, S. E. (2004). Cover- and density-based vegetation classifications of the Sonoran Desert using Landsat TM and ERS-1 SAR imagery. *Remote Sensing of Environment*, *93*, 131–149.

Sieber, A., Kuemmerle, T., Prishchepov, A. V., Wendland, K. J., Baumann, M., Radeloff, V. C., Baskin, L. M., & Hostert, P. (2013). Landsat-based mapping of post-Soviet land-use change to assess the effectiveness of the Oksky and Mordovsky protected areas in European Russia. *Remote Sensing of Environment*, *133*, 38–51.

Siebert, S., Portmann, F. T., & Döll, P. (2010). Global patterns of cropland use intensity. *Remote Sensing*, *2*, 1625–1643.

Skriver, H., Mattia, F., Satalino, G., Balenzano, A., Pauwels, V., Verhoest, N., & Davidson, M. (2011). Crop classification using short-revisit multitemporal SAR data. *Selected Topics in Applied Earth Observations and Remote Sensing, IEEE Journal of*, *4*, 423–431.

Souza, Jr, Carlos, Siqueira, J., Sales, M., Fonseca, A., Ribeiro, J., Numata, I., Cochrane, M., Barber, C., Roberts, D., & Barlow, J. (2013). Ten-Year Landsat classification of deforestation and forest degradation in the Brazilian Amazon. *Remote Sensing*, *5*, 5493–5513.

State Statistics Committee of Ukraine (2001). All-Ukrainian Population Census 1979-2001., `http://www.ukrcensus.gov.ua/eng/` (accessed on 5 June 2014).

Stefanski, J., Mack, B., & Waske, B. (2013). Optimization of object-based image analysis with Random Forests for land cover mapping. *IEEE Journal of Selected Topics in Applied Earth Observations and Remote Sensing*, *6*, 2492–2504.

Stehman, S. V. (2009). Model-assisted estimation as a unifying framework for estimating the area of land cover and land-cover change from remote sensing. *Remote Sensing of Environment*, *113*, 2455–2462.

Stumpf, A., & Kerle, N. (2011). Object-oriented mapping of landslides using Random Forests. *Remote Sensing of Environment*, *115*, 2564–2577.

Sulla-Menashe, D., Friedl, M. A., Krankina, O. N., Baccini, A., Woodcock, C. E., Sibley, A., Sun, G., Kharuk, V., & Elsakov, V. (2011). Hierarchical mapping of Northern Eurasian land cover using MODIS data. *Remote Sensing of Environment*, *115*, 392–403.

Tilman, D., Balzer, C., Hill, J., & Befort, B. L. (2011). From the cover: Global food demand and the sustainable intensification of agriculture. *Proceedings of the National Academy of Sciences*, *108*, 20260–20264.

Turner, B. L., & Doolittle, W. E. (1978). The concept and measure of agricultural intensity. *The Professional Geographer*, *30*, 297–301.

Turner, B. L., Lambin, E. F., & Reenberg, A. (2007). Land change science special feature: The emergence of land change science for global environmental change and sustainability. *Proceedings of the National Academy of Sciences*, *104*, 20666–20671.

UNEP (2005). *One Planet Many People: Atlas of Our Changing Environment*. Division of Early Warning and Assessment (DEWA), United Nations Environment Programme (UNEP), Nairobi, Kenya.

USGS (2013). Landsat Processing Details. United States Geological Survey (USGS) `http://landsat.usgs.gov/Landsat_Processing_Details.php` (accessed on 5 June 2014).

Václavík, T., Lautenbach, S., Kuemmerle, T., & Seppelt, R. (2013). Mapping global land system archetypes. *Global Environmental Change*, *23*, 1637–1647.

Verburg, P. H., Neumann, K., & Nol, L. (2011). Challenges in using land use and land cover data for global change studies. *Global Change Biology*, *17*, 974–989.

Von Thünen, J. H. (1966). *Von Thünen's Isolated State: An English Edition of: (1826) Der Isolierte Staat. Edited with an Introduction by Peter Hall*. Pergamon Press.

Waske, B., & Benediktsson, J. (2007). Fusion of support vector machines for classification of multisensor data. *IEEE Transactions on Geoscience and Remote Sensing*, *45*, 3858–3866.

Waske, B., & Braun, M. (2009). Classifier ensembles for land cover mapping using multitemporal SAR imagery. *ISPRS Journal of Photogrammetry and Remote Sensing*, *64*, 450–457.

Waske, B., & van der Linden, S. (2008). Classifying multilevel imagery from SAR and optical sensors by decision fusion. *IEEE Transactions on Geoscience and Remote Sensing*, *46*, 1457–1466.

Wästfelt, A., Tegenu, T., Nielsen, M. M., & Malmberg, B. (2012). Qualitative satellite image analysis: Mapping spatial distribution of farming types in Ethiopia. *Applied Geography*, *32*, 465–476.

Whiteside, T. G., Boggs, G. S., & Maier, S. W. (2011). Comparing object-based and pixel-based classifications for mapping savannas. *International Journal of Applied Earth Observation and Geoinformation*, *13*, 884–893.

Woodcock, C. E., Allen, R., Anderson, M., Belward, A., Bindschadler, R., Cohen, W., Gao, F., Goward, S. N., Helder, D., Helmer, E., Nemani, R., Oreopoulos, L., Schott, J., Thenkabail, P. S., Vermote, E. F., Vogelmann, J., Wulder, M. A., & Wynne, R. (2008). Free access to Landsat imagery. *Science*, *320*, 1011.

Yan, L., & Roy, D. P. (2014). Automated crop field extraction from multi-temporal Web Enabled Landsat Data. *Remote Sensing of Environment*, *144*, 42–64.

Zaks, D. P. M., & Kucharik, C. J. (2011). Data and monitoring needs for a more ecological agriculture. *Environmental Research Letters*, *6*, 1–10.

Zhu, Z., Woodcock, C. E., Rogan, J., & Kellndorfer, J. (2012). Assessment of spectral, polarimetric, temporal, and spatial dimensions for urban and peri-urban land cover classification using Landsat and SAR data. *Remote Sensing of Environment*, *117*, 72–82.

Chapter IV:

Mapping and monitoring of land use changes in post-Soviet western Ukraine using remote sensing data

Applied Geography, vol. 55, pp. 155–164, December 2014

Jan Stefanski, Oleh Chaskovskyy, and Björn Waske

© 2014 Elsevier Ltd. All rights reserved.
http://dx.doi.org/10.1016/j.apgeog.2014.08.003

Abstract

While agriculture is expanded and intensified in many parts of the world, decreases in land use intensity and farmland abandonment take place in other parts. Eastern Europe experienced widespread changes of agricultural land use after the collapse of the Soviet Union in 1991, however, rates and patterns of these changes are still not well understood. Our objective was to map and analyze changes of land management regimes, including large-scale cropland, small-scale cropland, and abandoned farmland. Monitoring land management regimes is a promising avenue to better understand the temporal and spatial patterns of land use intensity changes. For mapping and change detection, we used an object-based approach with Superpixel segmentation for delineating objects and a Random Forest classifier. We applied this approach to Landsat and ERS SAR data for the years 1986, 1993, 1999, 2006, and 2010 to estimate change trajectories for this time period in western Ukraine. The first period during the 1990s was characterized by post-socialist transition processes including farmland abandonment and substantial subsistence agriculture. Later on, recultivation processes and the recurrence of industrial, large-scale farming were triggered by global food prices that have led to a growing interest in this region.

1 Introduction

Substantial increase in land-based production (e.g., food, fiber, bioenergy) is needed as long as the global demand for agricultural products steadily increases and no changes in consumption occur (Godfray et al., 2010; Lotze-Campen et al., 2010; Tilman et al., 2011). To increase land-based production, either agriculture can be expanded into (other) ecosystems, existing farmland can be intensified, or abandoned farmland can be recultivated. While the transformation of forest to agricultural systems is widely studied and relatively well understood, particularly in the tropics, (Geist & Lambin, 2002; Hansen et al., 2008), patterns of agricultural intensification and abandonment remain unclear for most parts of the world (Kuemmerle et al., 2013; Fritz et al., 2013). However, monitoring status and trends of agricultural landscapes can provide important information to reduce the environmental impact of agricultural production (Zaks & Kucharik, 2011) and to identify potential regions for sustainable intensification or recultivation.

During the last decades remote sensing became a valuable tool for environmental monitoring and land cover mapping. In context of agriculture, existing studies mainly focused on mapping different crop types (Wardlow et al., 2007; McNairn et al., 2009a; Waske & Braun, 2009) as well as on monitoring changes in cropland extent and the proximate drivers so far (Shalaby & Tateishi, 2007; Zhang et al., 2013; Wagner et al., 2013). However, there are lacks of approaches sensitive to land use intensity because remote sensing can only rarely measure the complex terms of land use intensity (Kuemmerle et al., 2013).

One way for a more nuanced representation of agricultural landscapes is to map land management regimes as proxies of land use intensity (Verburg et al., 2011; Kuemmerle et al., 2013; Stefanski et al., 2014). Only a few studies have used such approaches at global (Ellis & Ramankutty, 2008; Václavík et al., 2013) or regional scales (Stefanski et al., 2014). Stefanski et al. (2014), for example, used the representation of management regimes that differed in field sizes, i.e., (1) large-scale, mechanized agriculture, (2) small-scale, subsistence agriculture, and (3) fallow or abandoned farmland. While large-scale, mechanized agriculture implied high management intensity, small-scale, subsistence agriculture had basically a low management intensity. Monitoring land management regimes, however, requires adequate data sets and methods.

Although optical remote sensing data are generally a powerful tool for mapping land use/cover changes (Loveland et al., 2008; El-Kawy et al., 2011), the problem of cloud cover is a potentially limiting factor (Moran et al., 2002). This seems particularly critical in context of agricultural landscapes. Managed cropland and grassland show typical temporal patterns due to the phenology of planted crops and management activities, while abandoned farmland is not affected by these activities. Nevertheless, a differentiation between grassland and cropland or grassland and abandoned farmland can be challenging due to spectral ambiguity of the multispectral remote sensing data. Accordingly, the use of multitemporal data seems promising. Prishchepov et al. (2012) recommends the use of three Landsat scenes - from spring, summer, and fall - for a reliable mapping of agricultural abandonment in Eastern Europe.

Moreover, besides the requirement of an adequate data set for one time period, the monitoring of land management changes requires multitemporal data sets from different years for the same study site. However, regarding the repetition rate of typical systems like Landsat and the problem of cloud cover, the generation of adequate multitemporal data sets can be challenging, while data with higher temporal coverage and wide swath (e.g., MODIS and MERIS) are inadequate in capturing land use/cover changes at fine scales.

Synthetic Aperture Radar (SAR) data on the other hand might overcome spectral ambiguities of multispectral data and are (almost) weather independent and thus useful to fill gaps in optical time series. Furthermore, multispectral and SAR systems operate in different wavelengths, ranging from visible to microwave and consequently provide different, but often complementary information (Pohl & Van Genderen, 1998). Thus, a combination of multispectral imagery with SAR data is worthwhile and it has been demonstrated in several studies that multisensor analysis significantly improves the accuracy of land use/cover classifications (Kuplich et al., 2000; Waske & Benediktsson, 2007; McNairn et al., 2009a).

Besides the availability of adequate image data for all relevant time periods, the use of adequate classifier algorithms and change detection approaches is critical. Standard classifiers are often not adequate for classifying multisensor and multitemporal data sets, because in most cases the class distributions cannot be modeled by adequate multivariate statistical models. However, machine learning algorithms such as support vector machines

and classifier ensembles have emerged over the past years in the remote sensing community and are well suited for handling diverse remote sensing data sets (Gislason et al., 2006; Waske et al., 2009; Mountrakis et al., 2011). Particularly the classifier ensemble Random Forests (Breiman, 2001) is well suited for handling multitemporal SAR and multisensor data and has proved to be simple and accurate (Waske & van der Linden, 2008; Waske & Braun, 2009; Rodriguez-Galiano et al., 2012).

Remote sensing based change detection includes basically bi-temporal and trajectory-based change detection methods (McRoberts, 2013). While bi-temporal change detection assesses only the type and extent of change between two defined points in time, trajectory analyses use three or more dates to additionally assess trends and temporal patterns of change over time (Mertens & Lambin, 2000; Kennedy et al., 2007; Carmona & Nahuelhual, 2012). However, using trajectory analyses for detailed characterization of land change dynamics typically requires extensive time series (Kennedy et al., 2007; Sieber et al., 2013). Since the backscatter intensity of SAR data is almost independent from weather conditions, time-series can be produced most reliably using SAR imagery.

In our study, we explored the potential of multispectral Landsat and ERS SAR data to monitor land management regimes in western Ukraine. After the collapse of the Soviet Union, Eastern Europe experienced drastic political and socio-economic changes. This led to farmland abandonment as well as the conversion of (collectivized) large-scale agriculture to small fields, used for subsistence agriculture (Müller & Sikor, 2006; Kuemmerle et al., 2006; Alcantara et al., 2012). While widespread farmland abandonment often results in land fragmentation and simplification of landscapes (Sikor et al., 2009; Peringer et al., 2013), small-scale agriculture or basically subsistence agriculture in rural areas can preserve natural resources (Ioja et al., 2014). Analyzing traditional agricultural land use with its positive aspects for natural and cultural biodiversity in a case study in Eastern Europe seems therefore particularly interesting (Angelstam et al., 2013; Munteanu et al., 2014). More recently, recultivation of abandoned farmland emerges, triggered by the global trend of food prices. Overall, this region is particularly interesting to monitor land management regimes over the past decades.

Farmland abandonment in Eastern Europe was successfully mapped in different studies, using optical remote sensing data at different scales (Alcantara et al., 2012; Kuemmerle et al., 2006, 2011; Griffiths et al., 2013). In contrast to this, the recultivation of abandoned farmland and extend of subsistence agriculture were rarely discussed. Stefanski et al. (2014) mapped current land management regimes in western Ukraine, including large-scale agriculture and small fields, using optical and SAR data. However, this study is based on a data set from one time period and consequently, temporal changes in land use management were not analyzed. Therefore, we explore the spatio-temporal patterns of land management regimes between 1986 and 2010 in this study.

We used an object-based approach based on Landsat and ERS SAR data to map land use/cover in the years: 1986, 1993, 1999, 2006, and 2010. Then, we used change trajectories

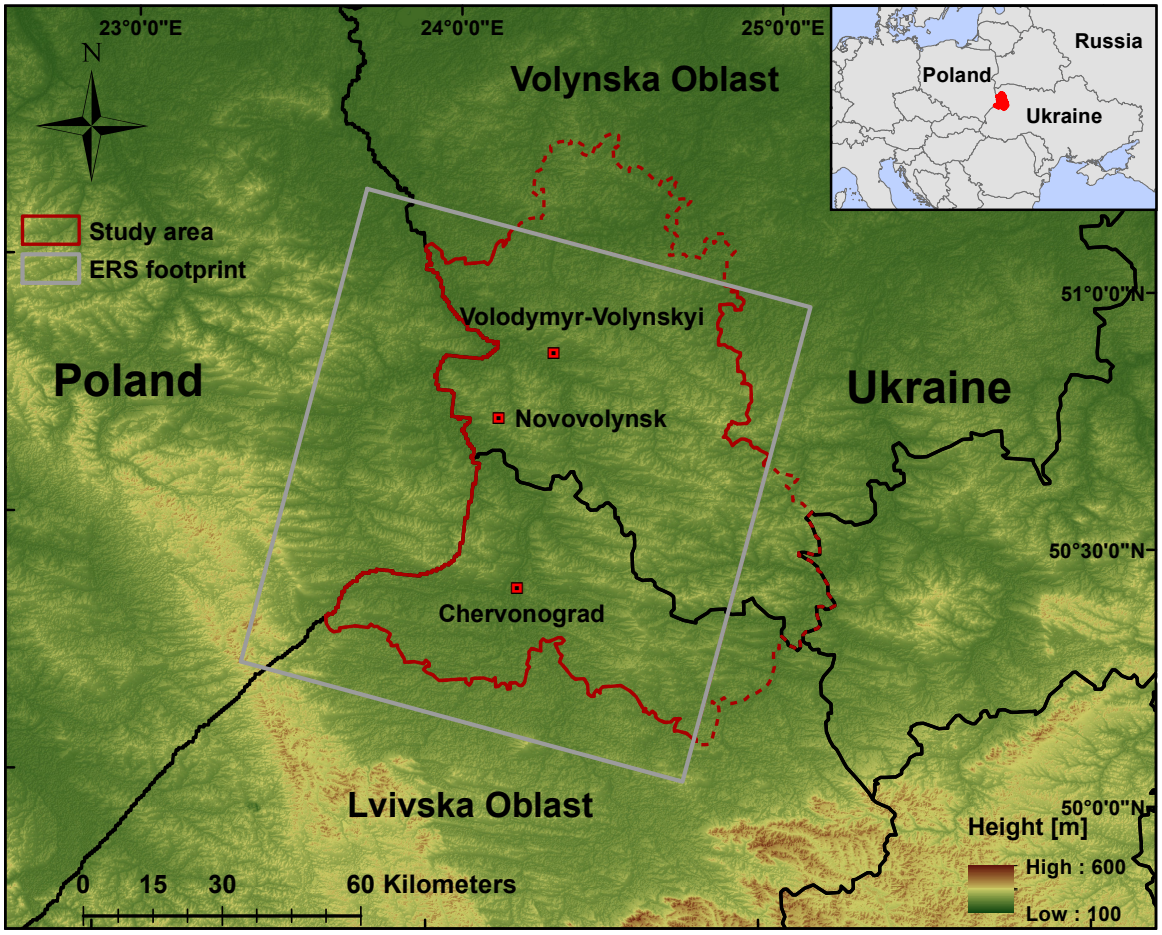

Figure IV-1: Map showing the study area in western Ukraine and a footprint of the used ERS data.

to derive changes of cropland (including large-scale and small-scale cropland), grassland, and fallow or abandoned land. Overall, we focused on the following objectives: (1) assessing the potential of SAR data to complement optical data for monitoring land management regimes, (2) analyzing the changes of land management intensities, i.e., the transformation of industrial, large-scale farming to subsistence agriculture, and (3) analyzing the spatio-temporal patterns of farmland abandonment and recultivation.

2 Material

2.1 Study area

Our study area is located in Volynska and Lvivska Oblasts in western Ukraine and covers about 7,500 km^2 (Figure IV-1). The study region is dominated by agriculture and forests. Agricultural land use types vary from large-scale, intensively managed farmland to small-scale, subsistence and low intensively managed farmland to fallow or abandoned farmland.

The study area is particularly interesting to monitor land management regimes because this

region is characterized by a large variability of socio-economic and environmental conditions, which caused marked spatial heterogeneity in management intensity. During the Soviet time, land management was characterized by collectivized, large-scale farmland (Mathijs & Swinnen, 1998). With the breakdown of the Soviet Union in 1991, drastic shifts in political and socio-economic conditions triggered widespread land changes such as land fragmentation, substantial abandonment of agricultural fields, and the emergence of subsistence agriculture (Sabates-Wheeler, 2002; Kuemmerle et al., 2006; Baumann et al., 2011). Yet, with the recent integration of this region into world markets, recultivation of abandoned land takes place.

2.2 Data set and preprocessing

To monitor land management regimes between 1986 and 2010, we used optical (Landsat) and SAR (ERS) data for different dates (Figure IV-2). As the ERS-1 satellite was launched in 1991, we used four Landsat scenes (path/row 185/25) recorded at 4 April, 8 August, 11 October, and 12 November 1986 to map land use and land cover during the Soviet period. To map the land use changes in the following years, we used six (1993) and eight (1999, 2006) ERS SAR images. For the mapping of land management regimes in 2010, we combined two Landsat (7 June 2010 and 14 November 2010) and nine ERS images (Figure IV-2).

We acquired the Landsat scenes already preprocessed on level L1T, which ensured a sufficient geometric and radiometric accuracy for our analysis (USGS, 2013). All ERS scenes were acquired in a single look complex (SLC) image format. We applied a standard SAR preprocessing using NEST-4C separate for each year, including radiometric and geometric corrections as well as Gamma speckle-filtering. Finally, we resampled all ERS images to 30 meter pixel size to match the resolution of Landsat data.

Reference data were acquired during an extensive field campaign in 2012 (Stefanski et al., 2014). By using a random clustered sampling technique, we allocated 357 points to be used for validation. Three surveying teams assessed the points in the field by using a survey protocol based on the Land Use and Cover Area frame Survey (LUCAS) guidelines (EUROSTAT, 2009). Additionally, high-resolution RapidEye images supported the field mission and generation of the reference set. To adjust the 357 points for validation to the years 1986, 1993, and 2006, we visually interpreted Landsat data for each year.

To acquire training data for 2010, we used information collected during the field campaign that was independent from validation data and, additionally, visually interpreted RapidEye data. During the generation of the training data, we ensured that training and test data were spatially disjoint. The adjustment of the training set to the years 1986, 1993, and 2006 was analogous to the validation set.

3 Methods

The monitoring of land management regimes was based on object-based approaches with the following steps: (1) generating a base map for 1986, including the land use classes cropland,

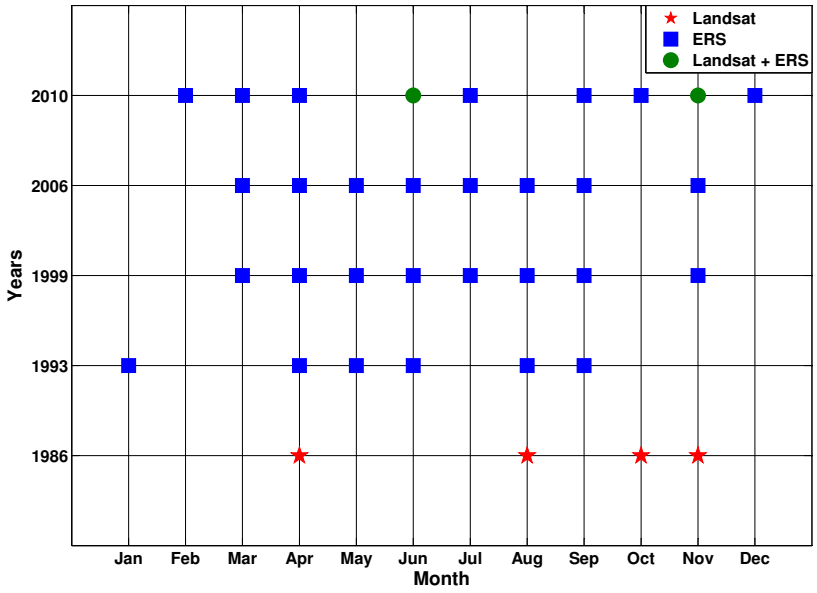

Figure IV-2: Acquisition dates of remote sensing data used in this study.

grassland, forest, and urban, (2) mapping cropland and grassland for the years 1993, 1999, and 2006, (3) mapping land management regimes for 2010, including *large-scale cropland*, *small-scale cropland*, and *grassland*, and finally (4) a trajectory analysis to determine changes of land management regimes. Based on our field campaign and visual interpretation of remote sensing data, we made three general assumptions in our study. First, the class *cropland* incorporated solely *large-scale cropland* in 1986. An explanation for this is the general collectivization of agricultural fields to large fields in the Soviet system. Second, as we did not find changes of forest and urban areas over the time, we summarized both classes in "*Forest and Urban*" and masked them. Third, we analyzed the abandonment of cropland (i.e., the transition of *cropland* to *grassland*) and did not differentiate managed/unmanaged grassland, which is not resolvable with Landsat and ERS SAR data.

For the classifications of step (1)–(3), we used an object-based approach by using the Superpixel Contour algorithm (Mester et al., 2011) for image segmentation and the Random Forest classifier (Breiman, 2001) for classification. The Superpixel Contour segmentation, the freely available Random Forest code (Jaiantilal, 2009), and the trajectory analysis were implemented in MATLAB.

3.1 Object-based classification

The Superpixel Contour (SPc) algorithm is an iterative, region-based segmentation approach introduced by Mester et al. (2011). The SPc proved well in context of remote sensing and provides very similar results in comparison to the widely-used segmentation algorithm in eCognition (Stefanski et al., 2013). The general principle of a segmentation algorithm is to separate an image into homogenous regions such as segments or superpixels, which ideally

represent real world objects. To do so, the SPc optimizes a non-specified initial segmentation along its boundaries based on the statistical distribution of each segment. An iteratively running maximum-a-posteriori (MAP) segmentation is used to assign the boundary pixels to the region that maximizes the posterior distribution. Because only the boundary pixels of each segment have to be optimized, the SPc algorithm is computationally efficient. To find adequate segmentation parameters, we used a semi-automatic parameter selection (Stefanski et al., 2013) that is based on the out-of-bag error provided by Random Forests.

The Random Forest (RF) classifier was introduced by Breiman (2001) and demonstrated excellent performance in classifying remote sensing data (Gislason et al., 2006; Waske & Braun, 2009; Ghosh et al., 2014). The RF has several advantages for its application in remote sensing. For example, the RF can efficiently handle large data sets and input variables, is robust to outliers and overfitting, and its parameter selection is user-friendly (Breiman, 2001). The principle of the RF is to build an ensemble of k randomly generated decision trees and using a majority voting over all trees to receive the final result. Each tree is build by choosing randomly m features at each split node of the tree, whereby m is a subset of all features. Furthermore, for each tree only a randomly selected subset of the training data is used for classifier training. Remaining training samples, the so called "out-of-bag" (OOB) samples, allow an estimation of the classification error. To estimate this OOB error, the out-of-bag samples are classified by the particular decision tree and the final OOB error is derived by the classification error of all OOB samples. Since the RF is relatively insensitive to the parameters k and m when using a certain amount of trees, standard values for the parameters can be used. We used 500 trees for k and the square root of the number of input features for m.

The features of our object-based classification contained for each pixel both the spectral values and object features (mean values). For training the classifier, we used 1000 training samples per class. The training samples were selected by an equalized random sampling out of the training set. We validated the classification results by calculating confusion matrices, producer's, user's, and overall accuracies (Foody, 2002; Olofsson et al., 2013), which were based on the randomly clustered field-based validation set.

3.2 Trajectory analysis

The change trajectories were defined by the successive transitions between the land use/cover categories between the years. To monitor land management regimes, we used every cropland and grassland pixel in 1986 to determine changes, while urban and forest areas have been masked. We defined the following eight major change trajectories with regard to 2010: (1) *permanent large-scale cropland*, (2) *permanent grassland*, (3) *permanently abandoned* (i.e., conversion of cropland to grassland with no subsequent use), (4) *LSC* $\rightarrow$ *abandoned* $\rightarrow$ *LSC* (i.e., large-scale cropland to abandonment to large-scale cropland), (5) *LSC* $\rightarrow$ *abandoned* $\rightarrow$ *SSC* (i.e., large-scale cropland to abandonment to small-scale cropland), (6) *LSC* $\rightarrow$ *SSC* (cropland parcellation, i.e., transformation of large-scale cropland to small-scale

cropland), (7) *grassland → large-scale cropland*, and (8) *grassland → small-scale cropland*. We summarized the remaining land use changes under the class "*Others*", including, for example, multiple changes of cropland to grassland (e.g., cropland 1986 → grassland 1993 → cropland 1999 → grassland 2006). The eight major change trajectories enabled the analysis of the pattern of land management regimes and potential changes of land use intensity: *large-scale cropland* to *small-scale cropland* as potentially decreasing land use intensity and cropland abandonment, which implied no active land use intensity. However, the time period of farmland abandonment and recultivation were not assessed with this approach.

Thus, for a more detailed analysis of the spatio-temporal patterns of abandonment and recultivation, we analyzed the following change trajectories: (1) *permanent cropland* (2) *permanent grassland*, (3) *permanently abandoned 1993* (i.e., conversion of *cropland* to *grassland* until 1993 with no subsequent conversion), (4) *permanently abandoned 1999*, (5) *permanently abandoned 2006*, (6) *permanently abandoned 2010*, (7) *recultivated 1999* (i.e., fields that became abandoned till 1993 and recultivated again until 1999), (8) *recultivated 2006*, (9) *recultivated 2010*, and (10) *grassland to cropland*. We summarized the remaining land use changes under the class "*Others*".

As the previous trajectory analysis investigated the permanent abandonment and the recultivation, a third trajectory analysis assessed the total abandonment rate for each year of investigation. Therefore, we used the trajectories of *cropland* to *grassland* between 1986 and 2010 without considering whether the field is permanently abandoned or recultivated afterwards. With other words, we detected the total rate of farmland abandonment for each year. Differences between permanent abandonment and total abandonment may result from the fact that total abandonment can also include multiple changes of cropland/grassland conversion, which is not included in the permanent abandonment, but in the class "*Others*".

4 Results

4.1 Object-based classification

We generated five different land use/cover maps: 1986 (Landsat), 1993, 1999, 2006 (ERS SAR), and 2010 (Landsat + ERS SAR), using an object-based approach. Our accuracy assessment was based on confusion matrices to calculate the overall, producer's, and user's accuracies.

The base map of 1986 showed an overall accuracy of 97.2% (Table IV-1). In addition, the classification resulted in high producer's and user's accuracies for the individual classes (*cropland*, *grassland*, *forest*, and *urban*).

In the next step, we classified the ERS data of the years 1993, 1999, and 2006 into *cropland* and *grassland* and achieved high class-specific as well as overall accuracies with 97.4%, 93.2%, and 92.1%, respectively (Table IV-2). Although the overall accuracy was lowest for 2006, the accuracy was still on a very high level (92.1%).

The classification 2010 achieved a good separation of the different land management regimes and showed an overall accuracy of 87.2% (Table IV-3). The producer's and user's accuracies of *large-scale cropland* and *grassland* reached accuracies between 85.1% and 90.0%. The producer's and user's accuracies of *small-scale cropland* was 91.8% and 71.4%, respectively.

Overall, these five land use/cover maps showed very high overall accuracies, which is essential for an accurate change trajectory analysis.

Table IV-1: Accuracy assessment: classification results for 1986 (PA = producer's accuracy, UA = user's accuracy, OA = overall accuracy).

Classes	**1986**	
	PA [%]	UA [%]
Cropland	97.3	98.6
Grassland	93.3	95.5
Forest	98.7	100.0
Urban	100.0	73.7
OA	97.2%	

Table IV-2: Accuracy assessment: classification results for 1993, 1999, and 2006 (PA = producer's accuracy, UA = user's accuracy, OA = overall accuracy).

Classes	**1993**		**1999**		**2006**	
	PA [%]	UA [%]	PA [%]	UA [%]	PA [%]	UA [%]
Cropland	99.1	97.7	93.2	97.3	89.7	96.5
Grassland	89.6	95.6	93.4	84.5	95.5	86.9
OA	97.4%		93.2%		92.1%	

Table IV-3: Accuracy assessment: classification results for 2010 (PA = producer's accuracy, UA = user's accuracy, OA = overall accuracy, LSC = large-scale cropland, SSC = small-scale cropland).

Classes	**2010**	
	PA [%]	UA [%]
LSC	85.1	89.7
SSC	91.8	71.4
Grassland	90.0	88.3
OA	87.2%	

4.2 Trajectory analysis

We used a change trajectory analysis to assess land management regimes changes between 1986 and 2010. Generally, our change detection showed substantial potential for monitoring land management regimes due to high accuracies of our classification of each year.

Table IV-4: Quantification of the land management regimes change (LSC = large-scale cropland, SSC = small-scale cropland).

Change estimation	[ha]	[%]
LSC permanent	105,867	24.5
Grassland permanent	22,340	5.2
Permanently abandoned	76,591	17.7
LSC → abandoned → LSC	46,593	10.8
LSC → abandoned → SSC	29,738	6.9
LSC → SSC	79,735	18.5
Grassland → LSC	8,402	1.9
Grassland → SSC	4,379	1.0
Others	58,412	13.5

The final land management regimes change map showed that large parts of the study area were permanently used for *large-scale cropland*, mainly in the center of the study area (Figure IV-3). In the central eastern part of the study area, the farmland parcellation, i.e., the transformation from *large-scale cropland* to *small-scale cropland* (dark yellow), frequently occurred. In contrast, in the south east of the study area, *large-scale cropland*, which was temporarily abandoned, was recultivated as *large-scale cropland* until 2010 (orange). Land use conversion from *grassland* to either *large-scale cropland* or *small-scale cropland* was spread over the study area, however, it was very rare in its extent.

The non-forest and non-urban area (from now on referred to as area) covered about 432,000 ha. About 24.5% of this area was permanently cultivated with *large-scale cropland* between 1986 and 2010 while 18.5% was transformed from large-scale cropland to small-scale cropland (Table IV-4). At the same time, 10.8% of the area was recultivated as *large-scale cropland* after becoming abandoned and 6.9% was recultivated as *small-scale cropland*. While about 17.7% (10.8% + 6.9%) of the area was only temporally abandoned and recultivated later on, 17.7% became permanently abandoned and was not recultivated during the observation period.

Analyzing the spatio-temporal patterns of farmland abandonment revealed that parts of the northern study area were the first that became permanently abandoned in the 1990s (yellow and orange). Thus, permanent grassland and abandonment were dominant in the northern part of the study area (Figure IV-4). Conversely, in the south and west of the study site farmland abandonment occurred at a later time, particularly between 2000 and 2006 as well as between 2007 and 2010 (dark red and light red). Moreover, selected areas were recultivated until 2010 (dark green).

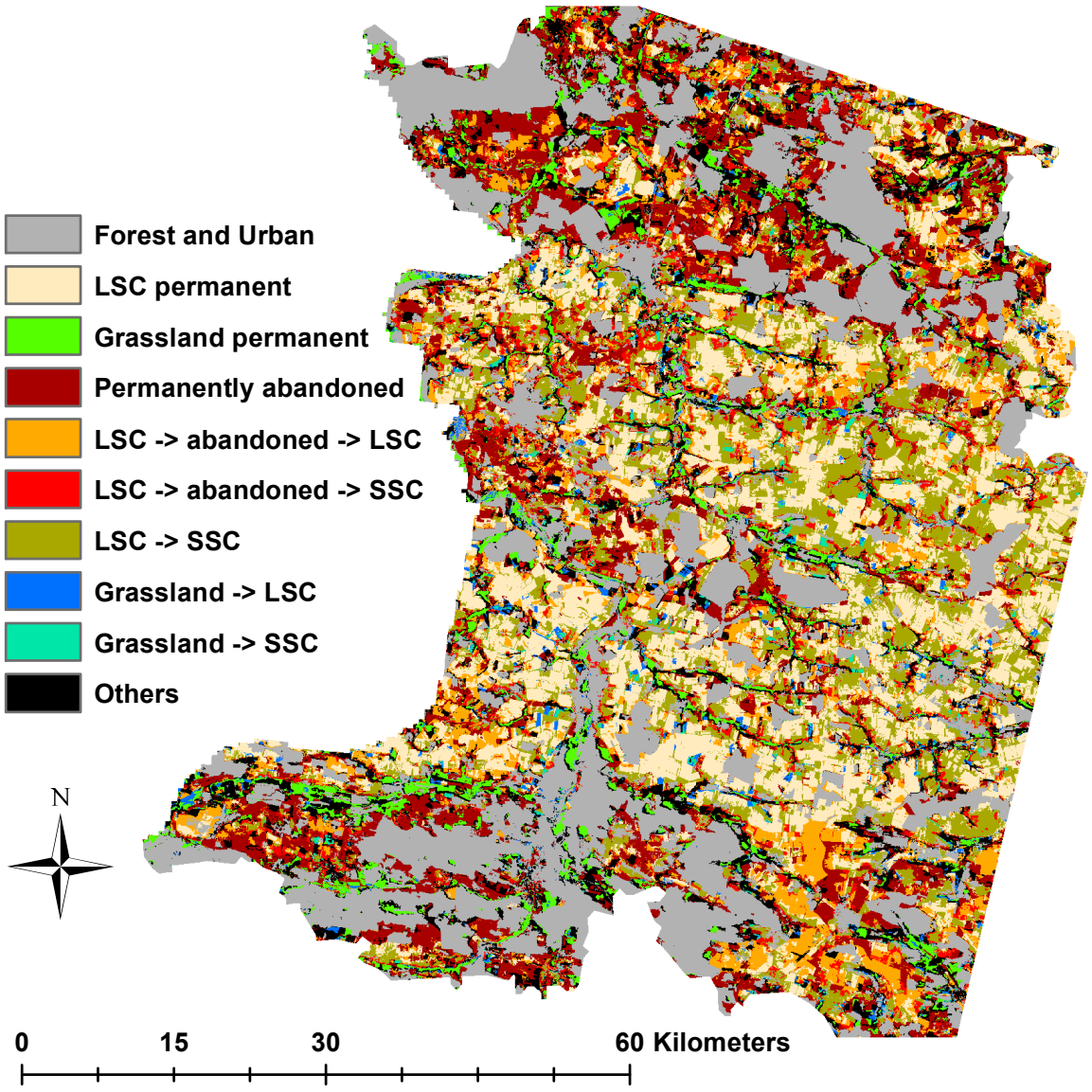

Figure IV-3: Land management regimes change map, based on Landsat and ERS data between 1986 and 2010 (LSC = large-scale cropland, SSC = small-scale cropland).

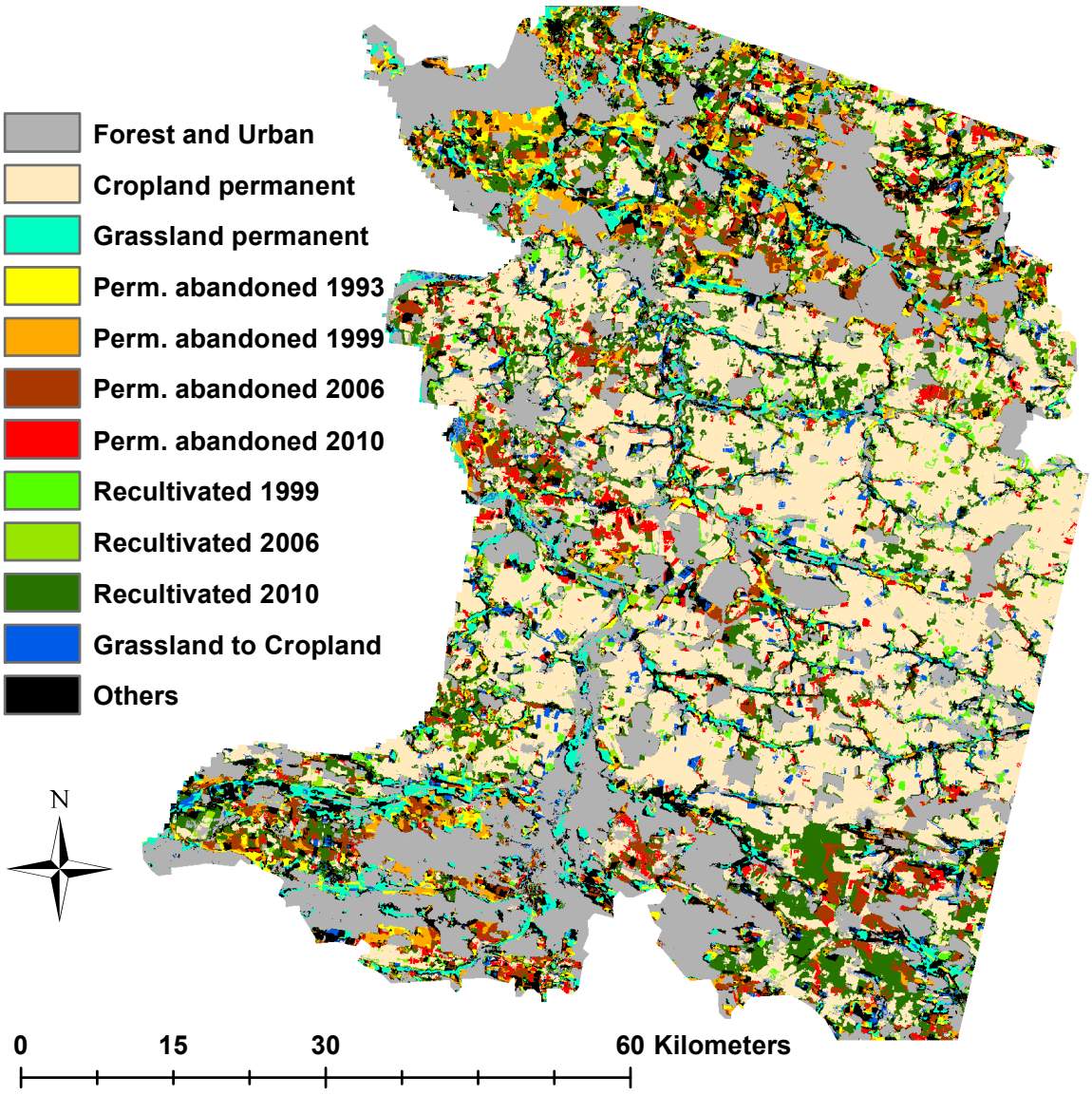

Figure IV-4: Change map showing farmland abandonment and recultivation, based on Landsat and ERS data between 1986 and 2010.

The analysis of the temporal stages of farmland abandonment revealed that only about 3.4% of the non-forest/non-urban area was permanently abandoned since 1993 (Table IV-5). In 1999, 7.9% (sum of 1993 and 1999) of the area was already permanently abandoned. The cumulative permanent farmland abandonment increased to 13.9% in 2006. Until 2010, we observed the highest permanent abandonment with 17.7% of the area, while about 3.8% became permanently abandoned between 2006 and 2010. Moreover, 17.7% of former abandonment was recultivated, particularly at the end of the 2000s (i.e., 13.5% recultivated 2010).

Table IV-5: Quantification of farmland abandonment and recultivation.

Change estimation	**[ha]**	**[%]**
Cropland permanent	185,602	43.0
Grassland permanent	22,340	5.2
Permanently abandoned 1993	14,734	3.4
Permanently abandoned 1999	19,500	4.5
Permanently abandoned 2006	26,134	6.0
Permanently abandoned 2010	16,223	3.8
Recultivated 1999	10,238	2.4
Recultivated 2006	7,670	1.8
Recultivated 2010	58,423	13.5
Grassland → Cropland	12,781	2.9
Others	58,412	13.5

The quantitative analysis of the total abandonment revealed that about 11.1% (47,897 ha) of the non-forest/non-urban area that was cropland in the 1980s was abandoned in 1993 (Table IV-6). In 1999, the total abandonment increased to 13.7% of the area. The highest total abandonment was in 2006 with 30.6% (132,406 ha) of the study area. In 2010, the total abandonment decreased in comparison to 2006 to 19.7%.

Table IV-6: Quantification of the total abandonment for each time step.

Change estimation	**[ha]**	**[%]**
Total abandonment 1993	47,897	11.1
Total abandonment 1999	59,120	13.7
Total abandonment 2006	132,406	30.6
Total abandonment 2010	85,171	19.7

5 Discussion

In the presented study, we monitored and analyzed changes in land use and management, including farmland abandonment, recultivation, and the transformation from common large-scale agriculture to small-scale agriculture. Due to spectral ambiguities, phenological variability, and limited data availability, a detailed and accurate mapping of these processes is

challenging. Therefore, an adequate strategy to monitor land management regimes is proposed, using an object-based approach with multitemporal SAR and multispectral remote sensing data.

By using Landsat and ERS SAR data, we received high overall classification accuracies between 87.2% and 97.4%. The good temporal coverage of at least one observation per season (Figure IV-2) has possibly favored the detection of land management. For example, grassland has a relatively constant signal signature during a year while, for example, plowing and harvesting can cause sharp changes in the signal of arable land. As expected, the use of spatial information due to object-based features in addition to the spectral information of each pixel ensured the precise mapping of classes that are hard to differentiate solely at pixel level, such as large-scale cropland and small-scale cropland (Hussain et al., 2013; Stefanski et al., 2014). This is in accordance with other studies that have shown the benefit of object-based classification of remote sensing data (Whiteside et al., 2011; Stefanski et al., 2013; Blaschke et al., 2014).

The analysis of change trajectories demand accurate classifications at every time step, which we achieved in general with relative high producer's and user's accuracies. Furthermore, the class "*Others*" summarized all remaining, not particularly investigated change classes, including implausible classes such as multiple changes of cropland to grassland. Therefore, inaccurate change classes were more likely assigned to this residue class, while the mapping of the relevant change classes was more reliably.

The first objective was the assessment of the value of SAR data for complementing optical data for monitoring land management regimes. Estimating land use and land cover changes by change trajectory analysis demand accurate land cover maps at each step. Our accuracy assessment clearly showed that SAR data are very well suited for mapping cropland and grassland with high classification accuracies (Table IV-2). The high accuracies for mapping agricultural classes, which are hard to separate by mono-temporal analyses, underline the value of multitemporal analyses. This is in accordance with the results in other studies (Blaes et al., 2005; McNairn et al., 2009b; Waske & Braun, 2009), where multitemporal C-Band data was used for crop type mapping. In general, these findings indicate that multitemporal SAR data are a promising alternative to complement optical data. SAR-based classifications can be used to fill temporal data gaps where no optical data is available for a particular year of interest and thus, enable a more detailed change analysis within time. Although most applications are based on C-band data, land cover information can be mapped by other frequencies such as X- and L-band data (McNairn et al., 2009b; Sonobe et al., 2014), for example, provided by TerraSAR-X and ALOS PALSAR. Nevertheless, for long-term monitoring the use of C-band is particularly interesting, because ERS-2, Envisat and RADARSAT have provided SAR data for several years. Moreover, data continuity is secured due to ongoing missions such as RADARSAT-2 and the recently launched Sentinel-1.

As discussed in other studies, the classification accuracy can be further increased by combining optical and SAR data (Waske & van der Linden, 2008; McNairn et al., 2009b;

Stefanski et al., 2014). The main reason for this is assumed to be the different nature of the used data types. SAR and optical systems operate in different wavelengths, ranging from visible to microwave domain. Consequently, the two systems provide different information. Moreover, optical data are characterized by a high spectral resolution, when compared to SAR data, while multi-temporal data sets within one growing season can be produced most reliably using SAR systems. The latter fact seems particularly relevant when the application demands specific acquisition periods. In context of mapping farmland abandonment, a spring observation is highly relevant to differentiate arable land and abandoned arable land. Moreover, a higher number of observations further increases the mapping accuracy (Prishchepov et al., 2012). The combination of SAR data with (a limited number of) optical images seems particularly relevant over larger areas, where the availability of adequate optical data sets is likely to decrease. Moreover, SAR-based maps can be used to fill-in spatial gaps in optical-based classifications, where clouds and haze result in missing values (McNairn et al., 2009b).

Our second objective was to analyze the changes of land management intensities between 1986 and 2010. The mapped changes such as the substantial permanent farmland abandonment (17.7% – Table IV-4) and the emerge of subsistence agriculture (26.4% – Table IV-4) can be traced back to the collapse of the Soviet Union and its planned-economy, which led to the end of guaranteed prices, the breakaway of former markets, and a rising foreign competition (Sabates-Wheeler, 2002; Kuemmerle et al., 2006; Baumann et al., 2011). The limits in infrastructure and migration from rural areas were additional issues that lead to increases in farmland abandonment (Ioffe & Nefedova, 2004; Müller & Munroe, 2008).

Economic transition in Eastern Europe led to the emergence of a large subsistence sector (Kostov & Lingard, 2004). Subsistence agriculture is often seen as a reaction of rural households to deal with hardships of transition (Mathijs & Noev, 2004), which is emphasized by the fact that the majority of subsistence agriculture (small-scale cropland) in our study area was directly converted from large-scale cropland. This process of land use intensity change was likely favored by the substantial political changes that led to the abandonment of the kolkhoz (i.e., collective farms in the Soviet Union) and thus, the ownership of the fields passed to the private property of the rural population.

However, about one quarter of the non-forest/non-urban area was permanently cultivated as large-scale cropland. The high rate of recultivation as large-scale cropland (i.e., potentially high intensive farming) led to a rate of 24.5% large-scale farming in 2010. The main reason for this may lie in the dominant soil types in this region. Stefanski et al. (2014) found that 54% of the large-scale cropland and even 60% of the small-scale cropland was cultivated on fertile Phaeozems and Chernozems, which are attractive for agriculture.

Our third objective was the analysis of spatio-temporal patterns of farmland abandonment and recultivation between 1986 and 2010. While about 11.1% of the area became abandoned until 1993, most fields were recultivated later on and only 3.4% in 1993 became permanently abandoned. That most fields became abandoned between 1999 and 2006 up to a rate of

30.6% was unexpected, as we expected the highest rates of abandonment in the 1990s (Table IV-6). However, we mentioned above that the kolkhoz collapsed in the 1990s and during these times a high amount of fields had to be used for subsistence farming. In the year 1999, an important page was turned in agricultural policy in Ukraine, including land reforms and a more stable trade policy (Aslund, 2002; OECD, 2004). This led to a period of improved efficiency-driven growth in the agricultural sector. Consequently, less farmland for self-sufficiency was needed and a continued decline in formal farm employment took place (OECD, 2004). This may explain the high rate of abandonment in 2006. With the recent integration in world markets and the emergence of agri-business, large areas were recultivated in 2010 while the abandonment rate decreased (Table IV-5).

Our agricultural land change rates are in accordance to previous case studies in Eastern Europe. For example, Kuemmerle et al. (2011) detected about 13% of farmland abandonment in western Ukraine in 2007. Likely reasons for the moderate differences to our results (17.7% permanent abandonment) are that their abandonment rate was based on the entire study area, and not just accounting the non-forest and non-urban area, as it was in our case. Alcantara et al. (2012) detected 15.1% abandoned cropland in Eastern Europe for 2005 by using MODIS data at a large scale (parts of the Baltic States, Belarus, Poland, and Ukraine). In contrast to this, other studies showed abandonment rates of 21% in Southern Romania (Kuemmerle et al., 2009) and 29% in the Carpathians Mountains (Griffiths et al., 2013). However, mountainous regions are marginal for agriculture and thus, farmland abandonment is more likely in such less suitable regions (Ioffe et al., 2012; Griffiths et al., 2013; Prishchepov et al., 2013).

6 Conclusions

We monitored land use changes, including large-scale cropland, small-scale cropland, farmland abandonment, and recultivation in western Ukraine by using an object-based approach with Landsat and ERS SAR data. With the utilization of a change trajectory analysis, we successfully estimated long term changes of land use intensity. We showed that SAR data is worthwhile to fill gaps of optical data. The good results that we received for separating different land use/cover classes at several time periods enabled a detailed trajectory analysis. This is especially beneficial as the availability of optical data can be limited due to cloud cover. This fact is particularly critical when mapping large areas and the accurate separation of individual land cover classes demands specific acquisitions. While the availability of adequate optical data sets can be limited in this context, data sets with high temporal coverage within a year can best be produced by using synthetic aperture radar. In our study region, we found substantial farmland abandonment both in the 1990s, basically characterized by the post-socialist transition processes, and in the 2000s. Some reasons for farmland abandonment in the 2000s might be land reforms and a more stable trade policy that led to a period of improved efficiency-driven growth in the agricultural sector.

Furthermore, we found a noticeable conversion of large-scale cropland to small-scale cropland in western Ukraine, showing the emerge of subsistence agriculture due to the demand of self-sufficiency. Especially between 2006 and 2010, we detected an increasing recultivation rate of abandoned cropland in western Ukraine, traced back to the recent integration in world markets and the emergence of agri-business. Overall, our approach constitutes a feasible and accurate approach for monitoring land management regimes over a long time period.

Acknowledgments

This work was supported by the German Research Foundation (DFG-WA 2728/2-1; WA 2728/2-2) and the State Fund of Fundamental Research of Ukraine (N 0113U002752). ERS data was provided by ESA (C1P.10962). RapidEye data was provided from the RapidEye Science Archive (RESA) by DLR under the proposal id490.

References

Alcantara, C., Kuemmerle, T., Prishchepov, A. V., & Radeloff, V. C. (2012). Mapping abandoned agriculture with multi-temporal MODIS satellite data. *Remote Sensing of Environment*, *124*, 334–347.

Angelstam, P., Elbakidze, M., Axelsson, R., Čupa, P., Halada, L., Molnar, Z., Pătru-Stupariu, I., Perzanowski, K., Rozulowicz, L., Standovar, T., Svoboda, M., & Törnblom, J. (2013). Maintaining cultural and natural biodiversity in the Carpathian mountain ecoregion: Need for an integrated landscape approach. In J. Kozak, K. Ostapowicz, A. Bytnerowicz, & B. Wyzga (Eds.), *The Carpathians: Integrating Nature and Society Towards Sustainability* Environmental Science and Engineering (pp. 393–424). Springer Berlin Heidelberg.

Aslund, A. (2002). *Why has Ukraine returned to economic growth?*. Technical Report Kiev, Ukraine: Institute for Economic Research and Policy Consulting, Working Paper No. 15.

Baumann, M., Kuemmerle, T., Elbakidze, M., Ozdogan, M., Radeloff, V. C., Keuler, N. S., Prishchepov, A. V., Kruhlov, I., & Hostert, P. (2011). Patterns and drivers of post-socialist farmland abandonment in western Ukraine. *Land Use Policy*, *28*, 552–562.

Blaes, X., Vanhalle, L., & Defourny, P. (2005). Efficiency of crop identification based on optical and SAR image time series. *Remote Sensing of Environment*, *96*, 352–365.

Blaschke, T., Hay, G. J., Kelly, M., Lang, S., Hofmann, P., Addink, E., Queiroz Feitosa, R., van der Meer, Freek, van der Werff, Harald, van Coillie, F., & Tiede, D. (2014). Geographic object-based image analysis - towards a new paradigm. *ISPRS journal of photogrammetry and remote sensing : official publication of the International Society for Photogrammetry and Remote Sensing (ISPRS)*, *87*, 180–191.

Breiman, L. (2001). Random Forests. *Machine Learning*, *45*, 5–32.

Carmona, A., & Nahuelhual, L. (2012). Combining land transitions and trajectories in assessing forest cover change. *Applied Geography*, *32*, 904–915.

El-Kawy, O. A., Rød, J., Ismail, H., & Suliman, A. (2011). Land use and land cover change detection in the western Nile delta of Egypt using remote sensing data. *Applied Geography*, *31*, 483–494.

Ellis, E. C., & Ramankutty, N. (2008). Putting people in the map: Anthropogenic biomes of the world. *Frontiers in Ecology and the Environment*, *6*, 439–447.

EUROSTAT (2009). LUCAS 2009 (Land Use / Cover Area Frame Survey) - Instructions for surveyors. `http://epp.eurostat.ec.europa.eu/portal/page/portal/lucas/documents/LUCAS2009_C1-Instructions_Revised20130925.pdf` (accessed on 11 June 2014).

Foody, G. M. (2002). Status of land cover classification accuracy assessment. *Remote Sensing of Environment*, *80*, 185–201.

Fritz, S., See, L., You, L., Justice, C., Becker-Reshef, I., Bydekerke, L., Cumani, R., Defourny, P., Erb, K., Foley, J., Gilliams, S., Gong, P., Hansen, M., Hertel, T., Herold, M., Herrero, M., Kayitakire, F., Latham, J., Leo, O., McCallum, I., Obersteiner, M., Ramankutty, N., Rocha, J., Tang, H., Thornton, P., Vancutsem, C., van der Velde, M., Wood, S., & Woodcock, C. (2013). The need for improved maps of global cropland. *Eos, Transactions American Geophysical Union*, *94*, 31–32.

Geist, H. J., & Lambin, E. F. (2002). Proximate causes and underlying driving forces of tropical deforestation. *BioScience*, *52*, 143.

Ghosh, A., Sharma, R., & Joshi, P. (2014). Random forest classification of urban landscape using Landsat archive and ancillary data: Combining seasonal maps with decision level fusion. *Applied Geography*, *48*, 31–41.

Gislason, P. O., Benediktsson, J. A., & Sveinsson, J. R. (2006). Random Forests for land cover classification. *Pattern Recognition Letters*, *27*, 294–300.

Godfray, H. C. J., Beddington, J. R., Crute, I. R., Haddad, L., Lawrence, D., Muir, J. F., Pretty, J., Robinson, S., Thomas, S. M., & Toulmin, C. (2010). Food security: The challenge of feeding 9 billion people. *Science*, *327*, 812–818.

Griffiths, P., Müller, D., Kuemmerle, T., & Hostert, P. (2013). Agricultural land change in the Carpathian ecoregion after the breakdown of socialism and expansion of the European Union. *Environmental Research Letters*, *8*, 1–12.

Hansen, M. C., Stehman, S. V., Potapov, P. V., Loveland, T. R., Townshend, J. R. G., DeFries, R. S., Pittman, K. W., Arunarwati, B., Stolle, F., Steininger, M. K., Carroll, M., & DiMiceli, C. (2008). Humid tropical forest clearing from 2000 to 2005 quantified by using multitemporal and multiresolution remotely sensed data. *Proceedings of the National Academy of Sciences*, *105*, 9439–9444.

Hussain, M., Chen, D., Cheng, A., Wei, H., & Stanley, D. (2013). Change detection from remotely sensed images: From pixel-based to object-based approaches. *ISPRS Journal of Photogrammetry and Remote Sensing*, *80*, 91–106.

Ioffe, G., Nefedova, T., & De Beurs, K. (2012). Land abandonment in Russia. *Eurasian Geography and Economics*, *53*, 527–549.

Ioffe, G., Nefedova, T., & Zaslavsky, I. (2004). From spatial continuity to fragmentation: The case of Russian farming. *Annals of the Association of American Geographers*, *94*, 913–943.

Ioja, C., Nita, M. R., & Stupariu, I. G. (2014). Resource conservation: Key elements in sustainable rural development. In Z. Andreopoulou, V. Samathrakis, S. Louca, & M. Vlachopoulou (Eds.), *E-Innovation for Sustainable Development of Rural Resources During Global Economic Crisis* (pp. 80–97). Hershey, PA: Business Science Reference.

Jaiantilal, A. (2009). Classification and regression by randomForest-matlab. Available at http://code.google.com/p/randomforest-matlab (accessed on 11 June 2014).

Kennedy, R. E., Cohen, W. B., & Schroeder, T. A. (2007). Trajectory-based change detection for automated characterization of forest disturbance dynamics. *Remote Sensing of Environment*, *110*, 370–386.

Kostov, P., & Lingard, J. (2004). Subsistence agriculture in transition economies: Its roles and determinants. *Journal of Agricultural Economics*, *55*, 565–579.

Kuemmerle, T., Erb, K., Meyfroidt, P., Müller, D., Verburg, P. H., Estel, S., Haberl, H., Hostert, P., Jepsen, M. R., Kastner, T., Levers, C., Lindner, M., Plutzar, C., Verkerk, P. J., van der Zanden, E. H., & Reenberg, A. (2013). Challenges and opportunities in mapping land use intensity globally. *Current Opinion in Environmental Sustainability*, *5*, 484–493.

Kuemmerle, T., Hostert, P., St-Louis, V., & Radeloff, V. C. (2009). Using image texture to map farmland field size: A case study in Eastern Europe. *Journal of Land Use Science*, *4*, 85–107.

Kuemmerle, T., Olofsson, P., Chaskovskyy, O., Baumann, M., Ostapowicz, K., Woodcock, C. E., Houghton, R. A., Hostert, P., Keeton, W. S., & Radeloff, V. C. (2011). Post-Soviet farmland abandonment, forest recovery, and carbon sequestration in western Ukraine. *Global Change Biology*, *17*, 1335–1349.

Kuemmerle, T., Radeloff, V. C., Perzanowski, K., & Hostert, P. (2006). Cross-border comparison of land cover and landscape pattern in Eastern Europe using a hybrid classification technique. *Remote Sensing of Environment*, *103*, 449–464.

Kuplich, T., Freitas, C. d. C., & Soares, J. (2000). The study of ERS-1 SAR and Landsat TM synergism for land use classification. *International Journal of Remote Sensing*, *21*, 2101–2111.

Lotze-Campen, H., Popp, A., Beringer, T., Müller, C., Bondeau, A., Rost, S., & Lucht, W. (2010). Scenarios of global bioenergy production: The trade-offs between agricultural expansion, intensification and trade. *Ecological Modelling*, *221*, 2188–2196.

Loveland, T. R., Cochrane, M. A., & Henebry, G. M. (2008). Landsat still contributing to environmental research. *Trends in Ecology & Evolution*, *23*, 182–183.

Mathijs, E., & Noev, N. (2004). Subsistence farming in Central and Eastern Europe: Empirical evidence from Albania, Bulgaria, Hungary, and Romania. *Eastern European Economics*, *42*, 72–89.

Mathijs, E., & Swinnen, J. F. M. (1998). The economics of agricultural decollectivization in East Central Europe and the former Soviet Union. *Economic Development and Cultural Change*, *47*, 1–26.

McNairn, H., Champagne, C., Shang, J., Holmstrom, D., & Reichert, G. (2009a). Integration of optical and Synthetic Aperture Radar (SAR) imagery for delivering operational annual crop inventories. *ISPRS Journal of Photogrammetry and Remote Sensing*, *64*, 434–449.

McNairn, H., Shang, J., Jiao, X., & Champagne, C. (2009b). The contribution of ALOS PALSAR multipolarization and polarimetric data to crop classification. *Geoscience and Remote Sensing, IEEE Transactions on*, *47*, 3981–3992.

McRoberts, R. E. (2013). Post-classification approaches to estimating change in forest area using remotely sensed auxiliary data. *Remote Sensing of Environment*, *in press*.

Mertens, B., & Lambin, E. F. (2000). Land-cover-change trajectories in southern Cameroon. *Annals of the Association of American Geographers*, *90*, 467–494.

Mester, R., Conrad, C., & Guevara, A. (2011). Multichannel segmentation using contour relaxation: Fast super-pixels and temporal propagation. In *Proceedings of the 17th Scandinavian conference on Image analysis* SCIA'11 (pp. 250–261). Berlin, Heidelberg: Springer-Verlag.

Moran, M., Hymer, D. C., Qi, J., & Kerr, Y. (2002). Comparison of ERS-2 SAR and Landsat TM imagery for monitoring agricultural crop and soil conditions. *Remote Sensing of Environment*, *79*, 243–252.

Mountrakis, G., Im, J., & Ogole, C. (2011). Support vector machines in remote sensing: A review. *ISPRS Journal of Photogrammetry and Remote Sensing*, *66*, 247–259.

Müller, D., & Munroe, D. K. (2008). Changing rural landscapes in Albania: Cropland abandonment and forest clearing in the postsocialist transition. *Annals of the Association of American Geographers*, *98*, 855–876.

Müller, D., & Sikor, T. (2006). Effects of postsocialist reforms on land cover and land use in South-Eastern Albania. *Applied Geography*, *26*, 175–191.

Munteanu, C., Kuemmerle, T., Boltiziar, M., Butsic, V., Gimmi, U., Halada, L., Kaim, D., Király, G., Éva Konkoly-Gyuró, Kozak, J., Lieskovský, J., Mojses, M., Müller, D., Ostafin,

K., Ostapowicz, K., Shandra, O., Štych, P., Walker, S., & Radeloff, V. C. (2014). Forest and agricultural land change in the Carpathian region – A meta-analysis of long-term patterns and drivers of change. *Land Use Policy*, *38*, 685–697.

OECD (2004). Achieving Ukraine's agricultural potential. Organization for Economic Co-operation and Development & the Environmentally and Socially Sustainable Development Unit, Europe and Central Asia Region, The World Bank, Washington.

Olofsson, P., Foody, G. M., Stehman, S. V., & Woodcock, C. (2013). Making better use of accuracy data in land change studies: Estimating accuracy and area and quantifying uncertainty using stratified estimation. *Remote Sensing of Environment*, *129*, 122–131.

Peringer, A., Siehoff, S., Chételat, J., Spiegelberger, T., Buttler, A., & Gillet, F. (2013). Past and future landscape dynamics in pasture-woodlands of the Swiss Jura Mountains under climate change. *Ecology and Society*, *18*.

Pohl, C., & Van Genderen, J. L. (1998). Review article multisensor image fusion in remote sensing: Concepts, methods and applications. *International Journal of Remote Sensing*, *19*, 823–854.

Prishchepov, A. V., Müller, D., Dubinin, M., Baumann, M., & Radeloff, V. C. (2013). Determinants of agricultural land abandonment in post-Soviet European Russia. *Land Use Policy*, *30*, 873–884.

Prishchepov, A. V., Radeloff, V. C., Dubinin, M., & Alcantara, C. (2012). The effect of Landsat ETM/ETM+ image acquisition dates on the detection of agricultural land abandonment in Eastern Europe. *Remote Sensing of Environment*, *126*, 195–209.

Rodriguez-Galiano, V., Ghimire, B., Rogan, J., Chica-Olmo, M., & Rigol-Sanchez, J. (2012). An assessment of the effectiveness of a Random Forest classifier for land-cover classification. *ISPRS Journal of Photogrammetry and Remote Sensing*, *67*, 93–104.

Sabates-Wheeler, R. (2002). Consolidation initiatives after land reform: Responses to multiple dimensions of land fragmentation in Eastern European agriculture. *Journal of International Development*, *14*, 1005–1018.

Shalaby, A., & Tateishi, R. (2007). Remote sensing and GIS for mapping and monitoring land cover and land-use changes in the northwestern coastal zone of Egypt. *Applied Geography*, *27*, 28–41.

Sieber, A., Kuemmerle, T., Prishchepov, A. V., Wendland, K. J., Baumann, M., Radeloff, V. C., Baskin, L. M., & Hostert, P. (2013). Landsat-based mapping of post-Soviet land-use change to assess the effectiveness of the Oksky and Mordovsky protected areas in European Russia. *Remote Sensing of Environment*, *133*, 38–51.

Sikor, T., Müller, D., & Stahl, J. (2009). Land fragmentation and cropland abandonment in Albania: Implications for the roles of state and community in post-socialist land consolidation. *World Development*, *37*, 1411–1423.

Sonobe, R., Tani, H., Wang, X., Kobayashi, N., & Shimamura, H. (2014). Random Forest classification of crop type using multi-temporal TerraSAR-X dual-polarimetric data. *Remote Sensing Letters*, *5*, 157–164.

Stefanski, J., Kuemmerle, T., Chaskovskyy, O., Griffiths, P., Havryluk, V., Knorn, J., Korol, N., Sieber, A., & Waske, B. (2014). Integrating optical and radar images for mapping land management regimes in western Ukraine. *Remote Sensing*, *6*, 5279–5305.

Stefanski, J., Mack, B., & Waske, B. (2013). Optimization of object-based image analysis with Random Forests for land cover mapping. *IEEE Journal of Selected Topics in Applied Earth Observations and Remote Sensing*, *6*, 2492–2504.

Tilman, D., Balzer, C., Hill, J., & Befort, B. L. (2011). From the cover: Global food demand and the sustainable intensification of agriculture. *Proceedings of the National Academy of Sciences*, *108*, 20260–20264.

USGS (2013). Landsat Processing Details. United States Geological Survey (USGS) `http://landsat.usgs.gov/Landsat_Processing_Details.php` (accessed on 11 June 2014).

Václavík, T., Lautenbach, S., Kuemmerle, T., & Seppelt, R. (2013). Mapping global land system archetypes. *Global Environmental Change*, *23*, 1637–1647.

Verburg, P. H., Neumann, K., & Nol, L. (2011). Challenges in using land use and land cover data for global change studies. *Global Change Biology*, *17*, 974–989.

Wagner, P. D., Kumar, S., & Schneider, K. (2013). An assessment of land use change impacts on the water resources of the Mula and Mutha rivers catchment upstream of Pune, India. *Hydrology and Earth System Sciences*, *17*, 2233–2246.

Wardlow, B. D., Egbert, S. L., & Kastens, J. H. (2007). Analysis of time-series MODIS 250 m vegetation index data for crop classification in the U.S. Central Great Plains. *Remote Sensing of Environment*, *108*, 290–310.

Waske, B., & Benediktsson, J. (2007). Fusion of support vector machines for classification of multisensor data. *IEEE Transactions on Geoscience and Remote Sensing*, *45*, 3858–3866.

Waske, B., & Braun, M. (2009). Classifier ensembles for land cover mapping using multitemporal SAR imagery. *ISPRS Journal of Photogrammetry and Remote Sensing*, *64*, 450–457.

Waske, B., Chi, M., Benediktsson, J., van der Linden, S., & Koetz, B. (2009). Algorithms and applications for land cover classification - a review. In *Li, D., Gong, J., & Shan (Eds.). Geospatial Technology for Earth Observation*. Springer.

Waske, B., & van der Linden, S. (2008). Classifying multilevel imagery from SAR and optical sensors by decision fusion. *IEEE Transactions on Geoscience and Remote Sensing*, *46*, 1457–1466.

Whiteside, T. G., Boggs, G. S., & Maier, S. W. (2011). Comparing object-based and pixel-based classifications for mapping savannas. *International Journal of Applied Earth Observation and Geoinformation*, *13*, 884–893.

Zaks, D. P. M., & Kucharik, C. J. (2011). Data and monitoring needs for a more ecological agriculture. *Environmental Research Letters*, *6*, 1–10.

Zhang, H., Qi, Z., Ye, X., Cai, Y., Ma, W., & Chen, M. (2013). Analysis of land use/land cover change, population shift, and their effects on spatiotemporal patterns of urban heat islands in metropolitan Shanghai, China. *Applied Geography*, *44*, 121–133.

Chapter V:

Synthesis

1 Summary and main findings

The overarching goal of this thesis was to develop a framework for monitoring land management regimes that differ in land use intensity and to apply this to a case study in western Ukraine to advance the mapping and understanding of broad-scale land use changes. Eastern Europe is a prime example for studying such land changes because of the profound political and socio-economic upheavals within the past three decades. To advance object-based image analysis, its prerequisite, the image segmentation process, was optimized by the development of a semi-automatic parameter selection. This method was integrated into an overall mapping framework consisting of a hierarchical, object-based analysis, using a joint data set of multispectral and SAR imagery. In addition to the remote sensing data, auxiliary data was used for a more detailed analysis of the land use patterns, which revealed interesting interconnections. Finally, land use and land cover changes were monitored between 1986 and 2010 in order to assess the spatio-temporal patterns of land use intensity during the Soviet and post-Soviet time.

In the following, each research question corresponding to one of the core chapters of this dissertation is answered, the main conclusions are presented, and future perspectives are discussed.

Research Question 1: How can object-based image analysis be optimized and simplified in order to improve both the accuracy and feasibility of remote sensing analysis?

In Chapter II, a new semi-automatic parameter selection approach for the Superpixel Contour segmentation algorithm was developed. It advances the image segmentation process in order to get optimal segmentation results with regard to the classification accuracy. The Superpixel Contour algorithm was newly introduced in the remote sensing context and proved to be useful to partition images into multiple homogenous regions. Its segmentation-based object features, such as mean value and standard deviation, led to significant higher classification accuracies in comparison to pixel-based approaches. Since image segmentation parameters have to be selected for each individual segmentation task, which can even include multiple segmentations for one image to capture different object-sizes, the segmentation parameter selection is often time consuming and requires a certain user knowledge. To optimize this process with regard to the segmentation quality and the users' expenditure of time, the proposed semi-automatic parameter selection supports the user in finding overall and class-specific optimal segmentations. The parameter selection strategy is based on the internal accuracy assessment of the Random Forest, which is fast and only requires training data. Optionally, the segmentation quality can also be assessed by using validation data. The Random Forest is very suitable for the parameter selection process because it does not need a specific parameter selection itself and provides fast and robust classifications. Furthermore, the proposed approach is scale-invariance due to the classification-based segmentation quality assessment, which means that the parameter selection works independently from the image

resolution. The semi-automatic parameter selection was successfully evaluated by land cover classifications of two study areas and the general performance (i.e., independently from the parameter selection approach) of the Superpixel Contour algorithm was similar to the widely-used multiresolution segmentation in eCognition. Finally, the semi-automatic parameter selection supported the finding of optimal image segmentations for the object-based analysis of land use and land cover in western Ukraine.

Research Question 2: How can the representation of land use intensity be improved in order to efficiently map land use management based on remote sensing data and what are the methodological and data requirements for mapping land management regimes?

In Chapter III, land management regimes were used to represent different land use intensity stages: 1) large-scale, intensive farmland; 2) small-scale, subsistence farmland; and 3) farmland abandonment that implies no active land use. Since land use intensity is a complex and multidimensional term and not directly mappable with remote sensing data, the use of field size as a proxy variable for the degree of mechanization enabled the mapping of land management regimes in western Ukraine. While large fields tend to require a high degree of mechanization and are typically intensively used in industrialized agriculture, small fields indicate low management intensity with a low degree of mechanization and are often accompanied by low levels of fertilizer and pesticide inputs. The identification of large-scale and small-scale cropland is not possible when using only spectral per pixel information. This makes object-based analysis with its spatial information essential for mapping land management regimes. To adequately distinguish pasture and fallow/abandoned farmland, it is necessary to have a good temporal resolution of the remote sensing data, because both classes account basically to grassland and the extraction of different phenological stages over the time is the key difference to distinguish both classes. As multispectral data depends on cloud-free image acquisition dates, the relatively weather independent SAR data ensured detailed temporal information. Overall, a hierarchical classification framework was used to integrate multispectral and SAR data as well as object-based features from different scales to map the land management regimes. Based on the generated land management regimes map and auxiliary data, the spatial patterns of land use and management were explored. In general, the observed patterns were as expected and in accordance with the classical land rent theory so that the land use intensity is lower on plots marginal for agricultural land use (e.g., on less suitable soils, high elevations, or far away from markets). Only small-scale cropland as subsistence agriculture with a potentially low management intensity showed slightly different patterns, as this was mostly found on soils suitable for agriculture. However, this is not very surprising as small-scale cropland became important after the collapse of the Soviet Union and many fertile soils in the vicinity of the cities were transformed from the former large-scale cropland to subsistence agriculture.

Research Question 3: What were the specific rates and patterns of land use and management changes in western Ukraine since 1986?

In Chapter IV, the monitoring of land management regimes between 1986 and 2010 was presented and discussed. The results clearly showed widespread changes of land management after the collapse of the Soviet Union in 1991, such as the emerge of farmland abandonment and subsistence agriculture. Substantial farmland abandonment of large, collectivized fields during the Soviet era were detected in the 1990s and 2000s. While the abandonment in the first period was characterized by post-socialist transition processes due to the dissolution of former collective farms (*kolkhoz*), the farmland abandonment in the 2000s likely goes back to land reforms, which improved the farmland efficiency so that less farmland was required for self-sufficiency. With the integration in world markets and the emerge of agri-business at the end of the 2000s, about 13.5% of the former abandoned farmland was recultivated between 2007 and 2010 and the total abandonment rate decreased to around 19.7% in 2010. In total, 17.7% of the abandoned farmland between 1994 and 2010 was recultivated. Another consequence of the collapse of socialism was the emerge of subsistence agriculture. Since the beginning of the 1990s, around 18.5% of the large-scale cropland was directly converted to small-scale cropland, 6.9% of the abandoned farmland was recultivated as small-scale cropland, and about 1.0% of the former grassland was used as small-scale cropland. In total, the rate of small-scale cropland added up to about 26.4% in 2010. Large-scale cropland was the most widespread agricultural class in 2010 with a rate of 37.2%, composed of 24.5% of permanent large-scale cropland, 10.8% recultivation as large-scale cropland, and about 1.9% of grassland to large-scale cropland conversion.

2 Main conclusions and future perspectives

The rising demand for agricultural products, based on the growing world population, diet changes, and an increasing role of bioenergy is expected to require a doubling of the agricultural production by 2050 (FAO, 2009; Godfray et al., 2010; Foley et al., 2011). Increasing agricultural production by expanding agriculture into natural ecosystems entails negative consequences for the environment and biodiversity. In comparison to agricultural expansion, the intensification of existing farmland in sustainable ways (e.g., based on efficient organic farming on underperforming fields or improving the management of nutrient and water) and the recultivation of abandoned farmland are promising avenues for increasing agricultural production with minimal environmental disadvantages. To assess where such strategies can be pursued requires advanced spatial information about land use intensity that goes beyond broad land use and land cover classes. In general, a spatially detailed map of regions with potentials for increasing agricultural production would be highly beneficial.

This dissertation makes a step into the direction for a more nuanced mapping of land use and land cover and to examine proxies for land use intensity with a resolution on field plot basis. With the approach for mapping and monitoring land management regimes, a

framework was developed to explore land use classes in more detail by detecting large-scale cropland, small-scale cropland, and farmland abandonment, representing high, low, and no management intensity, respectively. In Chapter IV, a rate of 26.4% of small-scale cropland and 19.7% of total farmland abandonment was identified in western Ukraine for 2010, suggesting a considerable potential for agricultural intensification respective recultivation in general. However, the analysis in Chapter III showed that 45% of the abandoned farmland was on Podzols, 28% on Histosols, and 2% on Leptosols, which means that about 75% of the former farmland is not very suitable for agriculture. This likely results from the massive agricultural expansion during the Soviet era (Ioffe & Nefedova, 2004). Around 60% of the small-scale cropland was located on fertile soils (Phaeozems and Chernozems). Altogether, 25% of the abandoned farmland and 60% of the small-scale cropland was on fertile soils, which suggests still an interesting potential for increasing agricultural production. The identified potential for increasing agricultural production offers the opportunity to further strengthen Ukraine's position in the global agricultural sector, which is in concordance with other studies, predicting Ukraine an important future role in the global agricultural market (USDA, 2010; Liefert et al., 2010; Deininger et al., 2013). The consequences of farmland abandonment are manifold. On the one hand, negative consequences of farmland abandonment are an increasing fire risk or sometimes desertification, depending on the individual local conditions such as climatic influences, soil type, and the former intensity of land use (Hölzel et al., 2002; Romero-Calcerrada & Perry, 2004). On the other hand, the positive mid- and long-term impacts of abandoned farmland are a result of revegetation (i.e., shrub land, forest succession), increasing biodiversity, sometimes even including rare species, and the recovery of ecosystem services like soil recovery or carbon sequestration, which can finally result in new natural landscape types, for example, steppe or secondary forests (Hölzel et al., 2002; Romero-Calcerrada & Perry, 2004; Rey Benayas, 2007; Navarro & Pereira, 2012). In the end, the environmental trade-offs of increasing agricultural production should be taken into consideration from case to case.

The methodological core of this research was an object-based approach based on multi-sensor data, using the Superpixel Contour segmentation with a semi-automatic parameter selection and the Random Forest classifier. The combination of both approaches to one comprehensive framework proved to be very suitable for an accurate and robust mapping and monitoring of land management regimes. Object-based image analysis with its geospatial information has generally great potential for improving various remote sensing applications, for example in the context of farmland/rangeland, vegetation, forest inventory, or urban mapping (Stefanski et al., 2014a; Laliberte et al., 2007; Yu et al., 2006; Chubey et al., 2006; Thomas et al., 2003). Particularly, the combination of the presented mapping framework of land management regimes with the direct linking with indicators of agricultural suitability (e.g., soil type, elevation, slope, remoteness to cities) can complete an optimal approach for creating a mapping system that systematically evaluates the direct agricultural potential for each field. For a systematic and broad-scale mapping of land management regimes, the

combination of the developed hierarchical, object-based mapping framework with a chain classification technique could be an interesting methodological approach. The principle of a chain classification is that the initial scene is traditionally classified and its result – in the overlapping part with the neighboring scene – is used to derive training samples for the next classification, which allows generally an accurate broad-scale mapping with a reduced demand for expensive in-situ data (Knorn et al., 2009). Furthermore, the use of Import Vector Machines (IVM) could be interesting, as they perform similar as the widely used Support Vector Machines (SVM), but provide additionally reliable probabilities (Zhu & Hastie, 2005; Roscher et al., 2012). These probabilities could be used to improve the classification accuracy and compensate small training sets to a certain degree by performing a self-training to identify new training samples. However, a systematic and broad-scale mapping of land management regimes would require the availability of adequate remote sensing and auxiliary data as well as suitable proxies for land use intensity, which may vary according to the study region. The opened Landsat archive and the current Landsat-8 mission as well as the upcoming Sentinel missions offer a huge potential for such mapping and monitoring applications for the future (Woodcock et al., 2008; Malenovský et al., 2012; Wulder et al., 2012). The Sentinel-1A (C-band SAR) satellite has already started and operates in a single or dual polarization mode with a resolution of up to five meters and is supposed to continue the tradition of the ERS and Envisat SAR missions (Torres et al., 2012). The Sentinel-2 (multispectral) mission will operate with up to 13 spectral bands and with a resolution between 10–60 meters and is supposed to complement the Landsat and SPOT satellite missions (Drusch et al., 2012).

With the use of optical and SAR multisensor data, different yet complementary information about the Earth's surface could be used to significantly improve the land use and land cover classification accuracy. In the case of, for example, pasture and fallow, which have a similar land cover but differ in their phenological stages, the SAR data with its high temporal resolution provided elementary information to differentiate both classes. In general, the joint use of optical and SAR data can contribute to a more precise mapping for many applications (Kuplich et al., 2000; Blaes et al., 2005; Waske & Benediktsson, 2007). Furthermore, with the relatively weather independent SAR sensors, temporal constrains regarding specific target dates can be satisfied with SAR data if cloud cover prevents the use of optical image acquisitions. This is especially relevant in time critical situations like natural hazards or disaster management (DiGiacomo et al., 2004; Joyce et al., 2009), in which the satellite systems provide nearly real-time information. Furthermore, SAR data is very useful if a constant time series is required, for example to observe different phenological stages, surface deformations, or for a detailed monitoring of soil moisture (Lanari et al., 2004; Balenzano et al., 2011). For the monitoring of land use changes in Chapter IV, a combined optical and SAR time series was successfully used and it was shown that SAR can be a reliable alternative to fill gaps of optical time series. Overall, the synergistic effects of optical and SAR data sets are valuable for both inter- and intra-annual analysis.

References

Alcantara, C., Kuemmerle, T., Prishchepov, A. V., & Radeloff, V. C. (2012). Mapping abandoned agriculture with multi-temporal MODIS satellite data. *Remote Sensing of Environment*, *124*, 334–347.

Altieri, M. A. (1999a). Applying agroecology to enhance the productivity of peasant farming systems in Latin America. *Environment, Development and Sustainability*, *1*, 197–217.

Altieri, M. A. (1999b). The ecological role of biodiversity in agroecosystems. *Agriculture, ecosystems & environment*, *74*, 19–31.

Aslund, A. (2002). *Why has Ukraine returned to economic growth?*. Technical Report Kiev, Ukraine: Institute for Economic Research and Policy Consulting, Working Paper No. 15.

Aslund, A. (2009). *How Ukraine became a market economy and democracy*. Washington DC: Peterson Institute for International Economics, USA.

Attema, E., Desnos, Y.-L., & Duchossois, G. (2000). Synthetic aperture radar in Europe: ERS, Envisat, and beyond. *Johns Hopkins APL technical digest*, *21*, 155–161.

Attema, E., Duchossois, G., & Kohlhammer, G. (1998). ERS-1/2 SAR land applications: Overview and main results. In *Geoscience and Remote Sensing Symposium Proceedings, 1998. IGARSS'98. 1998 IEEE International* (pp. 1796–1798). IEEE volume 4.

Baatz, M., & Schäpe, A. (2000). Multiresolution Segmentation: An optimization approach for high quality multi-scale image segmentation. In J. Strobl, T. Blaschke, & G. Griesebner (Eds.), *Angewandte Geographische Informationsverarbeitung XII* (pp. 12–23). Wichmann Verlag.

Balenzano, A., Mattia, F., Satalino, G., & Davidson, M. (2011). Dense temporal series of C-and L-band SAR data for soil moisture retrieval over agricultural crops. *Selected Topics in Applied Earth Observations and Remote Sensing, IEEE Journal of*, *4*, 439–450.

Barlow, J., Gardner, T. A., Araujo, I. S., Avila-Pires, T. C., Bonaldo, A. B., Costa, J. E., Esposito, M. C., Ferreira, L. V., Hawes, J., Hernandez, M I M, Hoogmoed, M. S., Leite, R. N., Lo-Man-Hung, N. F., Malcolm, J. R., Martins, M. B., Mestre, L A M, Miranda-Santos, R., Nunes-Gutjahr, A. L., Overal, W. L., Parry, L., Peters, S. L., Ribeiro-Junior, M. A., da Silva, M N F, da Silva Motta, C, & Peres, C. A. (2007). Quantifying the

biodiversity value of tropical primary, secondary, and plantation forests. *Proceedings of the National Academy of Sciences of the United States of America*, *104*, 18555–18560.

Barthlott, W., Schmit-Neuerburg, V., Nieder, J., & Engwald, S. (2001). Diversity and abundance of vascular epiphytes: A comparison of secondary vegetation and primary montane rain forest in the Venezuelan Andes. *Plant Ecology*, *152*, 145–156.

Bengtsson, J., Ahnström, J., & Weibull, A.-C. (2005). The effects of organic agriculture on biodiversity and abundance: A meta-analysis. *Journal of Applied Ecology*, *42*, 261–269.

Bennet, E. M., Carpenter, S., & Caraco, N. F. (2001). Human impact on erodable phosphorus and eutrophication: A global perspective. *BioScience*, *51*, 227–234.

Blaes, X., Vanhalle, L., & Defourny, P. (2005). Efficiency of crop identification based on optical and SAR image time series. *Remote Sensing of Environment*, *96*, 352–365.

Blanchard, O., & Kremer, M. (1997). Disorganization. *The Quarterly Journal of Economics*, *112*, 1091–1126.

Blaschke, T. (2010). Object based image analysis for remote sensing. *ISPRS Journal of Photogrammetry and Remote Sensing*, *65*, 2–16.

Campbell, J. (2002). *Introduction to Remote Sensing*. New York: Guilford Press, USA.

Cassman, K. G. (1999). Ecological intensification of cereal production systems: Yield potential, soil quality, and precision agriculture. *Proceedings of the National Academy of Sciences*, *96*, 5952–5959.

Chubey, M. S., Franklin, S. E., & Wulder, M. A. (2006). Object-based analysis of Ikonos-2 imagery for extraction of forest inventory parameters. *Photogrammetric Engineering & Remote Sensing*, *72*, 383–394.

Clough, Y., Barkmann, J., Juhrbandt, J., Kessler, M., Wanger, T. C., Anshary, A., Buchori, D., Cicuzza, D., Darras, K., Putra, D. D., Erasmi, S., Pitopang, R., Schmidt, C., Schulze, C. H., Seidel, D., Steffan-Dewenter, I., Stenchly, K., Vidal, S., Weist, M., Wielgoss, A. C., & Tscharntke, T. (2011). Combining high biodiversity with high yields in tropical agroforests. *Proceedings of the National Academy of Sciences of the United States of America*, *108*, 8311–8316.

Csaki, C., & Lerman, Z. (1997). Land reform and farm restructuring in East Central Europe and CIS in the 1990s: Expectations and achievements after the first five years. *European Review of Agricultural Economics*, *24*, 428–452.

Deininger, K., Nizalov, D., & Singh, S. K. (2013). Are mega-farms the future of global agriculture? Exploring the farm size-productivity relationship for large commercial farms in Ukraine. Washington DC: World Bank, USA.

Del Frate, F., Petrocchi, A., Lichtenegger, J., & Calabresi, G. (2000). Neural networks for oil spill detection using ERS-SAR data. *IEEE Transactions on Geoscience and Remote Sensing*, *38*, 2282–2287.

DiGiacomo, P. M., Washburn, L., Holt, B., & Jones, B. H. (2004). Coastal pollution hazards in southern California observed by SAR imagery: Stormwater plumes, wastewater plumes, and natural hydrocarbon seeps. *Marine Pollution Bulletin*, *49*, 1013– 1024.

Drusch, M., Del Bello, U., Carlier, S., Colin, O., Fernandez, V., Gascon, F., Hoersch, B., Isola, C., Laberinti, P., Martimort, P., Meygret, A., Spoto, F., Sy, O., Marchese, F., & Bargellini, P. (2012). Sentinel-2: ESA's Optical High-Resolution Mission for GMES Operational Services. *Remote Sensing of Environment*, *120*, 25–36.

Du, Y., Teillet, P. M., & Cihlar, J. (2002). Radiometric normalization of multitemporal high-resolution satellite images with quality control for land cover change detection. *Remote Sensing of Environment*, *82*, 123–134.

Ehrlich, P. R., & Holdren, J. P. (1971). Impact of population growth. *Science*, *171*, 1212–1217.

Evenson, R. E., & Gollin, D. (2003). Assessing the impact of the green revolution, 1960 to 2000. *Science (New York, N.Y.)*, *300*, 758–762.

FAO (2006). *Global Forest Resources Assessment 2005. Progress towards sustainable forest management* volume 147. Rome: Food and Agriculture Organization of the United Nations (FAO).

FAO (2009). *The State of Food Insecurity in the World: Economic crises - Impacts and Lessons Learned*. Rome: Food and Agriculture Organization of the United Nations (FAO).

FAO (2011). *Global food losses and food waste: Extent, causes and prevention*. Rome: Food and Agriculture Organization of the United Nations (FAO).

Foley, J., Defries, R., Asner, G., Barford, C., Bonan, G., Carpenter, S., Chapin, F., Coe, M., Daily, G., Gibbs, H., Helkowski, J., Holloway, T., Howard, E., Kucharik, C., Monfreda, C., Patz, J., Prentice, I., Ramankutty, N., & Snyder, P. (2005). Global consequences of land use. *Science*, *309*, 570–574.

Foley, J. A., Ramankutty, N., Brauman, K. A., Cassidy, E. S., Gerber, J. S., Johnston, M., Mueller, N. D., O'Connell, C., Ray, D. K., West, P. C., Balzer, C., Bennett, E. M., Carpenter, S. R., Hill, J., Monfreda, C., Polasky, S., Rockström, J., Sheehan, J., Siebert, S., Tilman, D., & Zaks, D. P. M. (2011). Solutions for a cultivated planet. *Nature*, *478*, 337–342.

Gamanya, R., De Maeyer, P., & De Dapper, M. (2009). Object-oriented change detection for the city of Harare, Zimbabwe. *Expert Systems with Applications*, *36*, 571–588.

Gardner, T. A., Hernández, M. I., Barlow, J., & Peres, C. A. (2008). Understanding the biodiversity consequences of habitat change: The value of secondary and plantation forests for neotropical dung beetles. *Journal of Applied Ecology*, *45*, 883–893.

Gens, R., & van Genderen, J. L. (1996). Review article SAR interferometry—issues, techniques, applications. *International Journal of Remote Sensing*, *17*, 1803–1835.

Gibbs, H. K., Ruesch, A. S., Achard, F., Clayton, M. K., Holmgren, P., Ramankutty, N., & Foley, J. A. (2010). Tropical forests were the primary sources of new agricultural land in the 1980s and 1990s. *Proceedings of the National Academy of Sciences of the United States of America*, *107*, 16732–16737.

Godfray, H. C. J., Beddington, J. R., Crute, I. R., Haddad, L., Lawrence, D., Muir, J. F., Pretty, J., Robinson, S., Thomas, S. M., & Toulmin, C. (2010). Food security: The challenge of feeding 9 billion people. *Science*, *327*, 812–818.

Godwin, W. (1820). *Of Population: An Enquiry Concerning the Power of Increase in the Numbers of Mankind, Being an Answer to Mr. Malthus's Essay on that Subject.* London: Longman, Hurst, Rees, Orme & Brown, UK.

Goldewijk, K. K. (2001). Estimating global land use change over the past 300 years: The HYDE database. *Global Biogeochemical Cycles*, *15*, 417–433.

Griffiths, P., Müller, D., Kuemmerle, T., & Hostert, P. (2013). Agricultural land change in the Carpathian ecoregion after the breakdown of socialism and expansion of the European Union. *Environmental Research Letters*, *8*, 1–12.

Guo, L. B., & Gifford, R. M. (2002). Soil carbon stocks and land use change: A meta analysis. *Global Change Biology*, *8*, 345–360.

Henderson, F. M., & Lewis, J. (1998). *Principles and applications of imaging radar*. Manual of Remote Sensing, Volume II. New York: John Wiley & Sons, USA.

Hole, D. G., Perkins, A. J., Wilson, J. D., Alexander, I. H., Grice, P. V., & Evans, A. D. (2005). Does organic farming benefit biodiversity? *Biological Conservation*, *122*, 113–130.

Hölzel, N., Haub, C., Ingelfinger, M. P., Otte, A., & Pilipenko, V. N. (2002). The return of the steppe large-scale restoration of degraded land in southern Russia during the post-Soviet era. *Journal for Nature Conservation*, *10*, 75–85.

Hostert, P., Kuemmerle, T., Prishchepov, A., Sieber, A., Lambin, E. F., & Radeloff, V. C. (2011). Rapid land use change after socio-economic disturbances: The collapse of the Soviet Union versus Chernobyl. *Environmental Research Letters*, *6*, 1–8.

Ioffe, G., & Nefedova, T. (2004). Marginal farmland in european russia. *Eurasian Geography and Economics*, *45*, 45–59.

Jenson, J. (1983). *Urban/suburban land use analysis.* Manual of Remote Sensing, Second Edition. Falls Church: American Society of Photogrammetry, USA.

Johnson, D., Brooks, K., for Strategic, G. U. C., & Studies, I. (1983). *Prospects for Soviet Agriculture in the 1980s.* CSIS publication series on the Soviet Union in the 1980s. Indiana University Press.

Johnson, S. R., Bouzaher, A., Carriquiry, A., Jensen, H., & Lakshminarayan, P. G. (1994). Production efficiency and agricultural reform in Ukraine. *American Journal of Agricultural Economics*, *76*.

Jolly, C. L., & Torrey, B. B. (1993). Population and land use in developing countries. In *Report of a Workshop. Committee on Population, Commission on Behavioural and Social Sciences and Education, National Research Council ed. National Academy Press, Washington, DC*.

Joyce, K. E., Belliss, S. E., Samsonov, S. V., McNeill, S. J., & Glassey, P. J. (2009). A review of the status of satellite remote sensing and image processing techniques for mapping natural hazards and disasters. *Progress in Physical Geography*, *33*, 183–207.

Kennedy, R. E., Cohen, W. B., & Schroeder, T. A. (2007). Trajectory-based change detection for automated characterization of forest disturbance dynamics. *Remote Sensing of Environment*, *110*, 370–386.

Knorn, J., Rabe, A., Radeloff, V. C., Kuemmerle, T., Kozak, J., & Hostert, P. (2009). Land cover mapping of large areas using chain classification of neighboring Landsat satellite images. *Remote Sensing of Environment*, *113*, 957–964.

Kuemmerle, T., Olofsson, P., Chaskovskyy, O., Baumann, M., Ostapowicz, K., Woodcock, C. E., Houghton, R. A., Hostert, P., Keeton, W. S., & Radeloff, V. C. (2011). Post-Soviet farmland abandonment, forest recovery, and carbon sequestration in western Ukraine. *Global Change Biology*, *17*, 1335–1349.

Kuplich, T., Freitas, C. d. C., & Soares, J. (2000). The study of ERS-1 SAR and Landsat TM synergism for land use classification. *International Journal of Remote Sensing*, *21*, 2101–2111.

Laliberte, A. S., Fredrickson, E. L., & Rango, A. (2007). Combining decision trees with hierarchical object-oriented image analysis for mapping arid rangelands. *Photogrammetric engineering & Remote sensing*, *73*, 197–207.

Lambin, E. F., & Geist, H. (2006). *Land-use and land-cover change: Local processes and global impacts.* Berlin and New York: Springer.

Lanari, R., Lundgren, P., Manzo, M., & Casu, F. (2004). Satellite radar interferometry time series analysis of surface deformation for Los Angeles, California. *Geophysical Research Letters*, *31*.

Larsson, S., & Nilsson, C. (2005). A remote sensing methodology to assess the costs of preparing abandoned farmland for energy crop cultivation in northern Sweden. *Biomass and Bioenergy*, *28*, 1–6.

Lehner, S., Horstmann, J., Koch, W., & Rosenthal, W. (1998). Mesoscale wind measurements using recalibrated ERS SAR images. *Journal of Geophysical Research: Oceans (1978–2012)*, *103*, 7847–7856.

Lerman, Z., Kislev, Y., Biton, D., & Kriss, A. (2003). Agricultural output and productivity in the former Soviet republics. *Economic Development and Cultural Change*, *51*, 999–1018.

Liefert, W., Liefert, O., Vocke, G., & Allen, E. (2010). Former Soviet Union region to play larger role in meeting world wheat needs. *Amber Waves*, *8*, 12–19.

Lillesand, T., Kiefer, R., & Chipman, J. (2008). *Remote sensing and image interpretation*. New York: John Wiley & Sons, USA.

MacQueen, J. (1967). Some methods for classification and analysis of multivariate observations. In *Proceedings of the fifth Berkeley symposium on mathematical statistics and probability* (pp. 281–297). California, USA volume 1.

Malenovský, Z., Rott, H., Cihlar, J., Schaepman, M. E., García-Santos, G., Fernandes, R., & Berger, M. (2012). Sentinels for science: Potential of Sentinel-1, -2, and -3 missions for scientific observations of ocean, cryosphere, and land. *Remote Sensing of Environment*, *120*, 91–101.

Malthus, T. (1798). *An Essay on the Principle of Population, as it affects the future improvement of society with remarks on the speculations of Mr. Godwin, M. Condorcet, and other writers*. London: J. Johnson, UK.

Matson, P. A., Parton, W. J., Power, A. G., & Swift, M. J. (1997). Agricultural intensification and ecosystem properties. *Science*, *277*, 504–509.

McRoberts, R. E. (2013). Post-classification approaches to estimating change in forest area using remotely sensed auxiliary data. *Remote Sensing of Environment*, .

MEA (2005). *Ecosystems and Human Well-being: Synthesis*. Washington DC: Island Press, USA. [Millennium Ecosystem Assessment].

Mertens, B., & Lambin, E. F. (2000). Land-cover-change trajectories in southern Cameroon. *Annals of the Association of American Geographers*, *90*, 467–494.

Mika, A. M. (1997). Three decades of Landsat instruments. *Photogrammetric Engineering and Remote Sensing*, *63*, 839–852.

Möller, M., Lymburner, L., & Volk, M. (2007). The comparison index: A tool for assessing the accuracy of image segmentation. *International Journal of Applied Earth Observation and Geoinformation*, *9*, 311–321.

Moore, R. K. (1983). *Radar fundamentals and scatterometers.* Manual of Remote Sensing, Second Edition. Falls Church: American Society of Photogrammetry, USA.

Mueller, N. D., Gerber, J. S., Johnston, M., Ray, D. K., Ramankutty, N., & Foley, J. A. (2012). Closing yield gaps through nutrient and water management. *Nature*, *490*, 254–257.

Müller, D., & Munroe, D. K. (2008). Changing rural landscapes in Albania: Cropland abandonment and forest clearing in the postsocialist transition. *Annals of the Association of American Geographers*, *98*, 855–876.

Myint, S. W., Gober, P., Brazel, A., Grossman-Clarke, S., & Weng, Q. (2011). Per-pixel vs. object-based classification of urban land cover extraction using high spatial resolution imagery. *Remote Sensing of Environment*, *115*, 1145–1161.

Na, X., Zhang, S., Li, X., Yu, H., & Liu, C. (2010). Improved land cover mapping using Random Forests combined with Landsat Thematic Mapper imagery and ancillary geographic data. *Photogrammetric Engineering & Remote Sensing*, *76*, 833–840.

Navarro, L. M., & Pereira, H. M. (2012). Rewilding abandoned landscapes in Europe. *Ecosystems*, *15*, 900–912.

OECD (2004). Achieving Ukraine's agricultural potential. Organization for Economic Co-operation and Development & the Environmentally and Socially Sustainable Development Unit, Europe and Central Asia Region, The World Bank, Washington.

Ojima, D., Galvin, K., & Turner, B. (1994). The global impact of land-use change. *BioScience*, *44*, 300–304.

Pal, M. (2005). Random Forest classifier for remote sensing classification. *International Journal of Remote Sensing*, *26*, 217–222.

Pitas, I. (2000). *Digital Image Processing Algorithms and Applications.* New York: John Wiley & Sons, USA.

Prasad, A., Iverson, L., & Liaw, A. (2006). Newer classification and regression tree techniques: Bagging and Random Forests for ecological prediction. *Ecosystems*, *9*, 181–199.

Pretty, J. N., & Hine, R. (2001). *Reducing food poverty with sustainable agriculture: A summary of new evidence.* University of Essex Colchester.

Prishchepov, A. V., Radeloff, V. C., Baumann, M., Kuemmerle, T., & Müller, D. (2012). Effects of institutional changes on land use: Agricultural land abandonment during the transition from state-command to market-driven economies in post-Soviet Eastern Europe. *Environmental Research Letters*, *7*, 1–13.

Quegan, S., Le Toan, T., Yu, J. J., Ribbes, F., & Floury, N. (2000). Multitemporal ERS SAR analysis applied to forest mapping. *IEEE Transactions on Geoscience and Remote Sensing*, *38*, 741–753.

Rey Benayas, J. (2007). Abandonment of agricultural land: An overview of drivers and consequences. *CAB Reviews: Perspectives in Agriculture, Veterinary Science, Nutrition and Natural Resources*, *2*.

Richards, J., & Jia, X. (2006). *Remote Sensing Digital Image Analysis: An Introduction*. Springer.

Rodriguez-Galiano, V., Chica-Olmo, M., Abarca-Hernandez, F., Atkinson, P., & Jeganathan, C. (2012). Random Forest classification of Mediterranean land cover using multi-seasonal imagery and multi-seasonal texture. *Remote Sensing of Environment*, *121*, 93–107.

Romero-Calcerrada, R., & Perry, G. L. (2004). The role of land abandonment in landscape dynamics in the SPA 'Encinares del río Alberche y Cofio, Central Spain, 1984–1999. *Landscape and Urban Planning*, *66*, 217–232.

Roscher, R., Waske, B., & Förstner, W. (2012). Incremental import vector machines for classifying hyperspectral data. *IEEE Transactions on Geoscience and Remote Sensing*, *50*, 3463–3473.

Sandau, R. (2010). Status and trends of small satellite missions for Earth observation. *Acta Astronautica*, *66*, 1–12.

Schierhorn, F., Müller, D., Beringer, T., Prishchepov, A. V., Kuemmerle, T., & Balmann, A. (2013). Post-Soviet cropland abandonment and carbon sequestration in European Russia, Ukraine, and Belarus. *Global Biogeochemical Cycles*, *27*, 1175–1185.

Seufert, V., Ramankutty, N., & Foley, J. A. (2012). Comparing the yields of organic and conventional agriculture. *Nature*, *485*, 229–232.

Shepherd, M., Pearce, B., Cormack, B., Philipps, L., Cuttle, S., Bhogal, A., Costigan, P., & Unwin, R. (2003). An assessment of the environmental impacts of organic farming. *A review for DEFRA-funded Project OF0405*, .

Shulman, S. (1999). The cultural foundations of Ukrainian national identity. *Ethnic and Racial Studies*, *22*, 1011–1036.

Shupe, S. M., & Marsh, S. E. (2004). Cover- and density-based vegetation classifications of the Sonoran Desert using Landsat TM and ERS-1 SAR imagery. *Remote Sensing of Environment*, *93*, 131–149.

Singh, A. (1989). Review article digital change detection techniques using remotely-sensed data. *International Journal of Remote Sensing*, *10*, 989–1003.

Smith, K. A., McTaggart, I. P., & Tsuruta, H. (1997). Emissions of N_2O and NO associated with nitrogen fertilization in intensive agriculture, and the potential for mitigation. *Soil Use and Management*, *13*, 296–304.

Stefanski, J., Kuemmerle, T., Chaskovskyy, O., Griffiths, P., Havryluk, V., Knorn, J., Korol, N., Sieber, A., & Waske, B. (2014a). Mapping land management regimes in western Ukraine using optical and SAR data. *Remote Sensing*, *6*, 5279–5305.

Stefanski, J., Mack, B., & Waske, B. (2013). Optimization of object-based image analysis with Random Forests for land cover mapping. *IEEE Journal of Selected Topics in Applied Earth Observations and Remote Sensing*, *6*, 2492–2504.

Stefanski, J., Chaskovskyy, O., & Waske, B. (2014b). Mapping and monitoring of land use changes in post-Soviet western Ukraine using remote sensing data. *Applied Geography*, *55*, 155–164.

Strayer, R. W. (1998). *Why did the Soviet Union collapse? Understanding historical change*. Armonk: M.E. Sharpe, USA.

Striewe, L., & von Cramon-Taubadel, S. (1999). Grain production in ukraine: Missed opportunities and the need for immediate action. In A. Siedenberg, & L. Hoffmann (Eds.), *Ukraine at the Crossroads* (pp. 292–308). Heidelberg: Physica-Verlag, GER.

Thomas, N., Hendrix, C., & Congalton, R. G. (2003). A comparison of urban mapping methods using high-resolution digital imagery. *Photogrammetric Engineering & Remote Sensing*, *69*, 963–972.

Tilman, D. (1998). The greening of the green revolution. *Nature*, *396*, 211–212.

Tilman, D., Balzer, C., Hill, J., & Befort, B. L. (2011). From the cover: Global food demand and the sustainable intensification of agriculture. *Proceedings of the National Academy of Sciences*, *108*, 20260–20264.

Tilman, D., Fargione, J., Wolff, B., D'Antonio, C., Dobson, A., Howarth, R., Schindler, D., Schlesinger, W. H., Simberloff, D., & Swackhamer, D. (2001). Forecasting agriculturally driven global environmental change. *Science (New York, N.Y.)*, *292*, 281–284.

Torres, R., Snoeij, P., Geudtner, D., Bibby, D., Davidson, M., Attema, E., Potin, P., Rommen, B., Floury, N., Brown, M., Traver, I. N., Deghaye, P., Duesmann, B., Rosich, B.,

Miranda, N., Bruno, C., L'Abbate, M., Croci, R., Pietropaolo, A., Huchler, M., & Rostan, F. (2012). GMES Sentinel-1 mission. *Remote Sensing of Environment*, *120*, 9–24.

Tscharntke, T., Klein, A. M., Kruess, A., Steffan-Dewenter, I., & Thies, C. (2005). Landscape perspectives on agricultural intensification and biodiversity - ecosystem service management. *Ecology Letters*, *8*, 857–874.

Turner, B., Clak, W., Kates, R., Richards, J., Mathews, J., & Meyer, W. (1990). *The Earth as Transformed by Human Action: Global and Regional Changes in the Biosphere Over the Past 300 Years*. Cambridge: Cambridge University Press, UK.

USDA (2010). *USDA Agricultural Projections to 2019*. Long-term projections report. U.S. Department of Agriculture, Office of the Chief Economist, World Agricultural Outlook Board.

USDA-FAS (2008). *Russia: Grain Production Prospects and Siberia Trip Report*. Technical Report United States Department of Agriculture's (USDA) - Foreign Agricultural Service (FAS).

Vitousek, P. M. (1997). Human domination of Earth's Ecosystems. *Science*, *277*, 494–499.

Walker, B., Steffen, W., Canadell, J., & Ingram, J. (1999). *The Terrestrial Biosphere and Global Change: Implications for Natural and Managed Ecosystems*. International Geosphere-Biosphere Programme Book Series. Cambridge: Cambridge University Press, UK.

Wang, Z., Jensen, J. R., & Im, J. (2010). An automatic region-based image segmentation algorithm for remote sensing applications. *Environmental Modelling & Software*, *25*, 1149–1165.

Waske, B., & Benediktsson, J. (2007). Fusion of support vector machines for classification of multisensor data. *IEEE Transactions on Geoscience and Remote Sensing*, *45*, 3858–3866.

Waske, B., & Braun, M. (2009). Classifier ensembles for land cover mapping using multitemporal SAR imagery. *ISPRS Journal of Photogrammetry and Remote Sensing*, *64*, 450–457.

Waske, B., & van der Linden, S. (2008). Classifying multilevel imagery from SAR and optical sensors by decision fusion. *IEEE Transactions on Geoscience and Remote Sensing*, *46*, 1457–1466.

West, P. C., Gerber, J. S., Engstrom, P. M., Mueller, N. D., Brauman, K. A., Carlson, K. M., Cassidy, E. S., Johnston, M., MacDonald, G. K., Ray, D. K., & Siebert, S. (2014). Leverage points for improving global food security and the environment. *Science (New York, N.Y.)*, *345*, 325–328.

Whiteside, T. G., Boggs, G. S., & Maier, S. W. (2011). Comparing object-based and pixel-based classifications for mapping savannas. *International Journal of Applied Earth Observation and Geoinformation*, *13*, 884–893.

Williams, D. L., Goward, S., & Arvidson, T. (2006). Landsat. *Photogrammetric Engineering & Remote Sensing*, *72*, 1171–1178.

Woodcock, C. E., Allen, R., Anderson, M., Belward, A., Bindschadler, R., Cohen, W., Gao, F., Goward, S. N., Helder, D., Helmer, E., Nemani, R., Oreopoulos, L., Schott, J., Thenkabail, P. S., Vermote, E. F., Vogelmann, J., Wulder, M. A., & Wynne, R. (2008). Free access to Landsat imagery. *Science (New York, N.Y.)*, *320*, 1011.

World Bank (1996). Agricultural trade and trade policy: A multi-country analysis - commodity trends in agriculture: Production, gross margins, and trade: The experiences of Belarus, Moldova, and Ukraine - 1991-1994. Washington DC: World Bank, USA.

Wulder, M. A., Masek, J. G., Cohen, W. B., Loveland, T. R., & Woodcock, C. E. (2012). Opening the archive: How free data has enabled the science and monitoring promise of Landsat. *Remote Sensing of Environment*, *122*, 2–10.

Xiong, X., K Chiang, J Esposito, B Guenther, & W Barnes (2003). MODIS on-orbit calibration and characterization. *Metrologia*, *40*, 1–4.

Yu, Q., Gong, P., Clinton, N., Biging, G., Kelly, M., & Schirokauer, D. (2006). Object-based detailed vegetation classification with airborne high spatial resolution remote sensing imagery. *Photogrammetric Engineering & Remote Sensing*, *72*, 799–811.

Zhu, J., & Hastie, T. (2005). Kernel logistic regression and the import vector machine. *Journal of Computational and Graphical Statistics*, *14*, 185–205.